National University of Lesotho

An optimization approach for the economic dispatch incorporating renewable energy resources into the LEC power sources portfolio

Thato Nchakha Rateele (201602380)

A dissertation submitted in partial fulfilment of
the requirements for the degree of

Master of Science in Sustainable Energy

Offered by the

Energy Research Centre
Faculty of Science & Technology

June 2022

Abstract

Electricity demand in Lesotho has been constantly rising over the past years and has greatly surpassed the main domestic generation of 72 MW hydropower station in ‘Muela, which only supports a monthly average of 58% of the load and the deficit is imported from South Africa and Mozambique through fixed bilateral contracts. Although these contracts are regarded as uninterruptable as transmission paths are secured in advance, they come with heavy reliability premium costs endured by electricity utility, Lesotho Electricity Company (LEC). With the abundant renewable energy sources in Lesotho, Independent Power Producers (IPPs) could be invited to erect wind farms and solar photovoltaics (PV) plants to increase local energy security and diversify LEC power sources.

Because electrical power networks must be secure, reliable, and cost-effective, the study developed a power dispatching approach that includes solar PV and wind generators to aid 'Muela meet demand and be backed by imports. According to the analysis, main grid imports are minimized by 22.3% with the introduction of 50 MW Ha-Ramarothole solar PV and by 40.2% with wind farms (24 MW Masitise and 34 MW Lets'eng) working with 'Muela. A 59.7% minimization is obtained by combining solar PV at 50 MW, wind farms at 58 MW, and 'Muela at 72 MW. Furthermore, the study used the Monte Carlo approach to simulate generation adequacy analysis in order to establish the monthly average expected demand not supplied (EDNS) and loss of load probability (LOLP). The EDNS never drops below 0 MW, while the LOLP only reaches a minimum of 52% for all scenarios evaluated, according to generation adequacy analysis of all local generators.

Finally, the study assessed the influence of renewable energy absorption on LEC in terms of costs in procuring power locally and from imports using the South African Power Pool (SAPP) Markets: Day Ahead Market (DAM), Forward Physical Market (FPM) weekly and monthly. Since DAM yearly cost of energy is approximately half that of FPM weekly and monthly, it has been shown to be the most cost-effective market to procure under for renewables penetrations. Additionally, the cost of electricity anticipated to be incurred while purchasing from solar at 50 MW, ‘Muela, and DAM is around LSL 45 million less expensive than the fixed bilateral contracts. As a result, minimization of imports and their cost can be effectively accomplished with DAM because the total cost of energy (local prices plus DAM pricing) significantly reduces the potential expenses.

Acknowledgements

First and foremost, I would want to convey my heartfelt gratitude to my supervisor, Prof. Leboli Zak Thamae, for his devotion, encouragement, advice, and time spent on the project. His immense expertise and vast experience constantly motivated me to conduct and successfully complete my academic studies. I would also want to thank Mr. Mokeke and Mr. Kao for their unwavering support

during the research. I appreciate the help from ERC staff and LEC in providing me with the data I needed to complete the study.

My family (my parents and sister) deserve special thanks for their everlasting support and encouragement. It would have been impossible for me to finish my studies without them, thus I consider myself fortunate to have them as family. Finally, and most importantly, I praise God, the Almighty, for giving me the strength, wisdom, and bravery to pursue this research.

List of Acronyms

B&B	:	Branch and Bound
DAM	:	Day Ahead Market
DCS	:	Distributed Control Systems
DE	:	Differential Evolution
DED	:	Dynamic Economic Dispatch
DGO	:	Deterministic Global Optimization
EDM	:	Electricidade de Mozambique
EDNS	:	Expected Demand not Supplied
ELD	:	Economic Load Dispatch
EP	:	Evolutionary Programming
FPM	:	Forward Physical Market
GA	:	Genetic Algorithm
IPP	:	Independent Power Producer
IREGs	:	Intermittent Renewable Energy Generators
LEC	:	Lesotho Electricity Company
LHDA	:	Lesotho Highlands Development Authority
LOEE	:	Loss of Energy Expectation
LOLD	:	Loss of Load Duration
LOLE	:	Loss of load Expectation
LOLF	:	Loss of Load Frequency
LOLP	:	Loss of Load Probability
MPPT	:	Maximum Power Point Tracking
NOCT	:	Normal Cell Operating Temperature
POZ	:	Prohibited Operating Zones PPA
	:	Power Purchase Agreement
PSO	:	Particle Swarm Optimization
PV	:	Photovoltaic
QCQP	:	Quadratically Constrained Quadratic Programming
RES	:	Renewable Energy Sources

SA	:	Stimulated Annealing
SAPP	:	Southern African Power Pool
SCADA	:	Supervisory Control and Data Acquisition Systems
SED	:	Static Economic Dispatch
SQP	:	Sequential Quadratic Programming
WECS	:	Wind Energy Conversion Systems
WMO	:	World Meteorological Organization

Table of Contents

1. Introduction

1.1 Background

Acceleration in integrating renewable energy sources (RES) to electrical grids can be attributed to the whole world striving to achieve maximum energy security and economic development while also promoting environmental sustainability [1]. As of 2019, solar photovoltaic (PV) and wind have taken the lead as compared to other renewables with capacities of 760 GW and 743 GW [2], respectively. However, the power generated by intermittent renewable energy sources is variable and non-deterministic as it depends upon geographical and climate conditions [1]. Therefore, their variability and uncertainty creates challenges to the power planning and operation of the power system network [3]–[5].

Nevertheless, the basic requirements for electrical power networks are security, reliability and cost-effectiveness. Specifically, the normal operation and planning in conventional power systems is generally based on efficiently and economically meeting the future load forecast with considerations of random variations in the load and chances of major contingencies in the supply system [6]. Economical operation in power system networks is very crucial as it enables minimum operational costs and affordable tariffs to consumers while maximizing profits on the invested capital. This economic operation of the power system network can be achieved through economic load dispatch (ELD) which optimally allocates generating units to effectively match the load demand at all generating levels with minimum generating or operating costs and satisfying all system reliability constraints [5].

Adding on, the fundamental static economic dispatch (SED) optimally distributes the constant load demand among committed units while minimizing generational and operational costs satisfying all unit system equality and quality constraints to ensure power system network reliability [7]–[9]. Nonetheless, considering the variable load demand in practical networks, SED induces a practical difficulty as power cannot be altered to meet the demand. The dynamic economic dispatch (DED), an extension of SED, takes into consideration the dynamic costs involved as a result of changing from one-generation level to another and hence overcoming this difficulty [7]–[9]. Hence, DED is an optimization approach in power systems which aims at achieving an optimal scheduling of power available from generators to effectively and efficiently match the predicted load demand while minimizing generation costs and satisfying all system constraints [7], [9]–[11].

Integration of large-scale wind and solar generators to the grid implies a new source of uncertainty must be added to the operation and planning problem. Therefore, wind and solar generators are often treated as non-dispatchable or variable units which only inject the power to the grid network when available depending on climate conditions [5]. Furthermore, the unpredictable wind velocity and weather dependent solar irradiation, make it difficult to correctly predict output power, which consistently leads to under and over generation of power scheduling [5], [11]. For this reason, there is a need to determine the generation adequacy of these systems to analyze the power system's security of supply.

Generation adequacy refers to the generator's ability to meet system demand while simultaneously taking into account generators' unavailability, load volatility, and renewable energy generators (REGs) output variation [12], [13]. Although there are numerous indices that may be used to assess the adequacy of a country's or utility's power system, the basic ones are loss of load expectation (LOLE) or loss of load probability (LOLP) and loss of energy expectation (LOEE) or Expected demand not supplied (EDNS) [12], [14], [15]. The LOLE is the average number of days or hours over a given time period (usually a year) when daily peak load or hourly demand is expected to exceed available generation capacity. While, the predicted energy not provided by the generating system due to the load demand exceeding the available generating capacity is measured by the EDNS index. As such, this energy can be met by spinning reserves, battery storage or imports from external grids in an interconnected grid.

1.2 Problem Statement

The generation, supply and distribution of electricity in Lesotho has always been dominated by and reliant on two wholly state-owned entities: the Lesotho Electricity Company (LEC), which is the monopoly transmitter, distributor, and supplier of electricity, as well as the Lesotho Highlands Development Authority (LHDA), which is the main power producer through the 'Muela hydropower station [16]. In Lesotho, the energy demand has been constantly increasing over the past years and has greatly surpassed the domestic generation, which has been stagnant since 1998. The domestic electricity generation is mainly derived from a 72 MW hydropower station in 'Muela and other small generating utilities all over the country with a total of 2.6 MW [17]. Even so, the current installed capacities fail to meet the total energy demand which rose about 16% from 153 MW in 2015-2016, to an escalation of 177 MW in 2019 [17]. Since the local generating capacity fails to meet the peak

load and even the base load of about 100 MW, the deficit is met by importing power from Southern African Power Pool (SAPP) using bilateral contracts between South Africa (with Eskom) and Mozambique (with Electricidade de Mozambique (EDM)) [18].

The use of these bilateral contracts enables LEC to secure transmission paths in advance. Although these contracts are regarded as uninterruptable, they come with heavy reliability premium costs endured by the electricity supplier. On top of that, both contracts from Eskom and EDM are reviewed annually and subject to the volatile market conditions which can result in increased expense or an obstruction of the electricity supply to Lesotho [18]. As a result, in an effort to offset these costs, LEC may decide to set high charges for consumers and end users of electricity. Since Lesotho has about 50% poverty rate [19], setting heavy tariffs on consumers means that a bulk of households connected to the grid will fail to purchase electricity for their essential energy needs. Hence, there is a need to embark on exploring the feasibility of local generation mainly from renewable energy sources like solar PV and wind as a way to increase energy security and minimize heavy dependence on imports that come with higher energy costs.

1.3 Research Questions and Objectives

The current research project aims to implement a power dispatching approach for locally committed IREGs (wind and solar PV) and imports into the existing national grid. The emphasis will be on generation adequacy of these generators (‘Muela hydropower, Wind and solar PV farms) as they are dispatched to successfully match the dynamic local demand considering the LOLP and the EDNS.

The research will be guided the following questions:

i) How to meet the load demand using local generation, mainly from renewables?

ii) Is local generation using renewables more cost effective than imports? iii) What is the most economical way to combine local renewable sources and imports?

The objectives of the study are:

i) To assess the generation adequacy analysis of locally committed renewable energy generators and ‘Muela hydro power plant.

ii) To optimally schedule the locally committed generating unit outputs supported by imports in order to match the load demand at minimum cost while ensuring continual and reliable power supply.

iii) Analyze the cost implications for LEC in procuring power both locally and in SAPP markets considering the prices volatility.

1.4 Justification

Despite the crisis of energy security, Lesotho also faces a great challenge of low electricity access rate. The overall electricity access rate in Lesotho does is around 51% of population. In addition, the households' electrification is not equally proportioned over the country, with access rates estimated at 76% in urban areas and 32% in rural areas, as presented in the 2019 World Bank data [20]. As a response to meet the ever-escalating electricity demand and also increase energy access in Lesotho, the government has set out strategies to introduce penetration of renewables into the national grid. Such initiatives include the Grid Development Plan for 2017-2036 which has allocated M 150 million per annum and 80 % of it is budgeted for the grid expansion and 20 % of it would be allocated for off-grid electrification [21]. Lesotho also targets to achieve 375 MW from renewables by 2030, as drafted in the Lesotho Country Action Agenda [22]. Further, in January 2019, the Government of Lesotho was awarded a grant from the African Development Fund (ADF) towards Consultancy Services for Renewable Energy Grid Integration Study [23]. The objective of this initiative is intended towards analyzing the impacts on the transmission and distribution networks of the LEC when integrating variable renewable energy generation (VREG) and to establish the optimum absorption level, quantitatively and relative to intermittent nature of renewable energy generation in the LEC power system portfolio in the medium to long-term.

Since renewables are intermittent and depend on climate conditions, they can only inject power to the grid only when it is available. On that account, with the available renewables in Lesotho, the study presents a simple methodology to investigate the level of energy security (through generation adequacy analysis) that will be brought by these resources (wind and solar PV) as they will be featured into the national grid. Also, the study intends to assess how power can be dispatched to successfully match the ever increasing and fluctuating power demand considering their dynamic hourly output characteristics and how they can be supported through imports. In the same manner,

with increase in local energy security, this study will determine how LEC can still benefit from importing energy on Day, Week, and Month Ahead Markets offered by the SAPP despite their volatility in prices. This will assist in minimizing tariffs for customers together with operation and generating costs for the supplier while also achieving maximum profits. Hence, the study acts as an informative research document on power system operations and power planning and also, to the policy makers in accelerating the electricity access and security in Lesotho.

1.5 Report Structure

The thesis report is structured into five major chapters. The first chapter discusses the energy situation as well as challenges in Lesotho and background information on how power is dispatched. There is also the problem statement formulated together with the objectives of the thesis. From there, chapter two dwells into the literature review of methodologies or fundamental equations used for predicting wind and solar outputs and how they are given priority of dispatch. Furthermore, detailed overview of methodologies and constraints taken into account when dispatching power are reviewed. The third chapter discusses the methodology adopted for this study, data used and constraints observed. Having developed the methodology, results are obtained and discussed, and conclusions are drawn in the last two chapters of the thesis, respectively.

2. Literature Review/Theory

2.1 Overview of Electric Power System Network Operation

The electric power system is a complex network consisting of power generating facilities, transmission lines, transformers, buses, loads, etc. The simplified diagram of the power system network and how it operates can be represented by Figure 1, which shows the generating stations, transmission and distributions networks [24].

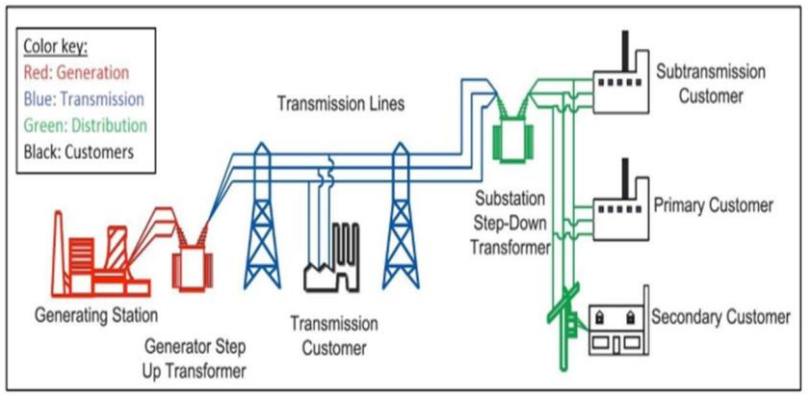

(a) Power grid network Schematic diagram

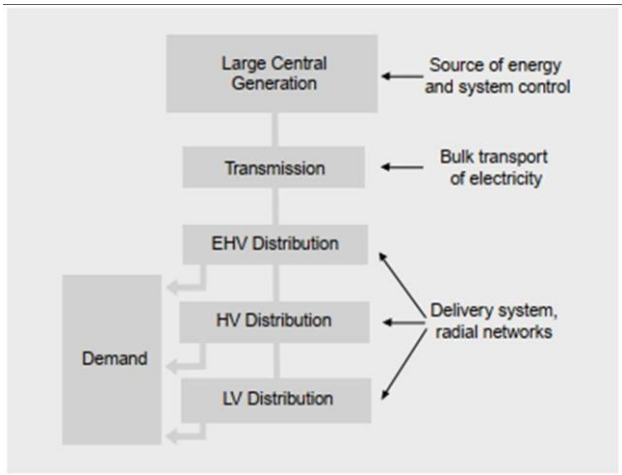

(b) Main Functions of Power system network

Figure 1: Outline of (a) Power System network and (b) its main functions[24]

Generating facilities are responsible for producing power at bulk from raw materials (coal, water, wind, solar, etc.), which is then transmitted using high voltage (HV) transmission lines. Transmission substations inside the generation plants use generation step-up transformers to increase voltage (e.g. from 11 kV to 220 kV) so that power can be transmitted over long distances with minimum losses due to resistance and therefore, allowing power to be carried efficiently over long distances. Apart from that, transmission network also links up adjacent national grids and creates opportunities for interconnections across multiple countries. These interconnections are essential for power trade, which enables sharing of resources in case of system stress, increases socio-economic benefit as well as enhancing security of power supply [24]. The high voltage power from the transmission lines is reduced to lower voltages (e.g. 220 kV to 33 kV) through the step-down transformer at the substation as it will be distributed through short distribution lines or

cables. Distribution transformer steps down the voltage (e.g. from 33 kV to 480 V) in order to distribute electricity to the required load or end users (industries, commercial buildings, household etc.) at low and medium voltages. Subsequently, the medium and low voltage distribution circuits are utilized as an economical way for interconnecting distribution lines with transmission lines.

Operation and planning of the power grid is generally based on reliability, security and delivering power economically [25]. Therefore, transmission and distribution system operators employ

sophisticated monitoring and control systems to safeguard and ensure predictable operations for the power system network. The control centers are on 24 hours alert to accomplish several key functions such as: economically matching electricity production with the varying load, maintaining synchronization of the power network, and sustaining reliability of the grid by bringing online or taking offline key components of the system in response to anticipated or present threats. In addition, these centers utilize Supervisory Control and Data Acquisition Systems (SCADA) and Distributed Control Systems (DCS) to remotely monitor the optimal power flow and control equipment such as switches, circuit breakers, relays, transformers and generators [24]. Hence, maintaining and improving the reliability, flexibility, efficiency and sustainability of the electric power grid.

2.2 Solar Photovoltaic (PV) Power Output

Solar radiation and ambient temperature are the two most influencing parameters on the produced power of PV systems, and their performance is strongly dependent on environmental conditions [26]–[28]. Also, the PV system efficiency varies depending on the different solar cell manufacturing technologies. Hence, solar cell datasheets provided by the manufacturer offer information such as the maximum rated power (□), optimum operating voltage (□) , optimum operating current (□) , open-circuit voltage (□), and the short-circuit current (□). An example of a solar cell (YL250C-30b) data sheet showing these parameters is depicted on Table 1: YL250C-30b solar cell data [27]. These parameters are based on standard test conditions (STC) being with solar irradiation of 1000 □/□ and ambient temperature of 25 ℃. The I-V curves and P-V curves of the YL250C-30b solar cell at constant temperature 25 ℃, and varying solar irradiance are shown in Figure 2. Furthermore, I-V and P-V curves under constant irradiance (1000 □/□) and varying temperature are shown in Figure 3.

Table 1: YL250C-30b solar cell data [27]

Manufacturer	Model	Dimension	Cell material
Yingli solar	YL250C-30b	156 × 156 mm	Mono-crystalline

Electrical characteristics					
Efficiency	P_{max}	V_m	I_m	V_{oc}	I_{sc}
17.5%	250 W	30.96 V	8.07 A	37.92 V	8.62 A

Temperature coefficients of (%/°C)		
P_{max}	V_{oc}	I_{sc}
−0.4	−0.35	+0.06

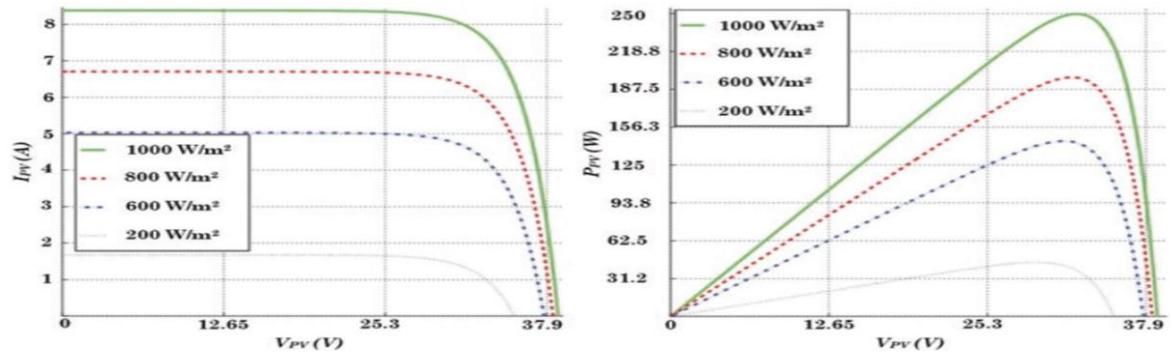

Figure 2:I-V curves and P-V curves of the YL250C-30b solar cell at constant temperature 25 ℃, and varying solar irradiance [27]

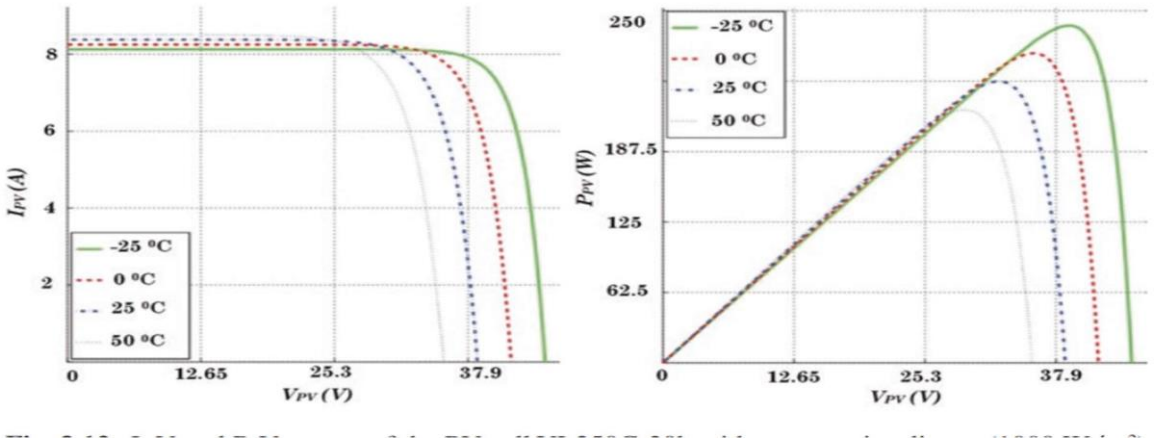

Figure 3: I-V and P-V curves under constant irradiance (1000 W/m^2) and varying temperature [27]

On the contrary, because of the varying solar radiation and ambient temperature, PV systems output varies instantaneously and this output can simply be modelled according to equation (1), where □ is the photoelectric efficiency of the PV system in (%), A (□) is the area of the PV array, □ (1000 □/□) is the incident solar radiation and □ (℃) is the cell operation temperature [27]–[29]. The output power of a solar panel is a function of radiation and ambient temperature, as shown by equation (1). Any solar system's output power appears to be calculable as long as the temperature of the solar radiation panels is precisely forecasted.

□ = □ □ □ [1 − 0.005(□ − 25)] (1)

Another model for PV generator output is presented in [30], which uses the equation (2)

□ = □ □ □ (2)

where □ is the PV generator efficiency and it is given by equation (3). The parameters □ , □ , □ and □ represent the reference module efficiency, power conditioning efficiency (this efficiency is equal to 1 if a perfect maximum power point tracker is used), the generator efficiency temperature coefficient, the reference cell temperature, respectively.

□ = □ □ 1 − □ □ − □ (3)

For these approaches, the cell temperature, □ , is given by equation (4), where □ is the normal cell operating temperature (NOCT), □ , = 20°C is the ambient temperature at NOCT conditions and □ = 800 □/□ is the NOCT solar radiation with respect to wind speed of 1 m/s.

$$T_c = T_a + \left(\frac{NOCT - T_{a,NOCT}}{S_{NOCT}}\right) S \quad (4)$$

2.2.1 Basic Structure of a Grid Connected PV System

Figure 4 illustrates the basic structure of a grid connected PV system. The PV cells, which are the power source, are connected in series or parallel to maximize the benefit of solar radiation. Another important component is the DC/DC converter, which is mostly controlled during the coupling of the Maximum Power Point Tracking (MPPT) control unit. The maximum power point for the functioning of the PV system is provided by an MPPT algorithm, which is achieved utilizing the Perturbation and Observation approach [29], [31]. This system uses the switches as a tracker to conserve energy to the greatest extent possible under all working environmental conditions. A DC/DC boost converter also guarantees that the output voltage is always higher than the grid peak voltage. The DC/AC three-phase bridge inverter circuit on the one hand, is connected to a grid via a typical step-up transformer. Furthermore, a DC/AC converter and a control unit offer an AC voltage that satisfies the grid's connection and synchronization requirements [31], [32].

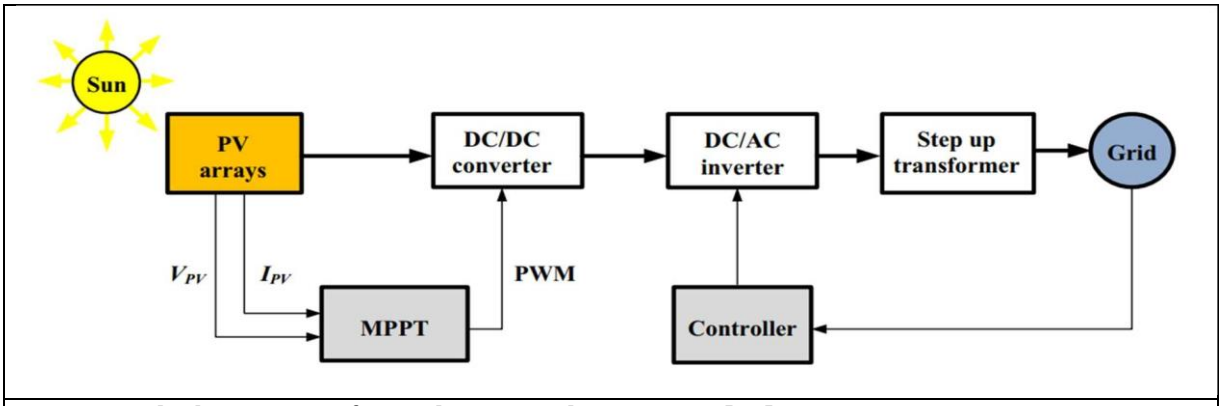

Figure 4: Block Diagram of a Grid connected PV system [32]

2.3 Wind Power Output

Wind turbines transform the kinetic energy of the wind into electrical energy, allowing them to create electricity using the natural power of the wind. The turbine's blades rotate as a result of the wind, generating mechanical energy. In the engine house at the top of the towers, this mechanical energy is transformed into electricity via a generator. Afterwards, the electricity is then distributed to end users or pumped into the grid. This process can be illustrated in Figure 5.

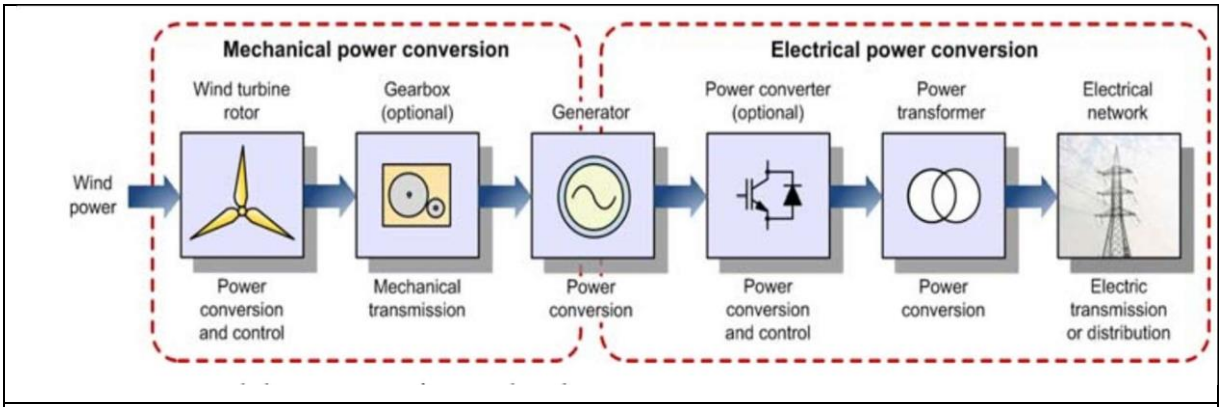

Figure 5: General description of wind energy conversion[33]

For a wind turbine with rotor blades of swept area A (□), exposed to wind (stream of air) with average wind speed □ (□/□) and density □ (□□/□), then the wind power can be expressed using equation (5) while the power captured by the blades can be expressed using equation (6) [33], [34].

$$□ \quad = \frac{1}{2} □ □ □ \qquad (5)$$

$$P_{wind} = \frac{1}{2} \rho A v^3 C_p(\lambda, \beta) \quad (6)$$

The term $C_p(\lambda, \beta)$ is called the power coefficient or coefficient of performance and it is a nonlinear function of the blade pitch angle β and tip-speed ratio λ. Lanchester and Betz proved that wind turbine can only convert a maximum of 59.26% of the wind kinetic energy to mechanical energy [34]. So $C_p = 0.5926$ is the rotor power coefficient known as the Lanchester- Betz limit.

The power delivered by the wind turbine can be represented by equation (7) [35] where v represent the wind speed at time t, P_r is the rated wind power output and P is the hourly power output, v is the turbine cut in speed, v is the turbine cut out speed and v is the turbine rated speed. The quantity $P(v)$ is the power output of the wind turbine when operating at the speed between the rated and the cut in speed.

$$P = P(v) = \begin{cases} 0, & v < v_{ci} \text{ or } v > v_{co} \\ P(v), & v_{ci} \le v \le v_r \\ P_r, & v_r \le v \le v_{co} \end{cases} \quad (7)$$

It can be estimated using various parametric functions formed from polynomial expressions [36]. These parametric models can be linear [37], quadratic [30], binomial [38], cubic [39], Weibull based [40] etc. Essentially, the quadratic model is good for simulating the power curve of a pitchcontrolled wind turbine, but not so much for stall-controlled or fixed blades, yaw-controlled wind turbines with a variable power range [41]. Nonetheless, because the machine's behavior is qualitatively similar, although with lesser accuracy, the model will be applied to these circumstances as well: this means that power outputs greater than P_r should be ignored, and a lower energy output should be considered [41]. All These models are explicitly discussed in [35].

These parametric models are used to model the wind turbine power output curve for all region 1, 2, 3 and 4 as shown in Figure 6. When the wind speed falls below a certain minimum, known as the cut-in speed, the power production is zero in region 1. There is a rapid increase in power produced in region 2 between the cut-in and the rated speed. However, in the third region the wind turbine produces a constant output (rated) until the cut-off speed is reached. The turbine is turned off above this speed (region 4) to safeguard its components from severe winds, that is why it produces no electricity in this region.

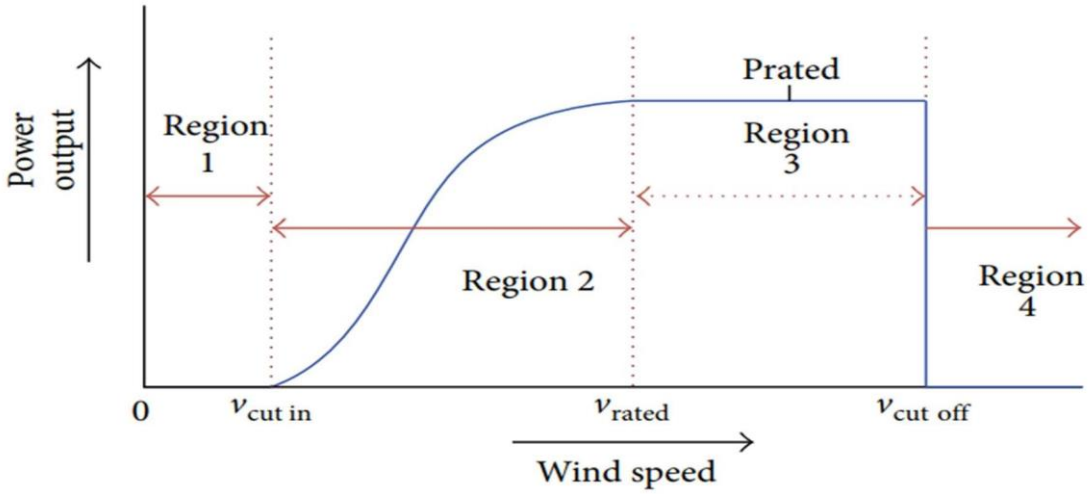

Figure 6: Typical pitch controlled wind turbine power output curve [35].

2.3.1 Extrapolation of Wind Speed

The World Meteorological Organization (WMO) recommends that data be logged at meteorological stations 10 meters above ground level (a.g.l), because the height of the turbine's rotor affects energy estimations [42]. The wind speed increases as the height above ground level rises, resulting in an increase in turbine output power. Turbines are built higher to capture more wind and to be higher than barriers (hills, buildings, tall trees, operational turbines, and so on) and ground roughness (mostly plants and vegetation) [43],[44]. Therefore the data collected at any height can be extrapolated to other heights of the turbine hub. The accuracy of converting observed wind speed to wind speed at hub height and at the turbine location is determined by parameters such as the vertical wind profile at the site, mast position relative to the turbine, and extrapolation method [35].

The extrapolation of wind speed is primarily done in two ways. The first method is based on the basis of the roughness height (□) of the terrain and finds the wind speed at the height (□) with the known wind speed □(□) at height □ as shown by equation (8) [45], [46].

$$□(□) = □(□) \_\_\_\_\_ \quad (8)$$

The second method predicts the wind speeds □(□) at any given height □ considering the reference wind speed □(□) at a reference height □ , using equation (9), where m represents the shear coefficient which is a number between 0 and 1 [45].

□(□) = □(□)(□ □⁄) (9)

2.4 Integration of Intermittent Solar and Wind Under Specified Grid Code and Priority of Dispatch

The actual flow of electric power from the power plant to the customers is controlled by power system operators. Above all, the reliability and security of the electricity grid are the main concerns of system operators. Regarding the widespread adoption of intermittent renewables (solar PV and wind farms), system operators are usually worried by the impacts of these renewables to stability and security of the grid. For this reason, to stimulate the injection of renewable electricity into the grid, open and non-discriminatory access is essential to assist renewable energy deployment. In most nations throughout the world, this is normally made compulsory by legislation (sometimes referred to as "obligation to take") [47]. Since, renewable energy costs have decreased [48] and grid operators have become less concerned about integrating renewables into the system, there is a growing consensus that renewables should be dispatched first due to their near-zero variable costs [47]. Alternatively, to minimize future synchronization and system balance concerns, technical standards for grid connection should be conveyed explicitly and openly to generators and enforced by system operators.

Moreover, the inherent resource constraints of renewable energy resources in terms of their usefulness under various atmospheric, environmental, and climatic circumstances limit their integration [49]. Again, their integration depends on the ease with which power can be transferred from the generator to the grid. Grid integration as well necessitates in-depth technical analysis to ensure proper grid operation stability and control (for example, through frequency stability, voltage magnitudes and stability, power balance, and congestion management), flexibility, and reliability in the presence of a significant share of wind and solar [49]. Essentially, grid codes are sets of technical analysis conditions which a power plant must meet in order to be connected (and sell energy) to the grid, as imposed by the power system operators. More detailed studies for grid codes are provided in studies such as [50], which outlined grid code requirements for integration of renewables in Spain. Another study by Sourkounis and Tourou [51], examined the grid requirements for wind generators in Europe. Furthermore, a study by Mokeke and Thamae[1] investigated the impacts of integrating

intermittent renewable energies into the Lesotho's national grid under the specified grid code requirements.

Accordingly, the grid codes are given to independent power producers (IPPs). These IPPs are privately developed, built, operated, and owned power plants that generate electricity and sell it to utilities, end users, or wholesale power traders [52]. They have a significant amount of private capital and are legally obligated to generate and sell power to a utility or other off-taker under long-term Power Purchase Agreements (PPAs). The PPA contract clearly defines the terms for buying and selling of power between the generating plant and off-taker. To this effect, it outlines the terms of power sale including the date the project will commence, the power delivery schedule, billing and payments terms, including termination terms [52].

European countries such as Germany and Denmark are admired for their well-structured Renewable Energy Acts and Policies which promote uptake and prioritize dispatch for renewable energies as they are usually accompanied by feed-in tariff schemes [53]. Significantly, the feed-in tariff system (minimum price standard) requires distribution network operators (DNO) to interconnect RES power plants and pay the plant operator a predetermined payment per kWh. In this case, the degree of remuneration is cost-based, with technology, plant capacity, and other factors influencing it. This remuneration is fixed for a set length of time (for example, 20 years), giving investors some assurance in terms of budgeting and recouping costs [54]. Also, other states in Latin America and Caribbean regions still offer priority of dispatch to renewables, guaranteed purchase and interconnection from IPPs as well as priority of interconnection for renewable power producers [55]. When power grid operators enter into interconnection agreements with renewable energy projects, these policies compel them to offer grid-connection services and related technical assistance, as well as to purchase and dispatch the total quantity of electricity generated by the projects. The priority of dispatch ensures that renewable energy generators are dispatched first ahead of non-renewable generators [55]. Guaranteed and priority interconnection reduces development risk by lowering the uncertainty surrounding project completion timeframes. Also, guaranteed purchase rules reduce the possibility of a project's failure to achieve a PPA. Revenue fluctuation and overall project risk are minimized by rules that ensure no curtailment or provide financial compensation for curtailment. Without a doubt, priority of dispatch lowers the chances of a generator being unable to secure transmission capacity [54] ,[[55].

2.5 Power Procurement in Electricity Markets and Economic Aspects of Electrical System Network

The main objective of economic operation of the power system network is to generate sufficient electrical energy at best-suited stations and then distribute it to consumers or end-users at an economic price while maintaining quality and reliability. Due to the diversified nature and activities of end-users (e.g. households, industries, agriculture, etc.), the load demand varies from instant to instant as shown in Figure 7, [56]. Because of this, generation of power must always be controlled to efficiently meet the base load, peak load as well as the varying load economically with minimum interruptions [25], [56].In essence, the base load refers to the unvarying minimum load a power system must always deliver at any point in time, whereas the peak load generally means the various peak demands of the load above the base load.

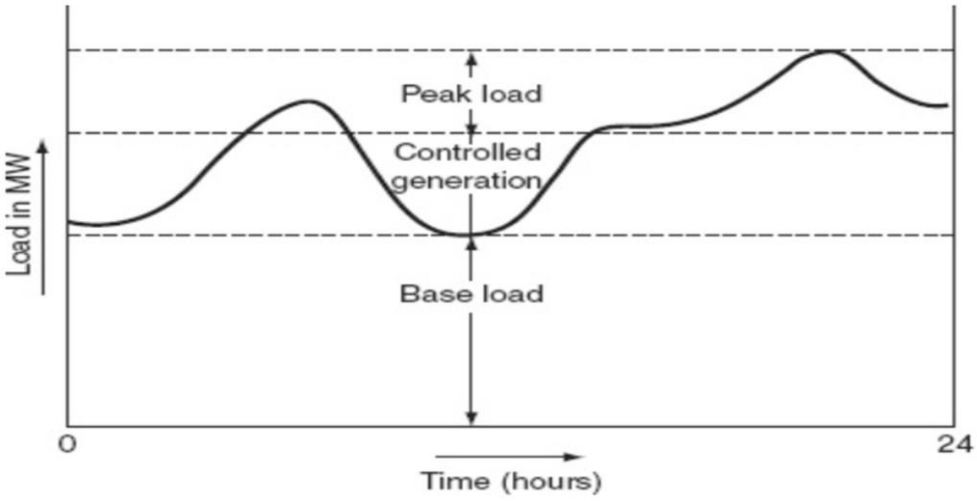

Figure 7: Daily variation of power demand [56]

The efficient and optimum economic operation of power systems plays an integral role in deciding the electricity price in both regulated and deregulated markets [25], [57]. Regulated electricity markets refer to utilities having complete control over operating, generating and transmission facilities, and sells electricity directly to consumers. And yet, in regulated states, utilities must set prices according to the public utility commissions. On the other hand, deregulated electricity markets, give way to competitors to purchase or procure and sell electricity by allowing all market participants to invest in generating facilities and transmission lines. Since an interconnected power

system network can provide national link between all markets participants, including generation and demand, it is possible to provide an optimal generation portfolio available thereby achieving cheapest possible generation [24], [25], [57]. Most importantly, in electricity markets, all participants have a great opportunity to opt for trade with the most competitive participant.

2.6 General Optimization and Economic Load Dispatch (ELD)

2.6.1 Optimization Description

The term "optimization" simply refers to the process of making the best or most efficient use of a situation or resource. Different fields study optimization problems, and various steps need to be taken to arrive at an optimal solution. Normally, engineering professionals are typically asked to design and operate systems that exceed specified goals while meeting numerous design and operational constraints. The process of optimization is sought to find such designs and operating modes. It specifies the activities or items that must be implemented in order to get optimal results. As a primary objective, optimization seeks to determine the maximum or minimum value of variables specified in a feasible range or space [25], [58]. It is important to recognize the problem parameters, which can either be continuous or discrete. To solve a problem, the objective function and the constraints must be known. In the end, it is necessary to choose and employ an optimizer that will solve the problem efficiently with satisfactory results.

2.6.2 Economic Load Dispatch Problem Description

Economic Load Dispatch (ELD) is an important optimization procedure applied in the operation and planning of the power system network. The aim of ELD is to optimally assign all the committed generating units to meet the varying load demand at minimum operation and generating costs while satisfying all the specified operational constraints [59] [25], [60]. Since the fundamental economic dispatch problem depends upon the generating unit cost function, then it is necessary to first understand the relationship between cost and power output of the generating units. Although the generation cost of energy (in MWh) varies widely due to the nature of unit technology, the cost and power relationship can be summarized using generator economic curves: Input-output curve and Incremental cost curve [25], [57]. Error! Reference source not found.(a) illustrates a typical input-output curve for a generating unit. The curve can be extrapolated from field data considering

variation of fuel consumption and power output that is within the operating limits (minimum and maximum power in MW). For majority of generators, generation costs constitute to fuel costs. However, other components of generation costs include operations and maintenances (O&M) as well as emission costs. Hence, the fuel or generation costs of a generating

unit can be represented by a continuous and monotonically increasing quadratic polynomial function shown in equation (10) as follows:

$$\square(\square) = \square + \square\square + \square\square \quad (10)$$

where $\square(\square)$ $\square\square$ ($/h) is the operating or generating cost for the $\square$ generator with output-power $\square$ $\square\square$ ($\square\square$) and $\square$, $\square$ $\square\square\square$ $\square$ are the coefficients which can be obtained from unit design data. The power output of each generator should be limited within the inequality constraint:

$$\square \leq \square \leq \square \quad (11)$$

where $\square$ and $\square$ are minimum and maximum power limit for each generator, respectively [25].

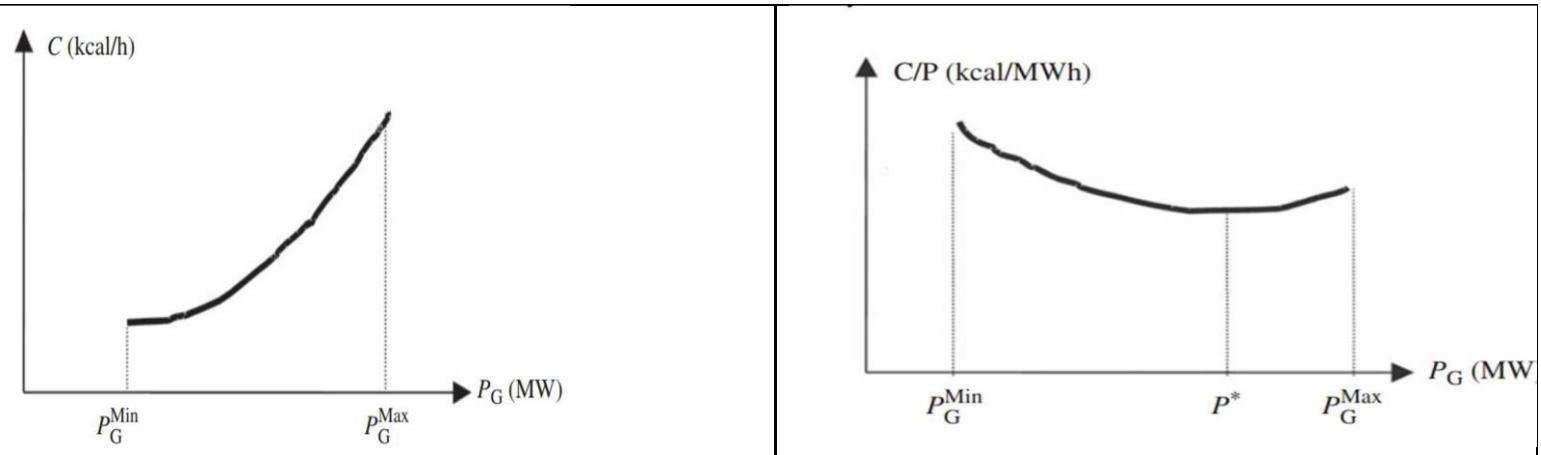

(a) Input-output curve of a typical generating unit

(b) Incremental Cost Curve

Figure 8: Generator economic curves [25]

Incremental cost curve, shown in Error! Reference source not found. is obtained from taking the derivative of the cost function, $\square(\square)$ with respect to power output of each generator, $\square$, as shown in equation (12) [56]. This curve represents the marginal costs of each unit, which is the cost of

generating one more power from that unit. Hence, it indicates the increase in cost rate per increase in one megawatt output.

$$\frac{\square\ \square\ (\square\ )}{\square\ \square} = \square + 2\square\ \square \quad (12)$$

The classic ELD problem assumes that a given collection of units will generate constant power for a specified time interval and that the cost of supplying this energy will be minimized subject to limits on the static behavior of the generating units [61]. The objective function minimizes the total generation costs or operational costs for the active power of each committed unit subject to power equality and inequality constraints [59], [61]. Equality constraint generally outlines that: total power generated from all units should be equal to the sum of power demand and the transmission losses. While inequality constraint states that: power output of each generating unit must be greater or equal to the minimum power permitted and should be less or equal to the maximum power permitted. Hence, this constraint ensures that the generated power from each unit is within the specified limits. Additional system constraints specifying the minimum or proper amount of reserve capacity required are often added to this basic problem. This basic problem can be referred to as the static ELD (SELD) problem which only optimizes the total operating costs or fuel costs in general in a specified time without considering the fundamental relation of systems and variation of load demand in different operating times [61]. Because of the wide range of customer load demand and the dynamic nature of power networks, it was necessary to look into a more practical means of optimally dispatching generated electricity that can meet the ever varying load in instant of time.

In practice, ELD problems are also called dynamic ELD problems, a continuation of the basic ELD problem. The main feature of practical ELD is the ability to match the ever changing load demand with a controlled generation. In practical ELD, the generation schedules for the committed units are designed to meet the predicted load demand over a time horizon at the lowest operating cost while taking into account more practical constraints such as generator ramp rate limits, prohibited operating zones (POZ), and in some cases, multiple fuel options for certain generators [62] [61] [63]. The ramp rate limitation is a dynamic requirement that is critical for the generators' longevity as it monitors operations and generation of online units to be within specified range. Because of the physical limitations of power plant components, a thermal or hydro power plant may have prohibited operating zones (e.g. vibrations in shaft bearings are amplified in certain operating regions). If there

is a prohibited zone, the unit is only permitted to operate above or below that zone and hence, results in disjoint convex regions [64]. A typical cost function which considers the POZs is shown in Error! Reference source not found.. Considering all these practical constraints, the resulting ELD problem becomes a non-smooth or non-convex and highly complex

optimization problem that requires well defined mathematical formulations and robust algorithms to solve.

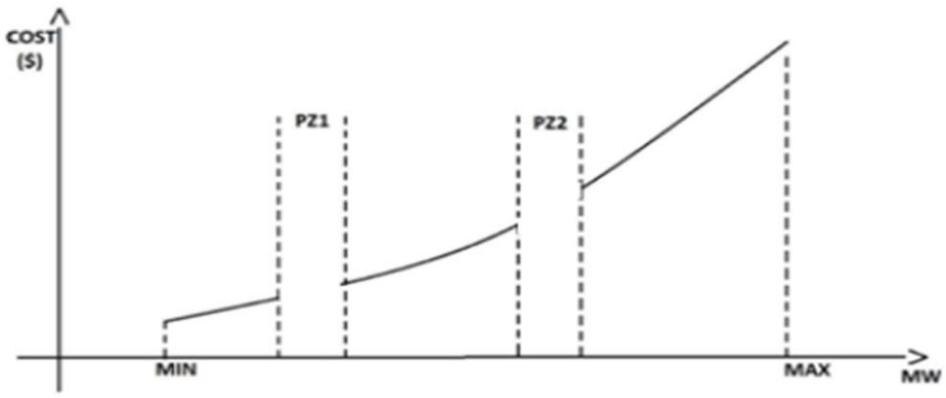

Figure 9: Cost function considering POZs [65]

2.7 Overview of Methods for ELD Incorporating Renewables

Integration of large-scale renewables (wind and solar) generators to the power network system suggests that a new source of uncertainty must be added to the operation and planning problem, making it more complex. Due to increasing penetration levels of renewables, it can be anticipated that the ELD problem can be approached by dispatching within smaller intervals so as to update all the operating set points while observing the updated forecasts [66]. On top of that, the challenge of finding the global optimal solution, minimizing the time to solve the problem makes it more challenging. Furthermore, for large scale and highly non-convex systems, the repeated failure of obtaining the global optimal solution of the non-convex ELD can result in significant monetary losses [66]. Numerous attempts have been made to solve the ELD problem through mathematical programming and optimization techniques, incorporating different kinds of constraints or multiple objectives. These approaches can generally be divided into two groups: Deterministic and Heuristic techniques [67], [68].

With advancements and review of these methodologies, another set of techniques were defined, which were referred to as hybrid methods as they emanate from a combination of either one of the groups or both. All the approaches have been very much useful in finding a balance between the

generation supply and the customer electricity consumption. Even so, each of its kind has some minor drawbacks or limited ability to effectively find the required optimal solution depending on the nature of objective function as well as operational constraints introduced.

2.7.1 Overview of Deterministic Methods

Deterministic global optimization (DGO) comprises numerical optimization methods that seek to find the best solution within a pre-defined tolerance from the global optimum [69]. In deterministic optimization problems, the objective function or feasible domain may have discrete or continuous variables with convexity as their characteristic feature [70]. In theory, DGO provides the theoretical guarantee that the solution returned is within the tolerance of the global optimum, or that the problem is not feasible. In addition, optimality gaps, also known as the difference between the bounds on the objective value, converge when it falls within the predefined tolerance [69], [70]. Because these optimization methods do not require stochastic rules to guide exploration of the search space, they are deterministic in nature. The search can instead be guided to convergence in a finite number of iterations by a sequence of deterministic bounding operations. A couple of examples for the deterministic approaches used for ELD problems are: Lambda (λ) iteration method [71] and Branch and Bound (B&B) technique [72].

In order to apply the -iteration method to an ELD problem, each generator's output power must be mapped to a value of marginal costs or . Generators collectively generate a total output of power for any common marginal cost. Then initially beginning with − values set below and above the optimal value (corresponding to too little and too much power output), the optimal value is bracketed iteratively [73]. The standard −method solves the non-convex ELD problem by iteratively solving the approximated convex problem when applied to a practical non-convex ELD situation. However, there are two significant disadvantages: 1) In large-scale mixed-generation systems, the method exhibits oscillating behavior, and 2) the method has limited ability to deal with the discontinuities created by prohibited operation zones [74]. As compared with the conventional −iteration method, the Distributed Augmented −iteration method proposed in [74] has the advantage of giving the

optimal dispatch in the presence of prohibited operating zones and effectively avoid the oscillatory behavior that the conventional −iteration method often exhibits. Moreover, the fast λ − Iteration Method is proposed in [75] to solve the non-convex ELD problem with consideration of prohibited operating zones and ramp rate limits for generating units. Nevertheless, the introduced method has limited ability to deal with generating units consisting of multiple fuel cost functions.

The B&B method enumerates all possible solutions to a problem by storing partial solutions referred to as sub-problems in a tree structure. Nodes in the tree that have not been explored are partitioned into smaller regions that can be solved recursively (i.e. branching), and pruning off regions of the search space that are demonstrably suboptimal (i.e. bounding) [76]. Following the exploration of the tree to its fullest extent, the best solution in the search is found. The study by Alowade et al [77] attempts to formulate the non-convex ELD problem as a rank-relaxed semidefinite programming problem, which is solved by B&B technique combined with convex iteration. A Bi-Level B&B method [78], which combines spatial and simple B&B techniques, is used for economic dispatch with disjoint prohibited zones considering network losses. A spatial B&B algorithm is used to solve the quadratically constrained quadratic programming (QCQP) problem at the higher level and a simple B&B algorithm to solve mixed-integer quadratic programming (MIQP) at the lower level. For this approach, the global solution is obtained within some predefined convergence tolerance. One of the greatest advantages of B&B methods is the ability to arrive at global optimal solution. However, applications of B&B techniques are limited to small sized systems with minimum constraints as addition of more grid constraints and generation sources, can increase computational time exponentially [79].

It has been stated that B&B and Lambda Iteration methods are just examples of deterministic techniques that have been used in past years to solve the ELD problem, other examples for deterministic techniques include: Lagrangian relaxation and linear, non-linear, and dynamic programming [80]. In summary, all these deterministic approaches have proven to be very effective and have given satisfactory results with strict proof of convergence and require very few, if any, problem-based parameters. There is, however, a requirement with these methodologies: the problem or objective function should satisfy certain mathematical requirements: complex calculusbased gradients should be deduced, or formulations may be approximated through linearity and/or convexity [80]. Convexification of the non-convex parts is essential in understanding the convexity

of the objective function or feasible domain. If the formulated problem is convex, effective numerical methods can be used to solve the optimization problem. In practice, nonetheless, many optimization problems for ELD involve non-convex functions due to multiple constraints considered, that require to be analyzed by robust and efficient methodologies to guarantee global optimality. Deterministic methods may not yield an optimal solution to non-convex or large-scale optimization problems within reasonable time because of the complexity of the problem. Hence, limiting their extensive applications in real or practical ELD problem. These kind of limitations or drawbacks viewed in deterministic methods have motivated the implementation of heuristic approaches for the ELD problem. Consequently, in the electric power business, traditional deterministic decision making is increasingly giving way to stochastic decision making, which explicitly accounts for the unpredictability in the power output of renewable energy generators [81].

2.7.2 Overview of Heuristic Techniques

The heuristics share the common characteristic of combining rules with randomness in order to mimic natural phenomena [62]. They are based on single-solution update and the population-based search [82]. In single-solution update, a number of successive iterations and calculations are performed and each time updating the solution only if the new one satisfies a predefined criterion. In contrast, the population-based search deals collectively with a set of solutions rather than a single solution. The intelligent heuristic methods have been introduced recently to solve problems in power systems networks such as network planning, distribution fault tracking, ELD [67], etc. Furthermore, such methods include: stimulated annealing (SA) [83], genetic algorithm (GA), evolutionary programming (EP) and particle swarm optimization (PSO), differential evolution (DE) [8], [67], [84]–[86] etc.

The GA is an example of population-based algorithm, where every solution corresponds to a chromosome and each parameter represents a gene. This method is a stochastic global search that replicates natural biological evolution metaphors like selection, crossover, and mutation [87]. GA evaluates the fitness of each individual in the population using a fitness (objective) function. The reliability of this approach stems from its capacity to estimate the global optimum for a particular problem by using the best solutions in each generation to enhance other solutions, so improving the entire population generation by generation [88]. This algorithm has been widely used in power system optimization problems, including the economic dispatch problem, for example

methodologies included in [89] and [90]. In [89] the GA was employed to solve economic dispatch problem incorporating thermal generators and wind farms. For this approach, the non-linear and quadratic cost functions of thermal units were considered while the stochastic nature and wind variability was modelled using the Weibull distribution function. A case study of Abu Dhabi presented in [90] formulated the economic dispatch model to optimize the thermal plants and solar generators. The approach delves into the usage of GA to minimize the operation costs of power production and serve the purpose of integrating renewable energy into the traditional power grid of United Arab Emirates.

Additionally, the PSO algorithm is a population-based optimization method that uses an array of particles in order to find the optimum solution [59]. Swarms are composed of particles, each of which is an individual. Solution spaces are formulated in PSO as search spaces where each position in the search space is a potential solution of the problem. In the search space (solution space), particles cooperate to find the best solution, with each particle moving in accordance to its velocity. Its implementation in power systems has yielded promising results for ELD optimization problems. The paper [91], establishes a practical or dynamic economic dispatch model to implement the minimization of the total generation cost of wind-hydro hybrid power systems. A probabilistic mathematical model of the wind farm output with regards to wake effect is presented here as the wind generation cost model. By employing a penalty function method and correction strategy, the proposed economic dispatch model is converted to an unconstrained optimization problem, which is then solved by the PSO algorithm with immunity (IA-PSO).

The study, [92], presents a short-term optimal hourly of hydro–wind–thermal hybrid scheduling based on PSO approach. The suggested model reduces the hybrid power system's generating costs to meet load needs over a predetermined time horizon while satisfying the network's different constraints on hydraulic, wind, and thermal electrical systems. In [93], an enhanced PSO strategy is proposed in an attempt to reduce fuel costs, as well as startup and start down costs, under the constraints of prohibited operating zones, hydro and thermal generation limits, and the water flow equation. In the original PSO, a concept of "Craziness function" was incorporated to give diversity, ergodicity, and stochastic behavior in the algorithm, improving its efficiency and limiting premature convergence. Another modified PSO algorithm is introduced in the research [94], for optimal power sharing among wind, solar, and combined heat and power plants inside a microgrid context. In this method, the probabilistic stochastic programming model is used to model the load uncertainty and

random nature of demand in addition to minimizing the overall costs of the power schedule. PSO is one of the algorithms that has been utilized in the past since it is simple to construct and has less parameters to establish.

Other heuristic approaches employed to solve the ELD problem in power systems include: SA [95] for wind-thermal power system and also chaotic fast convergence EP (CFCEP) utilized in [96] for solar–wind–thermal energy and hydroelectric energy storage. The heuristic techniques are considered stronger, efficient and more effective as largely compared with deterministic techniques, since they are capable of dealing with problems where non-differentiable objective functions and many nonlinear constraints as well as large-scale systems are taken into consideration. Furthermore, they are seen to more suitable than deterministic methods in handling non-convex problems, which are more practical problems. However they still also experience drawbacks as they are very sensitive to parameters and they can only guarantee a global optimal solution with a certain probability in a given feasible region [70]. GA may not provide an optimal global solution, but only a reasonable one due to a premature convergence [65]. Moreover, GA has significant flaws that result in longer calculation times and less guaranteed convergence, especially when dealing with an epistatic objective function with highly correlated parameters [62]. To make the annealing schedule precise, SA requires multiple runs, which would substantially reduce the algorithm's computation efficiency [65]. Furthermore, the premature convergence of PSO and EP may trap the algorithm into the local optimum, which may reduce its optimization ability [97].

2.7.3 Overview of Hybrid Techniques

Several advancements have occurred in combining flexible and soft computations with optimization techniques to solve the non-convex ELD problem. Hybridization can be seen as a method of improving one method and minimizing its shortcomings by incorporating the strengths of another method. For example, in [98], the paper introduces a novel heuristic technique for leading infeasible solutions to the feasible space using self-adaptive DE and a real-coded GA for resolving the dispatch problem. To improve its performance, the proposed method also implements constraint-handling mechanisms, dynamic relaxation of equality constraints, and diversity mechanisms. Furthermore, in [99] a combination of evolutionary programming (EP), PSO and sequential quadratic programming (SQP), is presented. Also in [100], a PSO-SQP is proposed to solve the non-convex ELD problem.

These combined techniques employ the local search property of SQP in fine tuning the solution and hence, guaranteeing the optimum solution.

2.8 Power System Reliability Assessment Through Generation Adequacy Analysis

The two essential aspects of power system reliability assessment are system security and system adequacy [13], [14]. The ability of a system to respond to dynamic or transient disturbances within the system is referred to as security. As a result, security is linked to the system's reaction to any disturbances it may encounter. These include the effects of both local and regional disturbances, as well as the sudden loss of key generation or transmission facilities, all of which can cause the system to become dynamic, transient, or voltage unstable [12], [14]. Adequacy refers to whether or not the system has enough facilities to meet the consumer load demand or the system's operating constraints. These include the facilities needed to generate enough energy, as well as the transmission and distribution infrastructure needed to get the energy to the actual consumer load locations. As a consequence, adequacy is linked to static conditions that exclude system dynamics and transient disruptions [14]. Prior to the 1990s, the majority of reliability studies relied on analytical approaches [101]. The size of the system state space influenced the computational complexity of these approaches significantly [102]. Later, approaches based on Monte Carlo simulation were favored for simulation of power systems with a large number of different operating states, because their computing complexity is independent of the size of the system state space [14], [102].

The ability to determine generation adequacy in an electrical system is an important tool for determining supply security [103]. It refers to the generator's ability to meet system demand while simultaneously taking into account common system restrictions such generation unavailability, load volatility, and REGs output variation [12], [13]. There are many possible indices which can be used to measure the adequacy of a power system for countries or utilities. However, Loss of load expectation (LOLE) and loss of energy expectation (LOEE), form the basic indices which are used to measure generating system adequacy, and they can be estimated using a variety of methods [12], [14], [15]. The mathematical expressions of these indices can be explained by equations:

a) Loss of load probability (LOLP) in days/year or hours/year:

The loss of load probability (LOLP) or loss of load expectation (LOLE) is the average number of days or hours over a specific time period (typically a year) that the daily peak load or hourly demand is predicted to surpass the available producing capacity. This indicator can be represented by equation (13) as shown below [14], [104], where □ is defined as the probability of system state s and S is the set of all system states associated with loss of load. It should be noted that, when LOLP is in days/year, □ then depends on a comparison between the daily peak load and the available generating capacity and when in hours/year, it depends on a comparison between the hourly load and the available generating capacity. Although, LOLP index does not reveal the severity of the insufficiency, nor does it provide the frequency or duration of load loss, it is the most extensively employed probabilistic criterion in capacity planning research.

$$\square\square\square\square = \sum_{s \in S} \square \quad (13)$$

b) Expected demand not supplied (EDNS) in MWh/year:

The predicted energy not provided by the generating system due to the load demand exceeding the available generating capacity is measured by the expected demand not supplied (EDNS) index or loss of energy expectation (LOEE). The EDNS considers the degree of deficiencies as well as the number of occurrences and their duration, allowing for an assessment of the impact of energy shortages as well as their likelihood. The representation of EDNS can be represented by equation (14), where □ is the loss of load for system state, s. This index is used in most studies to mainly assess the impact of replacement of conventional systems with renewable energies [14], [104].

$$\square\square\square\square = \sum_{\square \in \square} 8760 \square_{\square} \square_{\square} \quad (14)$$

Other indices such as Loss of load frequency (LOLF) and Loss of load duration (LOLD) are the basic extension of the LOLP index, identifying the expected frequency of meeting a deficit as well as the expected duration of the inadequacies [14], [15]. They have extra physical properties that make them more sensitive to additional generation system parameters and give power system

planners more information. Other indices that can still be considered include Probability of Load Curtailment (PLC) [105] and Expected Bulk Power Interruption Index (BPII) [14].

As more renewable generation has been considered in power systems, various reliability studies have assessed the impacts of renewables using reliability indices. For example, Vallee et al.,[106] used the Weibull probability distribution to examine the influence of wind power integration on power system reliability. The study in [15] provides a generation adequacy evaluation that includes wind energy conversion systems (WECS) at different locations as an example of a modeling technique that captures this. Hourly wind speeds are simulated using an autoregressive moving average time series model, and sequential Monte Carlo simulation is employed to make time series modeling of wind speeds easier. Furthermore, authors in [15] investigate the impact of wind speed correlation on system reliability indices and finds that the degree of wind speed correlation between two wind farms has a significant impact on the reliability indices that arise. The research in [107] presents a probabilistic analytical approach for evaluating the reliability of power systems with high penetration of wind and solar PV renewable power generation. The loss of load approach, which is one of the most successful probabilistic analytical methods, is used in this article. In accordance with Power Development Plan 7 (PDP7), the study provided in [108] evaluated generation adequacy for the Vietnamese power system while considering renewable energy integration. The Loss of Load Expectation (LOLE, expressed in hours) index was used to assess the generation's effectiveness.

2.9 Contributions of the Study

The power dispatching problem from the above methodologies is formulated mainly on reducing conventional generators (e.g. coal and thermal) in order to accommodate renewable energy sources like solar and wind. Also, the analysis of generation adequacy for power systems network is primarily based upon introducing wind and solar sources to the network in order to eradicate these conventional systems. However, power generation in developing countries like Lesotho, is primarily based on hydroelectricity, as there are no conventional energy sources or generators, which is still insufficient to supply the country's ever-increasing and fluctuating demand. In consequence, solar PV and wind energy power plants have emerged as viable alternatives to supplement hydropower. Motivations behind increasing solar PV and wind generations lie behind SDGs, falling prices of high capacity renewable plants, inviting IPPs for investments, fight against global warming as well as increasing local energy security. Another option is to purchase power from other neighboring

nations in order to improve energy security in developing and non-energysufficient countries. However, prices from imports (e.g. Eskom and EDM) come with wheeling charges and in some cases are subject to fluctuating prices and dollar exchange rate risks. Both of these possibilities still require further investigation to identify the best method for electrical utilities to determine the best way to procure power from local IREGs, operating under priority of dispatch, by weighing the viability of existing renewables as compared to imports.

Since solar and wind are intermittent, they cannot guarantee security of supply at all times. Therefore, planning for reliable power supply and procurement requires the need to evaluate the adequacy of locally committed wind, solar and hydro generators for security of supply. Since, the LOLP and EDNS indices of generation adequacy analysis are predicted for the overall period of the year in mostly presented methodologies considering uptake of wind or solar PV in order to reduce conventional systems, this study attempts to determine these indices on monthly basis, depending of the dynamic characteristics of wind farms, solar PV output and 'Muela hydro generators to reduce the consumption of imports. In addition, the study goes further to conduct a sensitivity analysis of these indices when taking cases: 1) 'Muela hydro generators alone, 2) 'Muela hydro generators plus solar PV, 3) 'Muela hydro generators plus wind farms and 4) 'Muela hydro generators, wind farms and solar PV combined. Using these indices as well as considering their time series output characteristics of local generators, the study attempts to find possible ways of power procurement from imports offered by SAPP markets. The proposed approach uses LEC network as the case study and handles all the above-mentioned constraints in a manner that can suit other developing countries that are in a similar or closely-related energy deficit situation.

3. Methodology

3.1 Overview

The addition of solar PV and wind farms brings a new dimension of uncertainty and complexity to the LEC power network's economic operation and planning. In dispatching power to satisfy demand, the major discussion centers on the decision between electricity pricing from imports and/or local renewables. In this study, all generating facilities in Lesotho are owned by the independent power producers (IPPs). Therefore, LEC buys power from these IPPs by paying a wholesale price tariff that would be agreed upon by LEC and the IPP, through PPAs. The cost of electricity (which is different for each IPP) must be proportional to the amount of power that is injected to the grid to meet the load at each time interval. For LEC, the aim is to achieve the most cost-effective energy mix in the grid that helps minimize costs of electricity and at the same time maximizes the reliability without violating the grid security constraints or transmission line limits, while considering variable and intermittent generation of solar and wind. So this means that, the power plants must be integrated to the grid in accordance with the grid code of LEC.

The major assumptions are:

1. The integrated plants are in accordance with the grid code and will not compromise the grid stability.
2. All renewable energy generators (REGs) in Lesotho are owned by IPPs and LEC buys power from them.
3. All power from REGs must be consumed first and imports must be suppressed to allow preference for REGs.
4. An hourly period schedule of power is considered.
5. The generation of wind and solar energy is non-schedulable. As a result, LEC will accommodate whatever generation is available from these sources at all times.
6. Surplus power from all the local energy and/or renewables will be assumed exported or unused.

The methodology flow chart for this study is illustrated by in Figure 10. Using respective sites' climate conditions, hourly radiation and wind speeds, hourly solar and wind power will be predicted for the whole year under study. From there, the hourly generating characteristics or output of

'Muela hydro generators and the yearly load demand together with the output of solar and wind, will be configured to the LEC network model in DigSILENT. Upon completion of dispatching all local generators, their generation adequacy and imports needed, the final stage is to assess the cost implications of different power dispatching scenarios.

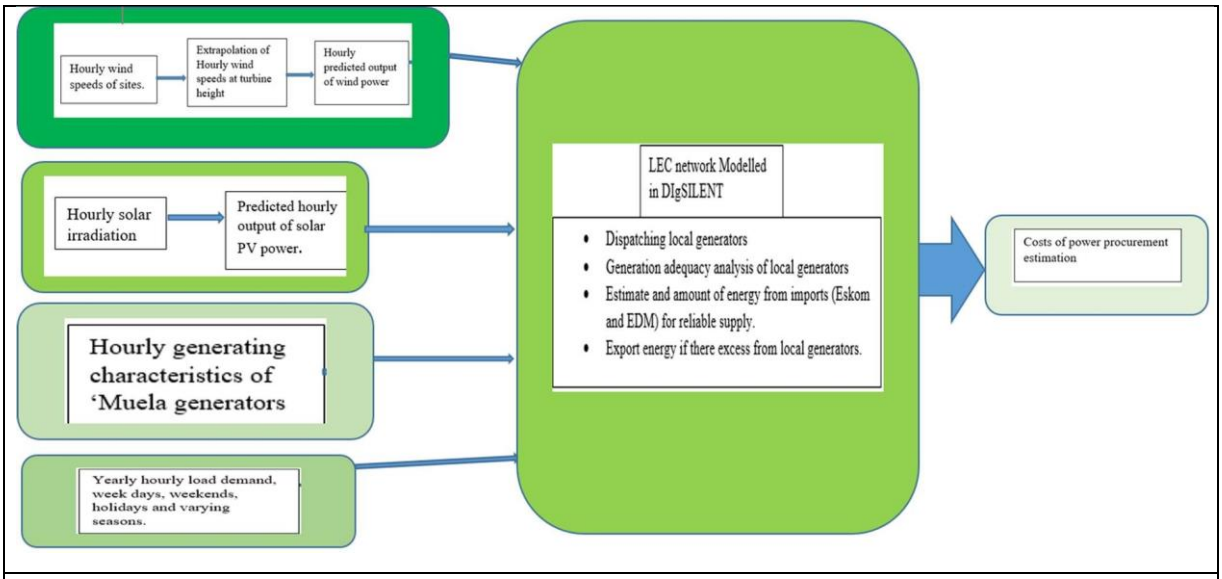

Figure 10:Flow chart of the overall methodology

3.2 Mathematical Description of Power Dispatching and Costs

The formulation of economic dispatch problem for utilities who own thermal generators is usually modelled using a quadratic function shown in Equation (15) which attempts to minimize the fuel costs of generators as well as incorporate renewable energy power sources by buying from IPPs. The quadratic function (formed by □ , which is the power from gth thermal generator) relates to the cost function of thermal generators in which the coefficients □ , □ □□□ □ relate to the units $\frac{\$}{\_\_\_}$ $\frac{\$}{\_\_\_}$ $ design cost coefficients having the dimensions , □□□ , respectively [10]. The linear cost function □ □ , Δ□ relates to the spinning reserve costs which is used for security of power supply, where □ is the spinning reserve cost coefficient for the gth thermal generator in $\frac{\$}{\_\_\_}$ and

□ , is the power from the spinning reserve. The wind power is represented by □ , and while solar power by □ , and the cost that is paid to the IPP for their scheduled power is represented by □ □□□ □ for wind and solar, respectively.

□ □ , = □ □ , + □ □ , + □ + □ □ , Δ□ + □ □ , Δ□ + □ □ , Δ□ (15)

LEC does not own any thermal generators or any generating units at all, it buys power from interconnected generating companies, then transmits and distributes it. Therefore, for this study, the cost functions that are considered are the linear parts of equation (15), which relate to the costs of power paid to IPP when incorporating renewables. Like any other utility company, the main objective of LEC is to minimize costs of buying or purchasing power from imports as well as incorporate the renewables to their power sources portfolio. Regardless, the major constraint is that LEC owns only the grid or power network as it does not own any generating units. This makes it to have only the control on the network for absorbing and dispatching power. Since the main hydro plant ('Muela) is owned by LHDA and solar and wind farms are assumed to be owned by IPPs, then LEC must pay the price of energy proportional to their injected or scheduled power through metered points. So, cost functions for wind and solar are given by equations (16) and (17). Considering the current status of LEC purchasing power from 'Muela hydropower plant also at a constant price, then, the cost function that can best relate to the situation is represented using equation (18). Also, since power from 'Muela cannot meet the demand, then power is sourced from imports, mainly Eskom and EDM, so the cost function is represented using equation (19).

$$\square_{,} \ \square_{,} = \square \ \square_{,}\Delta\square \quad (16)$$

$$\square_{,} \ \square_{,} = \square \ \square_{,}\Delta\square \quad (17)$$

$$\square_{,} \ \square_{,} = \square \ \square_{,}\Delta\square \quad (18)$$

$$\square \ \ _{,}(\square \ \ _{,}) = \square \ \ \square \ \ _{,}\Delta\square \quad (19)$$

where $\square_{,}, \square_{,}, \square_{,}, \square_{,}, \square_{,}, \square_{,}$ and $\square(\square)$ are the costs relating scheduled output of wind power $\square_{,}$, solar power $\square_{,}$, hydropower $\square_{,}$ and imports $\square$ in (MW) at time t in hours, respectively. The coefficients $\square, \square, \square \square\square\square \square$ ($/MWh) represent tariff or cost of electricity that must be paid by LEC to the power producer and imports per 1 MWh of injected energy to the grid. This cost of electricity is assumed to be constant for each power producer, in Lesotho, and it is named a flat rate tariff. However, considering the power exchange agreements between LEC and imported power, the import cost may vary.

Now the cost function will be represented as:

□ = □ , □ , + □ , □ , + □ , □ , + □ , □ , (20)

Or

□ = □ □ , Δ□ + □ □ , Δ□ + □ □ , Δ□ + □ □ , Δ□ (21)

The costs of electricity from imports is not usually constant, however in this study we consider two charging criteria 1) the flat rate tariff which is constant and is paid when the consumed power is within the specified limit signed bilaterally represented by □ , and 2) the price paid once the specified limit is exceeded, □ , + □, and □ becomes the increment to the flat rate charge.

Hence, using this translates the representation of prices from imports to be as shown in piece-wise function in equation (22), where P , . is the bilaterally signed power limit between LEC and Eskom or EDM.

$$\square = \begin{cases} \square \ , \ , \ , \ , \ . \\ \square \ , + \square, \square\square \ \square \ , > \square \ , \ . \end{cases} \quad (22)$$

For every system operator, the condition that must be met at all times, is the load demand, which is represented using equation (23).

$$\sum \square = \sum(\square , + \square , + \square , + \square ,) = \sum(\square , + \square ,) \quad (23)$$

The constraints that must be observed at all times is that power injected (□) or absorbed from any source, either local or imports, to serve the load and losses, cannot exceed the stipulated limit when serving the load. Hence for every power source, the injected power will always be within its minimum and maximum capacity as shown in equation (24),

$$\square \leq \square \leq \square \quad (24)$$

However, in the situation whereby the power injected to the grid by local sources (either by, ‘Muela, solar and wind farms) exceed the load demand as shown in equation (25), then LEC must reject power from imports, particularly Eskom and EDM, then export power. The exporting criterion assumes that the exported power will be absorbed in the interconnection point with external in-feed (Maseru Bulk). Furthermore, it assumes that power that is exported can be sold to Southern African Power Pool (SAPP) markets.

$$(\square_{,} + \square_{,} + \square_{,}) > \quad (\square \quad_{,} + \square \quad_{,}) \qquad (25)$$

3.3 Power Dispatching Scenarios

For every dispatching scenario, first being ‘Muela and Imports (Current Status) which will later be followed by introduction of renewables, ‘Muela hydropower station and other renewables are modelled as generating plants connected to the grid and Imports as External grids. For all the scenarios, the aim is to give every local plant, which is renewable, preference over imports. That is, every local power must be consumed first to serve the load and if there is any deficit, the external grids (Eskom+EDM) will come in and supply the load. However, if the local energy exceeds the demand, power is exported. The observed active power exchange patterns will be viewed in DIgSILENT using a quasi-dynamic simulation tool and exported to MS Excel or MATLAB to develop the cost implications graphs for every scenario which will be calculated using Equation (21) considering the electricity or energy trading prices obtained from the LEC annual reports (Table 3).

Since ‘Muela is a modelled as generator connected to the LEC grid and Imports (Eskom and EDM) are modelled as External Grids in the DIgSILENT, then, power is first consumed from ‘Muela and if it is insufficient to serve the required load, then the external grids (Eskom and EDM), are used as support to come in with the deficit. Also, if by any chance there is excess power, the external grid absorbs that power. This makes ‘Muela, the local generation, be given preference over imports. Again, the load flow analysis in DIgSILENT always ensures that power balance constraint explained in equation (23) is always satisfied. The active power flow for each hour and anytime or period, under steady state conditions are viewed, or observed using the Quasi-Dynamic simulation tool and

the results are exported to as an MS excel file to calculate the costs implications using last two parts of equation (21).

After setting up VREGs, they are also dispatched first collectively with ‘Muela ahead of imports from external grids. If power from ‘Muela and VREGs is insufficient to meet the dynamic demand, then Eskom+EDM will be absorbed at different entry points to ensure that the load is met at all times. However, if power from ‘Muela and VREGs, local generation exceeds the demand, the power from imports is rejected allowing exports to happen at any entry point and assumed to be sold to SAPP markets. In this study we do not curtail any energy from the local generators, as it discourages investments and may result in compensation charges as already discussed in the literature. The dispatching will consider four scenarios: (1) ‘Muela+imports, (2) ‘Muela+Solar PV+imports, (3) ‘Muela+Wind farms+Imports and (4) ‘Muela+Solar PV+Wind farms+Imports.

3.4 LEC Network Topology (Current Status) and Configuration in DigSILENT

Power is bought and dispatched from generation or main supply sources: Muela Hydropower (LHDA), Eskom (South Africa), and EDM (Mozambique) to LEC load centers via the transmission network. The distribution network, in general, transmits power from substations to energy users with voltages ranging from 11 kV to 220 volts and 380 V. The 132 kV lines carry the supply from 'Muela and Eskom plus EDM (at Maseru intake) to Maputsoe Substation and Mabote Substation, respectively. Eskom's (Clarens) supply enters Lesotho through an 88kV line at Khukhune Substation in Butha-Buthe, while Qacha's Nek import is through a 22kV line from Matatiele. The voltage levels of the transmission lines are 132kV, 88kV, 66kV, and 33kV. Nevertheless, in some areas, such as Thabana Morena in Mafeteng, LEC distributes with 33kV. Transmission voltages are stepped down to distribution voltages through 45 substations, six of which are crucial for the country's energy supply, notably Mabote, Mazenod, Maputsoe, Ramarothole, Litsoeneng, and Khukhune Substations. Only the district of Qacha’s Nek is not connected to the main national grid. The representation of the network is shown in Figure 11.

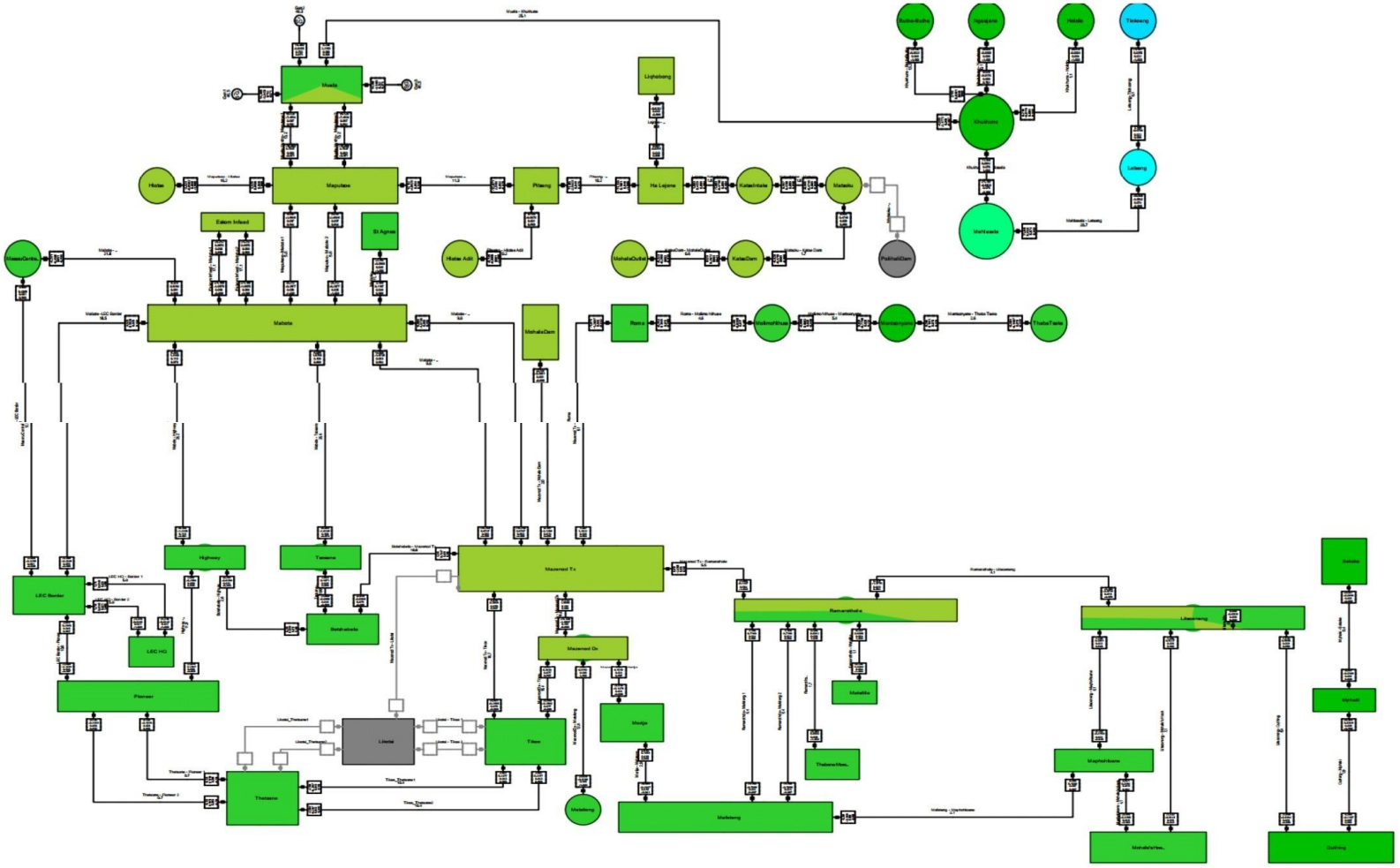

Figure 11:The LEC network representation in DIGSILENT

3.5 Baseline (Current Status) Modelling

3.5.1 Modelling of 'Muela Hydropower Station

The study uses recorded data in 2018 through statistical meters at different supply or infeed points for 'Muela, Eskom and EDM entry points. The raw data was recorded in half-hourly load but it was then converted to the hourly load by considering the maximum from the two half-hour readings, for all days: weekday, Saturdays and Sundays. From there, the load was prepared for three seasons, first being summer1 (from January to end of April), second being winter (from May to end of August) and third season being summer2 (from September to end of December). Thereafter, daily, weekly and monthly peaks as well as seasonal load patterns were calculated, observed and analyzed.

In order to model the 'Muela hydropower generators, a synchronous machine is used. Figure 12 shows the machine parameters such as power rating, stator resistance, synchronous reactance, and sub-transient reactance. The time characteristics of the three 'Muela generators was developed from the observed output generation recorded or metered at 'Muela station for each hour of the year as shown in Figure 13. These was done in order to be able to approximate the generation profile of each day or hour of the year.

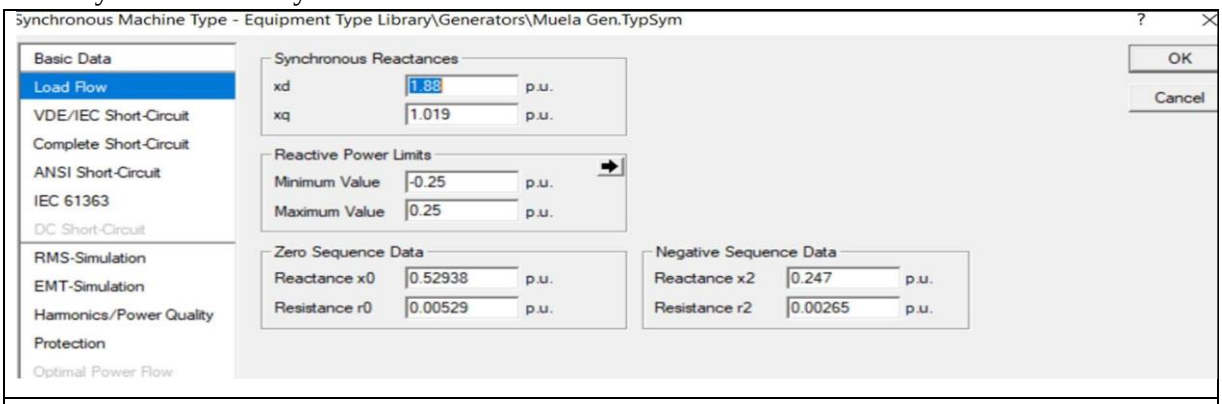

Figure 12:'Muela generator modelling

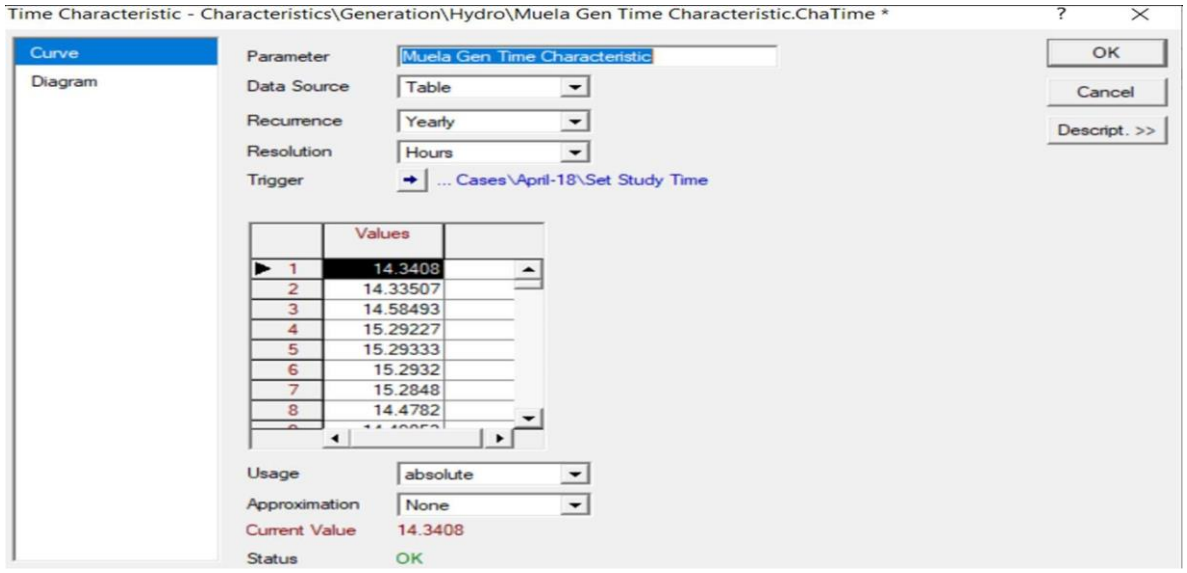

Figure 13: 'Muela Generators time characteristics

3.5.2 Load Modeling in DIgSILENT

The usual voltage dependent load is usually modelled using equation (26) and (27), where P is the active power, Q is the reactive power and V represents the instantaneous voltage while □ is the nominal voltage at load terminals. The values □ , □ represents the reference values of active power and reactive power respectively. The constant power, current, and impedance are represented by the exponents a and b, which have values of 0, 1, 2 [27], [109]. The constant power model, which assumes 0 for exponents a and b, was employed in this investigation.

$$□ = □ (□ □/) \quad (26)$$

$$□ = □ (□ □/) \quad (27)$$

The apparent power and power factor considering how the load was modelled are shown in Figure 14. Similarly, like the generators, time characteristic for each hourly load or consumption profiles of every substation was also defined using the same criteria as the generation load.

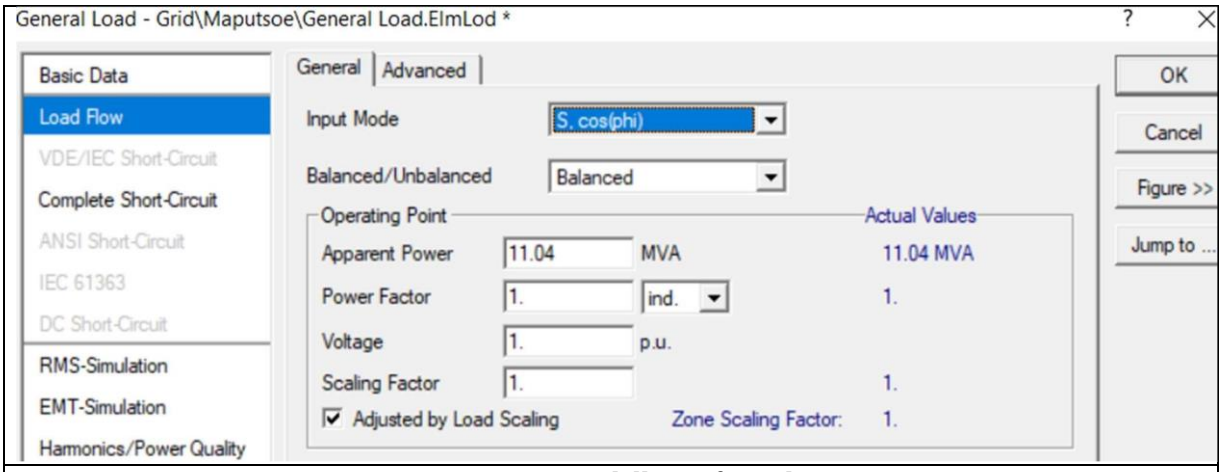

Figure 14: Modelling of Load

3.6 Modeling of Renewable Energy Generators

3.6.1 Wind Power Output Modelling

The wind power output was estimated using typical wind turbine model, which has the cut-in speed of 3.0 □/□, rated speed of 13 □/□ and the cut-out speed of 25 □/□. The wind power curve is estimated using equation (28) by considering the hourly wind speeds which were obtained from the 10 minutes measured data at 10 m above ground level and extrapolated to 50 m. As the modeling of the turbine power output is very crucial, the study chooses to model using the quadratic parametric model. This approach has also been used in researches [30], [41].

$$\square = \begin{cases} 0, & \square\square\square\ \square < \square \quad \square\square\square\ \square > \square \\ \square \times \dfrac{((\square) - (\square))}{((\square) - (\square))}, & \square\square\square\ \square \leq \square \leq \square \\ \square, & \square\square\square\ \square \leq \square \leq \square \end{cases} \tag{28}$$

Where □ represent the wind speed at time t, □ is the rated wind power output and □ is the hourly power output.

The hourly wind speeds at hub height (Z) of 50 m were estimated using equation (29), using Z , the reference height, in which the wind speed was measured in above ground level at 10 m for Masitise and 9 m for Lets'eng [45]. In this study the shear coefficient (m) or wind speed power law

coefficient is taken to be 1 7⁄ which is a typical value for low roughness surfaces and well exposed sites and it has been used in methodologies [1], [30], [110].

□ = □ × ( ) (29) □

The modelled wind turbine power output was configured in the DIgSILENT using the build in 2 MW doubly fed induction machine (DFI). The representation of the modelled yearly output for Lets'eng wind farm is shown in Figure 15 using the respective hourly wind speeds extrapolated at 50 m. Similarly with Masitise wind farm, this configuration was implemented. These turbines were connected in parallel to give the desired capacity for any wind farm.

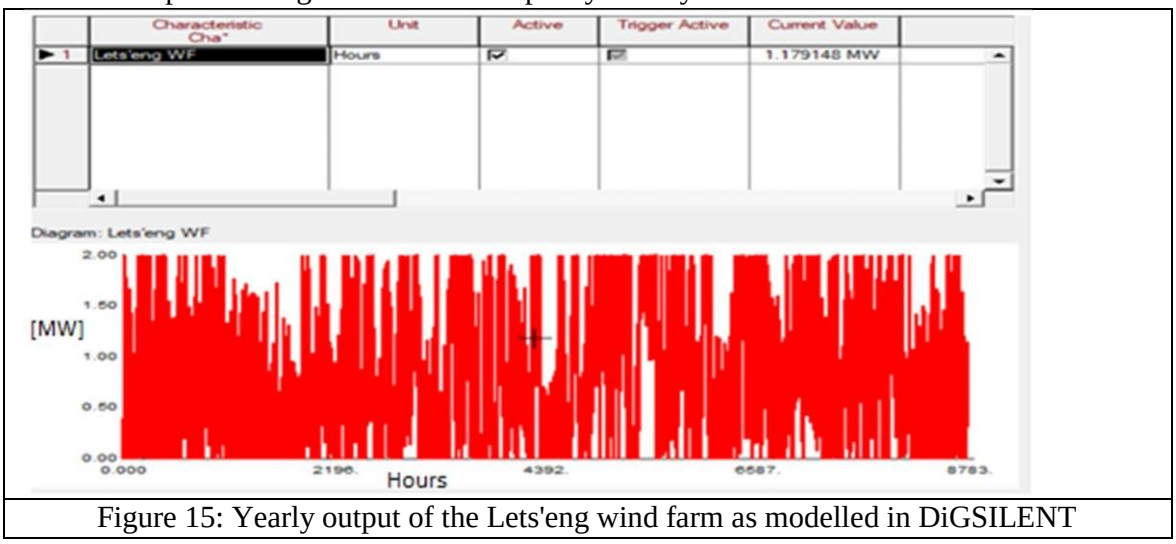

Figure 15: Yearly output of the Lets'eng wind farm as modelled in DiGSILENT

3.6.2 Solar PV Farm Generation Output

In order to model the instantaneous hourly solar farm output, equation (30) was used [26], and the hourly radiation at Ha-Ramarothole was downloaded from the PVGIS website [111].

$$\square = \frac{\square}{\square}\,\square \qquad (30)$$

Where, □ is the PV output, □ and □ are solar PV array efficiency under operating conditions and standard test conditions respectively, which are represented by the incident solar irradiance on the plane of the PV array (□) and the incident solar irradiance at standard test conditions □ . The power

output obtained were used to configure the general template of 0.5MW PV generator found in the DIgSILENT library. These generators were connected in parallel to give the desired capacity of the PV at Ha-Ramarothole. The instantaneous yearly output for the PV farm is illustrated by Figure 16.

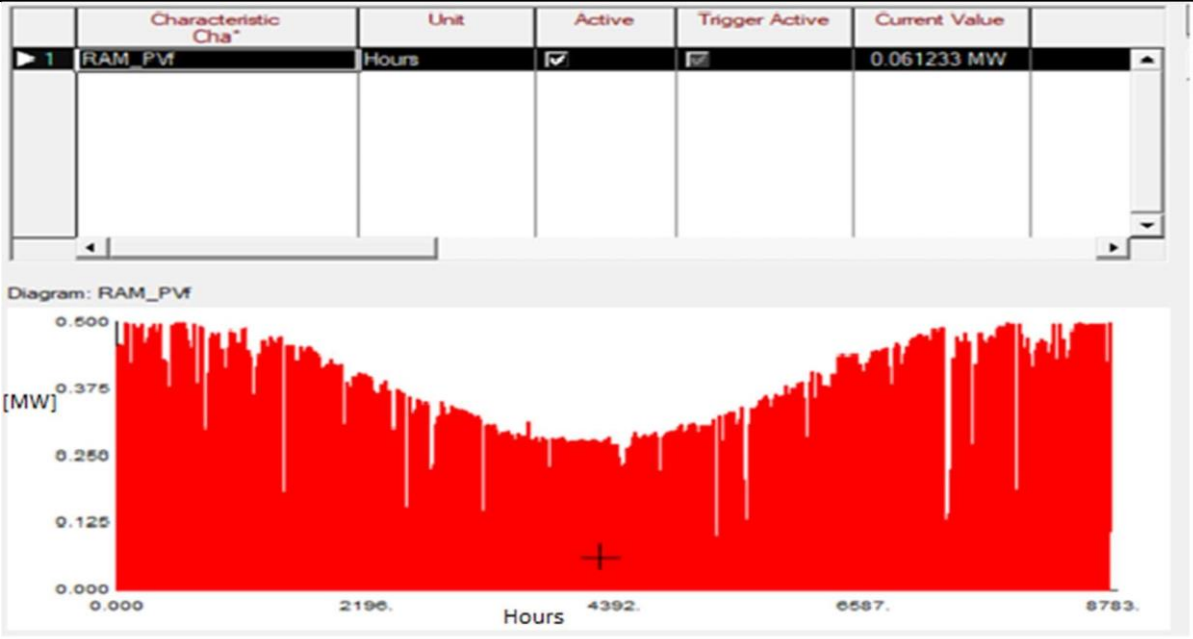

Figure 16: Yearly output profile of Ha-Ramarothole solar PV farm

3.7 Inputs for Generation Adequacy Analysis

The Generation Adequacy Analysis in DIgSILENT PowerFactory is the finest tool for evaluating generation unit reliability indices [27]. For this study it is used to assess how much renewable power generation (or local generation) contributes to overall system capacity, as well as the indices for LOLP and EDNS. The LOLP is a critical metric for assessing generation system reliability. It is based on probabilistic techniques and refers to the period when generating capacity is insufficient to meet system demand. The annual load duration curve or the daily load duration curve can be used to construct this index in DIgSILENT. It has a mathematical formula for calculating LOLP, which is given by equation (31) [27]. Where □ is the probability of a peak load equal to or greater than the generation capacity at a given point in time □ .

$$\square\square\square\square = \quad (\square \times \square)\ 100 \qquad (31)$$

The EDNS index which represents the energy not supplied to customers is calculated based on equation (32) as follows:

$$\square\square\square\square = \quad (\square \times \square) \qquad (32)$$

Where $\square$ is the average load demand and $\square$ is the outage time of the load at point $\square$.

The results of these indices will be obtained from the distribution plots, which depicts, total available capacities in (MW), available dispatchable and non-dispatchable capacities, total reserve generation and so on. Further, more detailed results for LOLP and EDNS will be determined from the Monte-Carlo convergence plots. The analysis will be carried out for the whole year based on the study period which will be disaggregated into 12 months for all the different scenarios of wind farms and solar PV with their rated capacities shown in Table 2. All the iterations are set at 100000 and the load time characteristics was enabled to consider the varying load.

Table 2: Capacities Modelled for power dispatching and Considered for generation Adequacy analysis

Lets'eng Wind farm (MW)	Masitise Wind Farm (MW)	Ha-Ramarothole Solar PV (MW)	'Muela Hydro (MW)
0	0	0	72 (base case)
34	24	50	72
34	24	90	72

In order to perform the generation adequacy analysis, the capacity available and probability of its availability must be set in percentages for all generators; that is availability of generation (in %) and probability of occurrence (in %). This means that for each state, the total available generation capacity in percent of maximum output, as well as the likelihood of this availability, must be stated.

Before setting up generation adequacy analysis in DIgSILENT, the Stochastic Multi State model for every committed generator should be defined [12], [27]. Since 'Muela generators are modelled using synchronous machines, considering their yearly generation data, their stochastic multi state model was set up considering the maximum output observed (which was 100% capacity) and all the

time series generation data was compared with the maximum state in order to know the available capacity (in %), to the maximum capacity as well as its number of occurrences. That is

for every available state □ at time t, it is compared with maximum capacity □ to get [(□ □⁄) × 100%] which is called a state available. For every state, the number occurrences were obtained throughout every hour of the year in order to calculate the probability of occurrence for the particular state. The sum of these probabilities add up to 100%. As such, the states of 'Muela generators are shown by Figure 17. Since the time series solar farm output was also modelled, the probability states were also set up the same way.

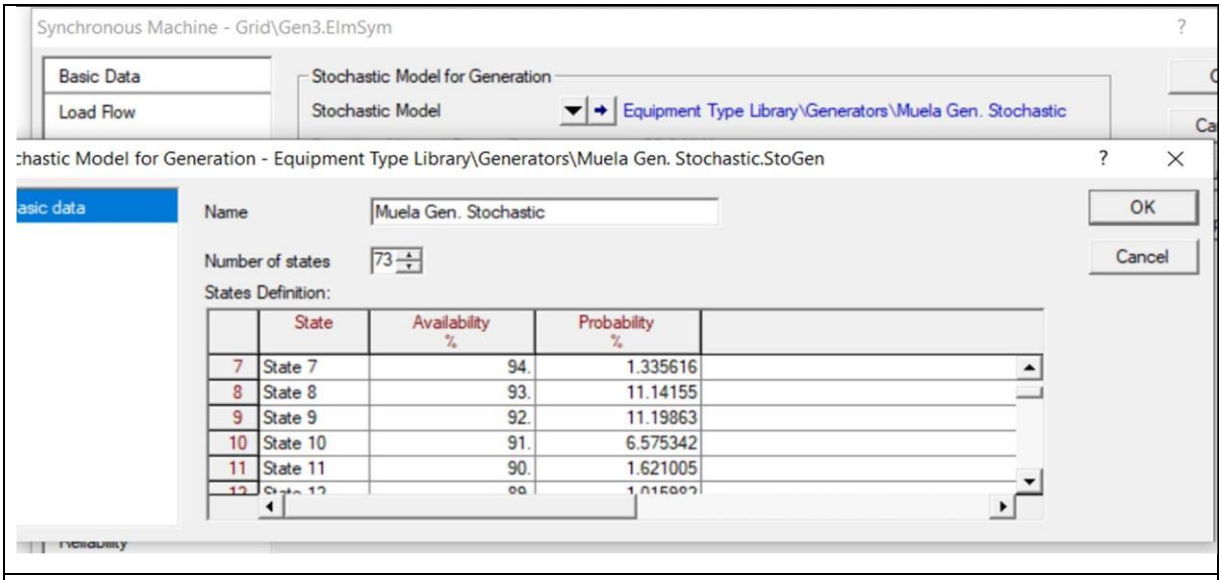

Figure 17: Multi-state model for 'Muela generators

The stochastic multi state model for wind generators is set up using the time series output contribution of active power. These was done by developing a time scale for each hour of the year and mapping it to each contribution or hourly output of the wind power with respect to the instantaneous wind speed. The multi state wind model of Masitise wind farm can be seen in Figure 18 as configured in DIgSILENT. A similar approach was adopted for Lets'eng wind farm.

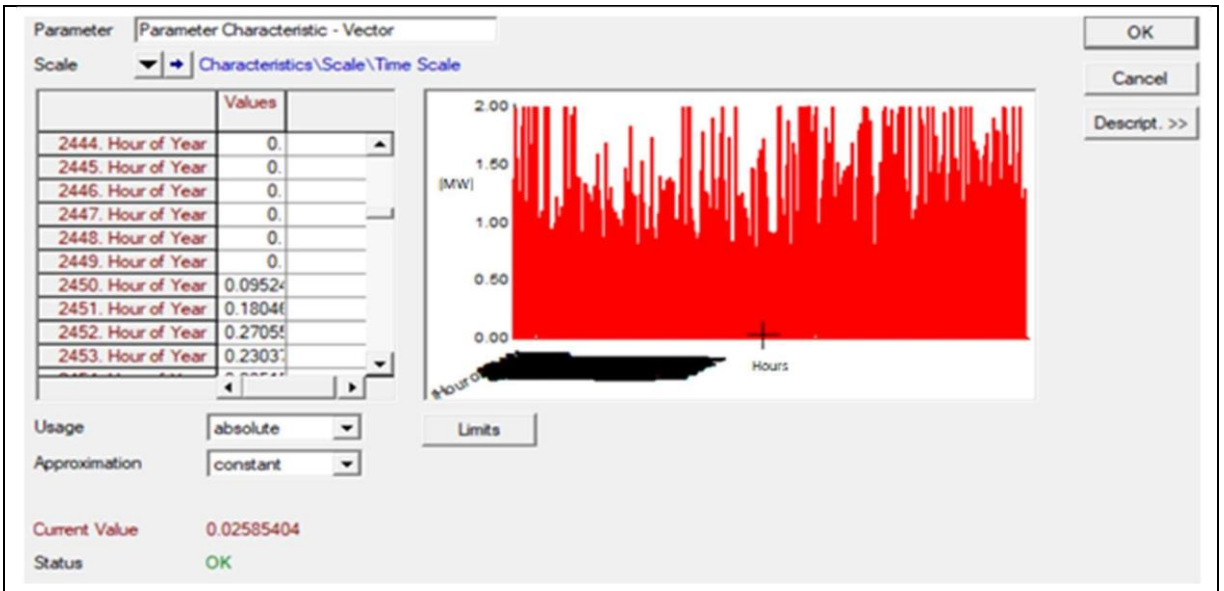

Figure 18: Multi state model for Masitise wind farm included in the generation adequacy analysis

After all these configurations were done, the generation adequacy analysis can be performed in the DIgSILENT environment for any selected time frame (e.g. months, week days, or the whole yearly). The generation adequacy analysis settings for the year under study is shown in Figure 19. For every power dispatching scenario, a generation adequacy analysis will be performed on monthly basis to assess the current scenario and security level in terms of supply of energy brought by the VREGs. Furthermore, this tool will be used to assess the amount of imports still needed under every scenario for reliable supply of energy and also assess in detail whereby local generators are insufficient to meet the demand through all months of the year considering critical times of the local demand peak and off peak hours. From the results, cost implications for power procurement will be performed.

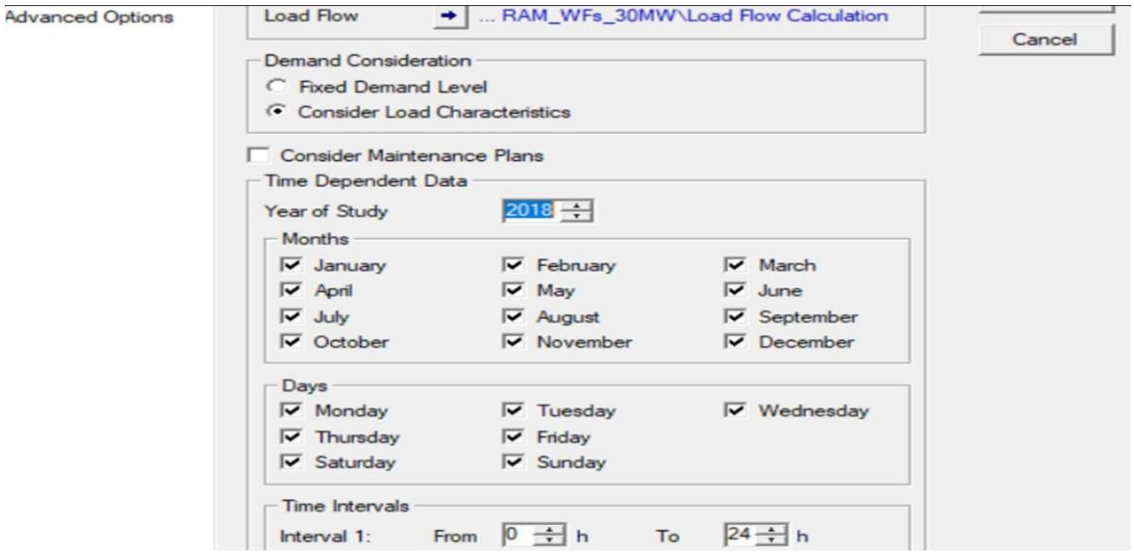

Figure 19: Generation adequacy analysis tab in DIgSILENT environment

3.8 Costs of Power Procurement

The costs of power procurement for every power dispatching scenario will be calculated according to the related costs of local generators and imports. For instance, the yearly average charges from imports and local generators for 2018_19 period is shown in Table 3 for the current status. The cost of solar for the study is 0.83 LSL/kWh (based on the approved generation tariff for Ramarothole solar form) and for wind is 1.05 LSL/kWh (based on tentative figures for planned wind projects). With the introduction of renewable energy generators, the costs of imports will be assessed through different SAPP markets (using real prices for 2018_19 year): Day Ahead Market (DAM), Forward Physical Market (FPM) Weekly and Monthly, based only on the energy consumed from imports.

Table 3: Bulk power costs from LEC in 2018_19 period and other years

Table 7: Bulk Supply Unit costs for Different Electricity Intake Points				
Intake Point or Supply Source	Bulk Supply Unit Costs for 2015/16 - 2018/19			
	2015/16	2016/17	2017/18	2018/19
'Muela	0.12	0.11	0.12	0.11
EDM	1.36	1.39	1.29	0.85
Clarens	0.68	0.74	0.75	0.82
Maseru Bulk Supply	0.95	0.84	0.98	0.97
Qacha's Nek	1.11	1.21	1.22	1.27
ESKOM (Clarens+Maseru+Qacha's Nek)	0.85	0.82	0.92	0.94
Total Imported Supply	0.99	1.00	1.01	0.91
Overall Average cost/kWh	0.42	0.48	0.49	0.47

4.0 Results and Discussions

4.1 Estimation of the Current Status – Baseline Modelling Results

Figure 20 illustrates the load demand for 2018 as presented from the DIgSILENT simulation. It is seen that most of the demand is high from May to Aug with peak month being July in 2018. The peak demand observed from the simulation is 177.196 MW which occurred at 10:00 AM in 2018.

In the summer seasons from September to April, the load demand follow almost a constant pattern that is usually in the range of 75 to 130 MW. The load duration curve in Figure 21 shows that less than 10% of the time the load demand is around its peak range of 140 to 177 MW (in winter) and about 99% of the time the load demand is around 80 MW.

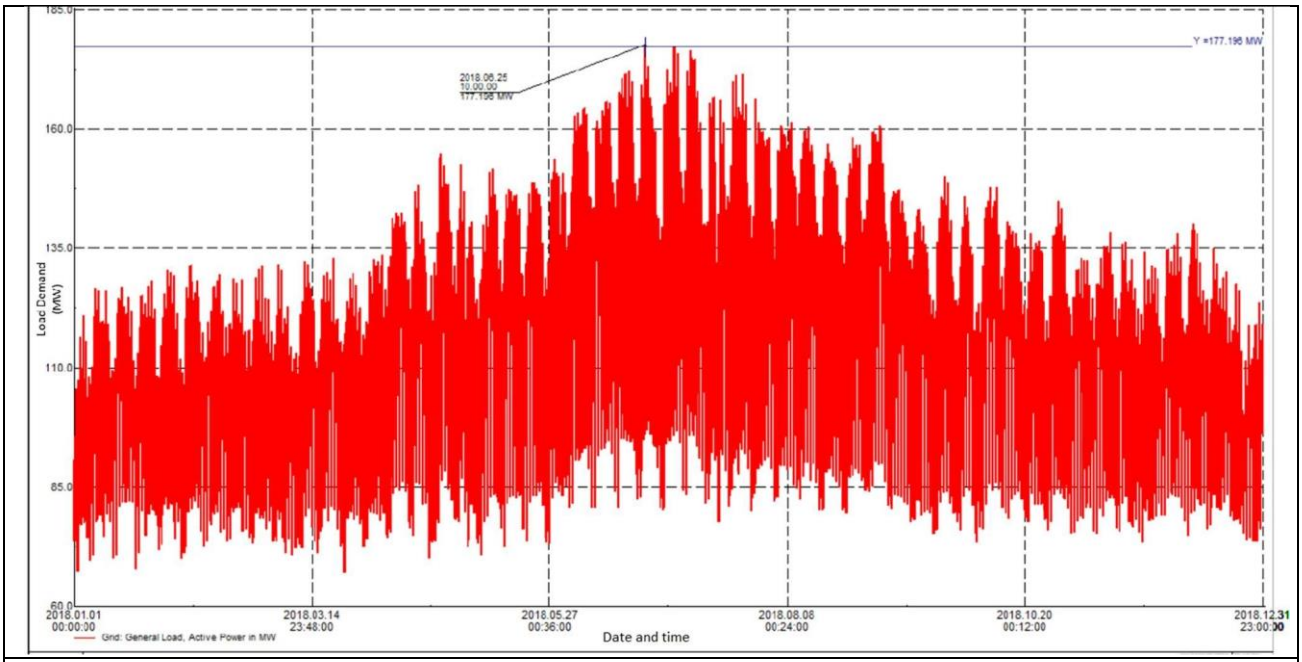

Figure 20: Yearly Load from 2018

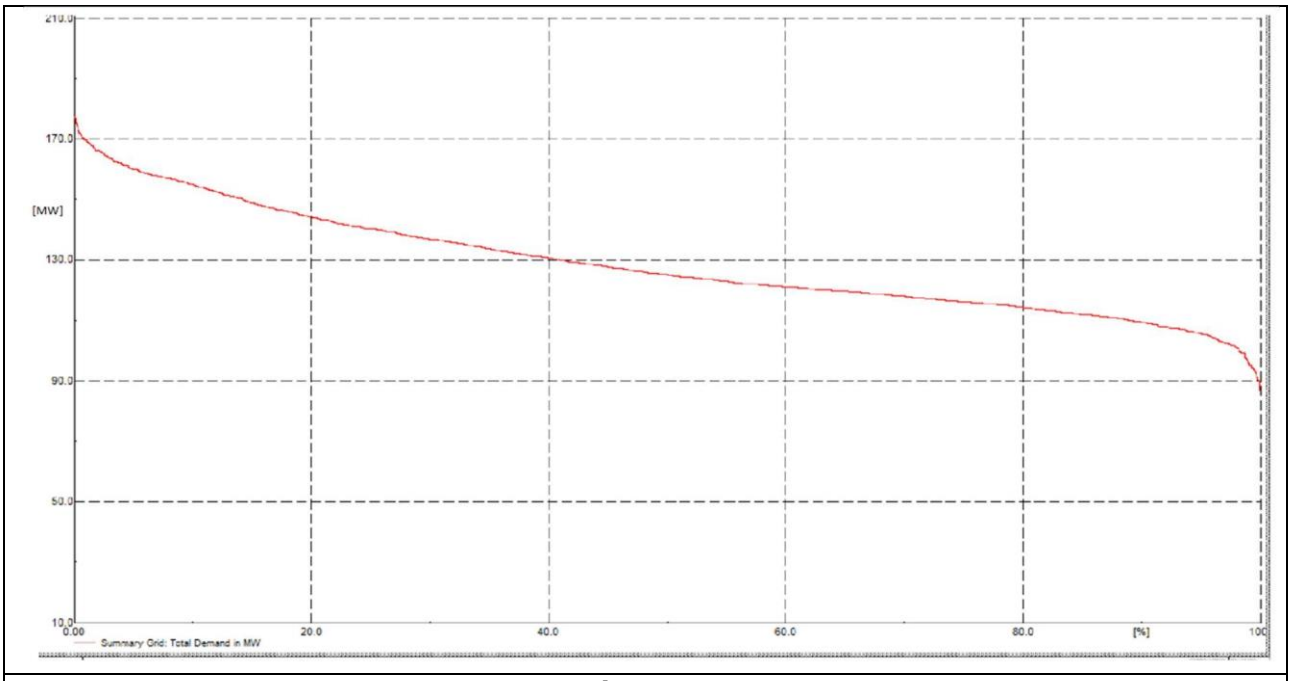

Figure 21:Load Duration Curve 2018

The observed active power exchange patterns as ‘Muela is dispatched first to serve the load depending on the availability and time characteristics profiles of the generators in the winter and summer weeks are illustrated in Figure 22 and Figure 23 respectively. Because winter is the high demand season, ‘Muela is always operating near its peak at around 70.2 MW at almost all the times and the imports happen most during winter season. Even so, it should be noticed from Figure 22 that, at around 01:00 to 03:00 HRS, the Maseru bulk (Eskom+EDM) power intake point (for imports) ranges from 23 MW to as low as 0 MW and drastically increases again (up to 95 MW) when the demand is high during morning peak hours (08:00 HRS to 11:00HRS). For night peak hours (18:00 HRS to 21:00 HRS), the Maseru bulk imports only reaches a maximum of about 80 MW. During these peak hours in winter, as power demand is always above ‘Muela’s total capacity, it can be seen that Maseru bulk infeed adjusts to the load changes as it rises and drops, in order to match the demand. The Khukhune (Clarens) intake point only brings a contribution ranging from 6 to 14 MW. Hence, on peak day (25.06.2018 at 10:00 HRS), main grid imports (Maseru bulk+Khukhune) contributes about 105 MW to supply the load. Furthermore, at night peak, around 20:00 HRS, main grid imports reaches a maximum of about 93 MW. However, since Qacha’s Nek (Letloepe) is an isolated grid in the east of the country, its Eskom intake is not affected by main grid load and it adjusts (from 0.9 to about 4 MW) to match the localized demand changes accordingly, ensuring reliable supply at all times of the day.

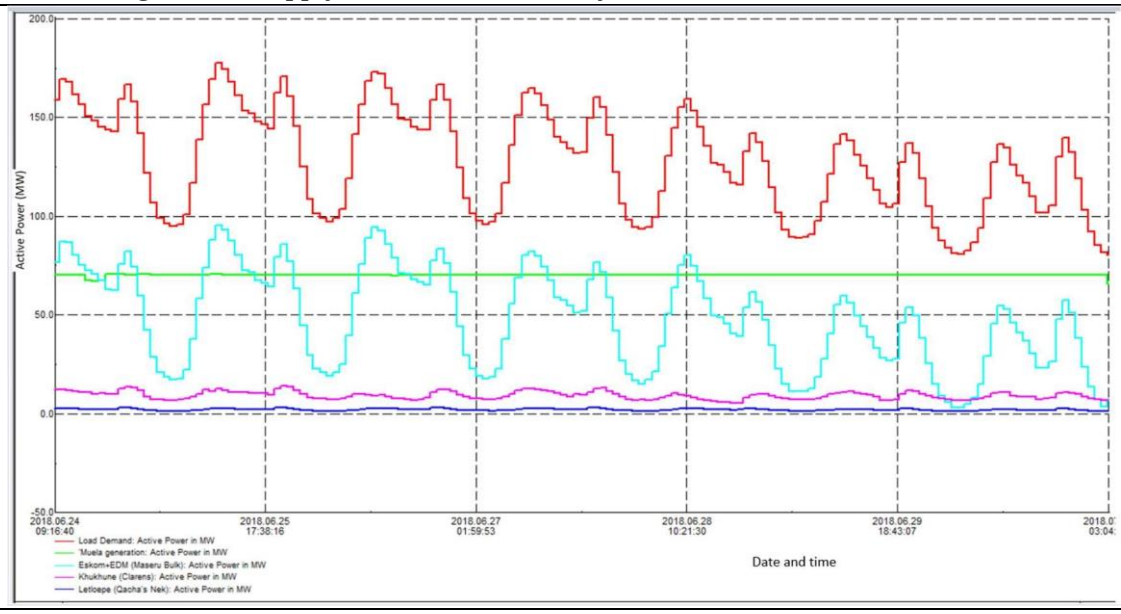

Figure 22: Typical Power exchange patterns in Winter season

The observed power exchange patterns in summer, shown in Figure 23, differs slightly from winter season. Power emanating from 'Muela is almost at 40 MW, when the demand is usually less than 80 MW and then Mabote infeed adjusts to the load changes. However, when the demand rises, typically above 80 MW, generation from 'Muela increases and therefore, decreasing the power intake from Mabote infeed. It should be acknowledged that, 'Muela operation is constrained mainly to reservoirs levels as well as scheduled maintenances, which enforces LEC to absorb whatever is available from generated power. Nonetheless, imports are mostly reliable despite of whatever inconsistencies encountered by Eskom and EDM. For this reason, using both Figure 22 and Figure 23 helps to establish a typical behavior of the current active power exchange patterns at metered points regarding the only two power sources of LEC; 'Muela and Imports, through various seasons, mainly summer and winter. Furthermore, the figures also illustrate that even though 'Muela is rated at 72 MW, it does not always operate at its peak. Therefore in dispatching it, all the available power will always be exhausted first and the deficit will be supported by imports.

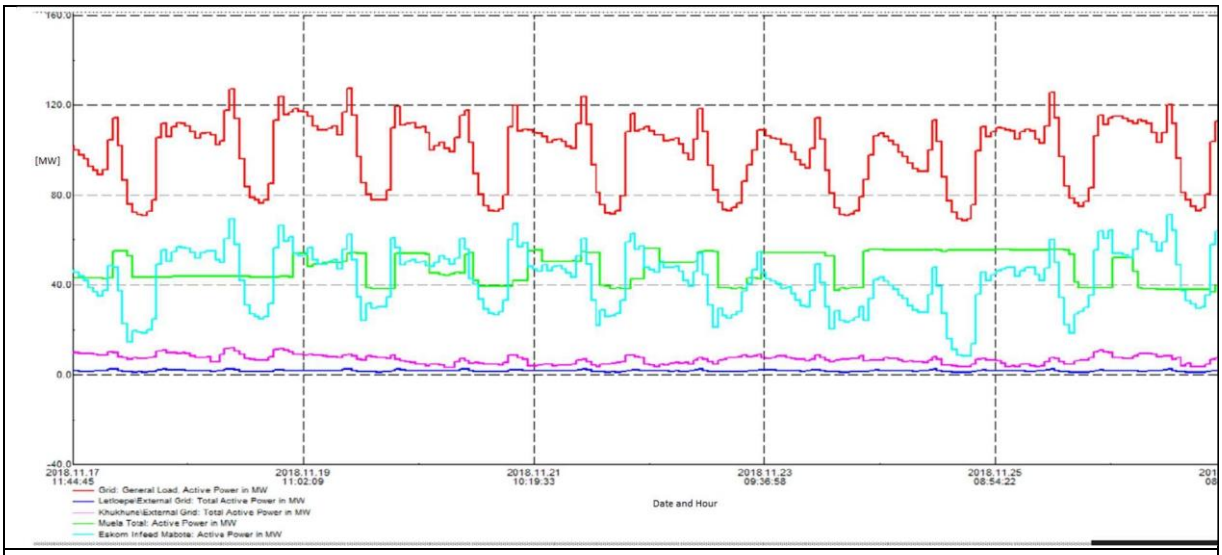

Figure 23:Typical active power exchange patterns in summer seasons

4.2 Performance of 'Muela and VREGs when dispatched vs imports

The performance of 'Muela combined with VREGs in June (winter season) is illustrated from Figure 24 and Figure 26. All the available power from Ha-Ramarothole solar PV is absorbed and fully utilized to serve the load. However, because of the insufficient radiation during the winter months, the maximum generated power is around 50% of the rated capacity (50 MW) as depicted in Figure

24.When solar PV generation is available, the imports needed in the main grid are seen to be reduced during the day (by a range of 0 to 28 MW, depending on solar output) and only support the deficit, with much imports (up to 93 MW) being needed at night peak. The solar output has reduced the large amount of imports needed at morning peak to a range of about 85 MW to 75 MW.

The wind farms (shown in Figure 25) are seen to almost have compensation profiles. That is, when Lets'eng wind farm generation drops, in most cases Masitise wind farm rises and vice versa. But, there are few times when both their generation is seen to be dropping and rising at the same time. In this case, imports are seen to be dropping (from 50 to 0 MW) when wind generation is available and excess energy from wind is exported to Eskom (about 18 MW) as shown by the negative profile of main grid imports. Most exports or unused energy are/is expected when the wind farms are almost at their rated capacities and also at night when the load drops and wind generation rises.

Combining Ha-Ramarothole solar PV with the wind farms (as shown in Figure 26) increases the local generation substantially and there is high absorption of local energy (ranging from 100 to 130 MW, when all local generators are almost at their peak). Every time the load is surpassed by local generation, wind energy (up to 28 MW) is exported but all the available solar energy is fully utilized. In all cases discussed above, the imports needed by the main grid are seen to be reduced and used as back up with introduction of renewable energy. Regardless, because Letloepe (Qacha's Nek) is an isolated grid, the imports in that area are not affected by the renewable generation, which is the same as the first scenario.

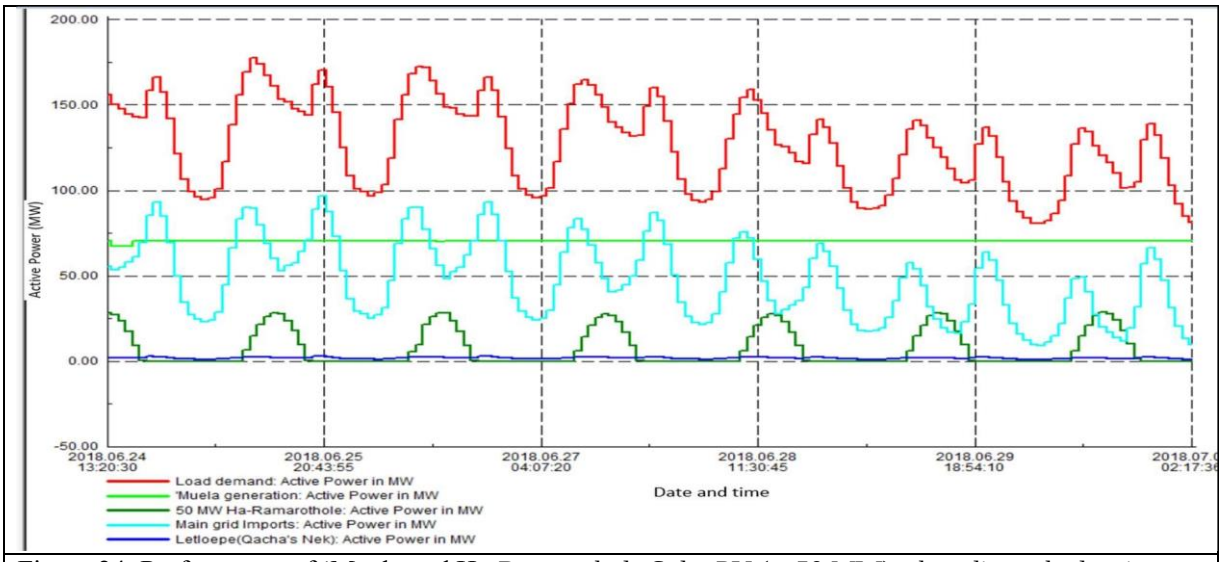

Figure 24: Performance of 'Muela and Ha-Ramarothole Solar PV (at 50 MW) when dispatched vs imports in winter season (June).

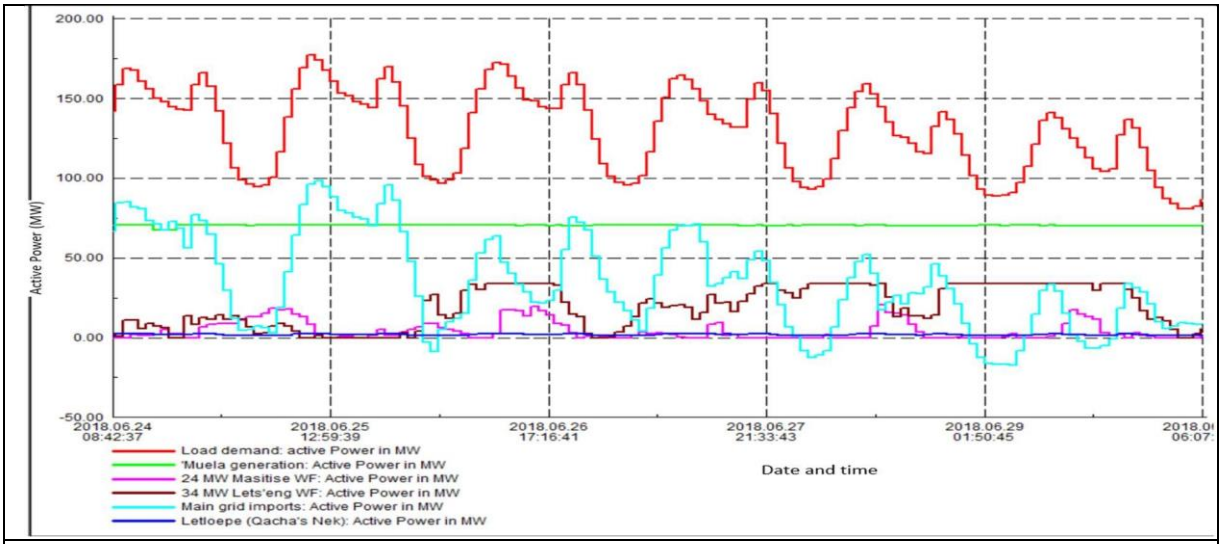

Figure 25:Performance of 'Muela, Masitise WF (at 24 MW) and Lets'eng WF (at 34 MW) when dispatched vs Imports in winter season (June)

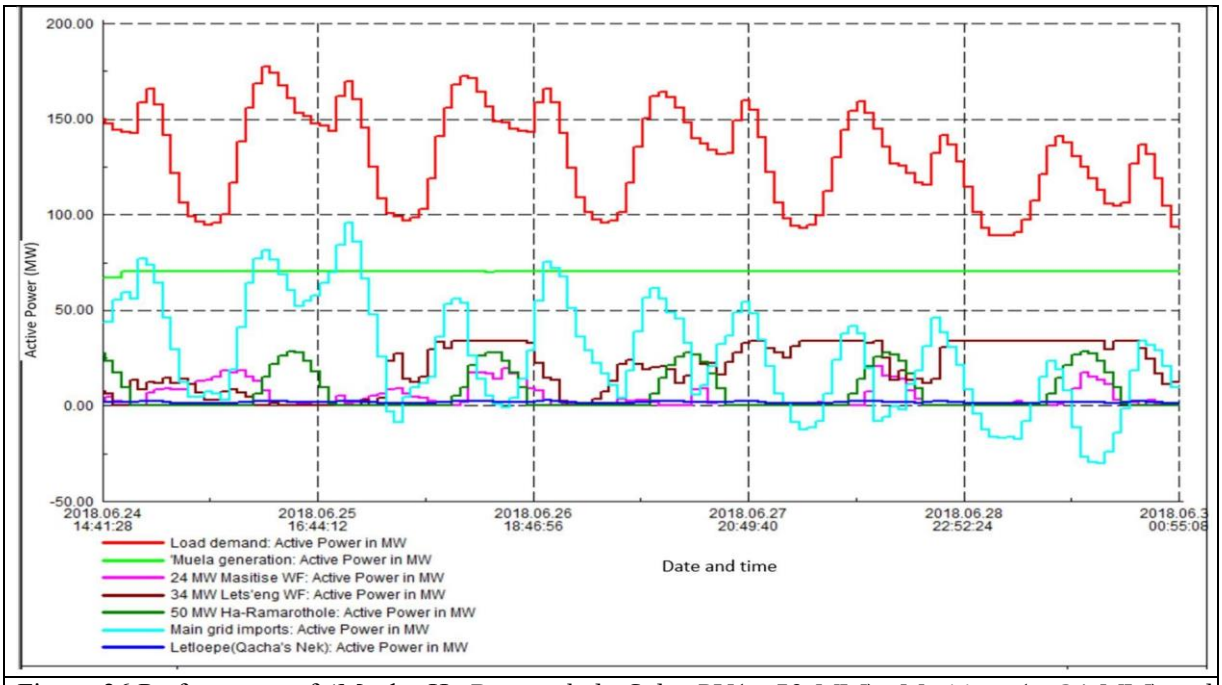

Figure 26:Performance of 'Muela, Ha-Ramarothole Solar PV(at 50 MW) Masitise (at 24 MW) and Lets'eng (at 34 MW) wind farms, when dispatched vs Imports in winter season (June)

4.3 Generation Adequacy Analysis of the Current Scenario ('Muela alone)

Figure 27 shows the observed distribution plots from Monte Carlo simulation illustrating the available dispatchable capacity for June. Considering the distribution curves in June, it can be seen that about 50% of the time 'Muela is always generating about 60 MW while the load demand reaches the peak of 177 MW less than 2% of the time. The total reserve generation is always negative (ranging from -138 MW to -38 MW) indicating that at all times there is insufficient capacity to meet the load. This can be clearly understood by Figure 28 considering the convergence plots from the Monte Carlo simulation as the LOLP is always 100% and the EDNS which is 92.121 MW for June. Although the EDNS results are in average, they paint a close enough picture of the amount of imports needed for each month in order for reliable energy supply. The summarized results for the indices of EDNS and LOLP are shown in Figure 29 depicting that, the LOLP is always 100% and therefore stressing the point that 'Muela alone is not sufficient to meet the demand. The EDNS varies according to each month and the highest is around 92 MW in June (high demand season) with a minimum being 54 MW in January (summer season, which is a low demand season).

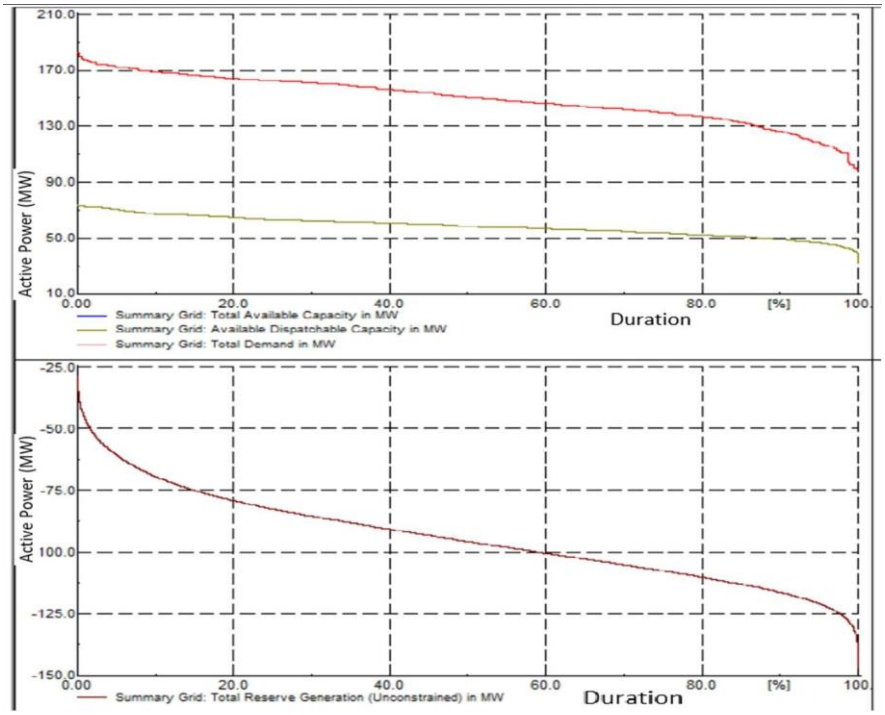

Figure 27: Distribution curves for 'Muela alone in June

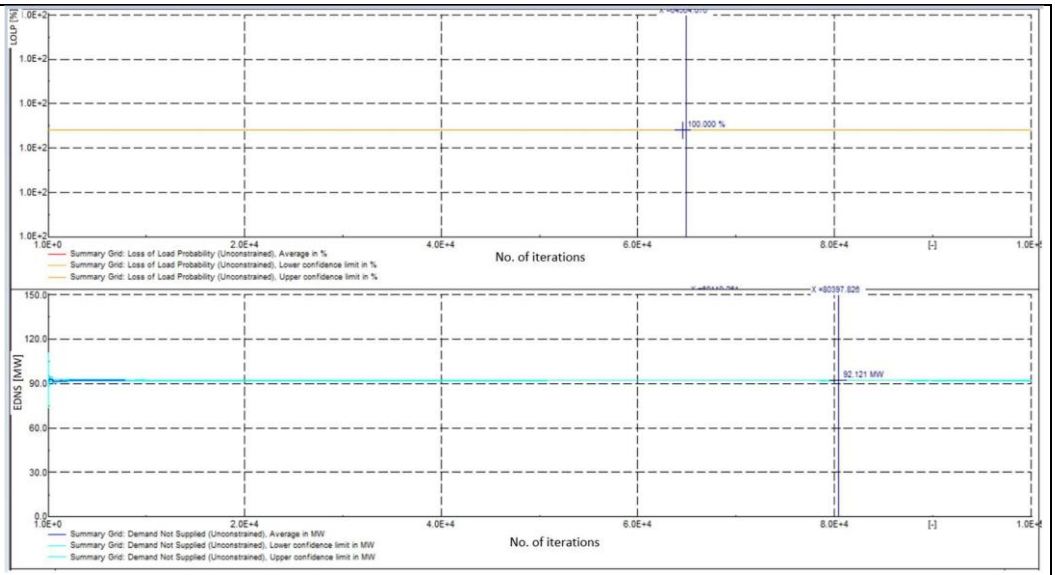

Figure 28: Convergence plots for Monte Carlo Simulation showing EDNS and LOLP for ‘Muela alone in June

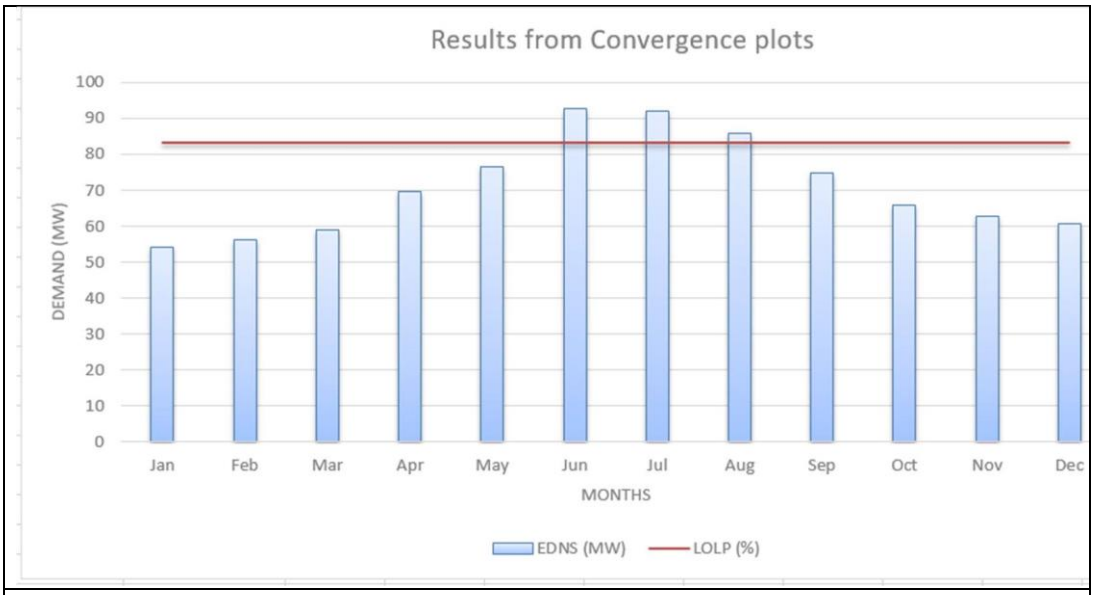

Figure 29: EDNS and LOLP for yearly period for 'Muela

4.4 Generation Adequacy Analysis of 'Muela and VREGs in June

Introducing solar PV and wind generators into the network implies that the local capacity would increase and therefore EDNS and LOLP must be lower than the base case. This can be confirmed

by the distribution plots and convergence plots (shown from Figure 30 to Figure 35) from Monte Carlo simulations. The distribution plots are all showing the increase with the total available capacity ('Muela+VREGs) as it is always greater than the dispatchable capacity ('Muela) for all different scenarios of renewable generators in June.

When 'Muela is combined with 50 MW Ha-Ramarothole solar PV in June (Figure 30) at about 50% of the time, the total available capacity will always be about 75 MW, showing an increment of about 15 MW (emanating from solar PV generation) when compared with the base case. Although Ha-Ramarothole solar PV is rated at 50 MW, in June, its maximum generation is around 28 MW due to insufficient radiation. This implies that around December or any of the summer months, the available generation from solar PV has a potential of increasing to a range of 40 and 50 MW due to sufficient radiation, thereby increasing the overall total available capacity to be dispatched into the network. Also, it implies that even when Ha-Ramarothole is operating at 90 MW (the expansion stage), around June or winter season, it would be operating at around half of its rated capacity due to radiation constraints. Similarly, like the total reserve generation in the base case, it is still below zero

margin, indicating that throughout, the total available capacity is insufficient to match the demand. Unlike the base case, the impact of solar PV can be appreciated by the fact that the total reserve generation now ranges from about -128 MW to -25 MW, which is an improvement of about 13 MW relative to the first baseline scenario. This illustrates that even though the LOLP is still 100% just like the base case, the EDNS will be reduced. Thus, under 'Muela and solar PV (at 50 MW) case, during operational hours of solar PV, the EDNS is reduced to 80.125 MW as shown by the convergence plots in Figure 31.

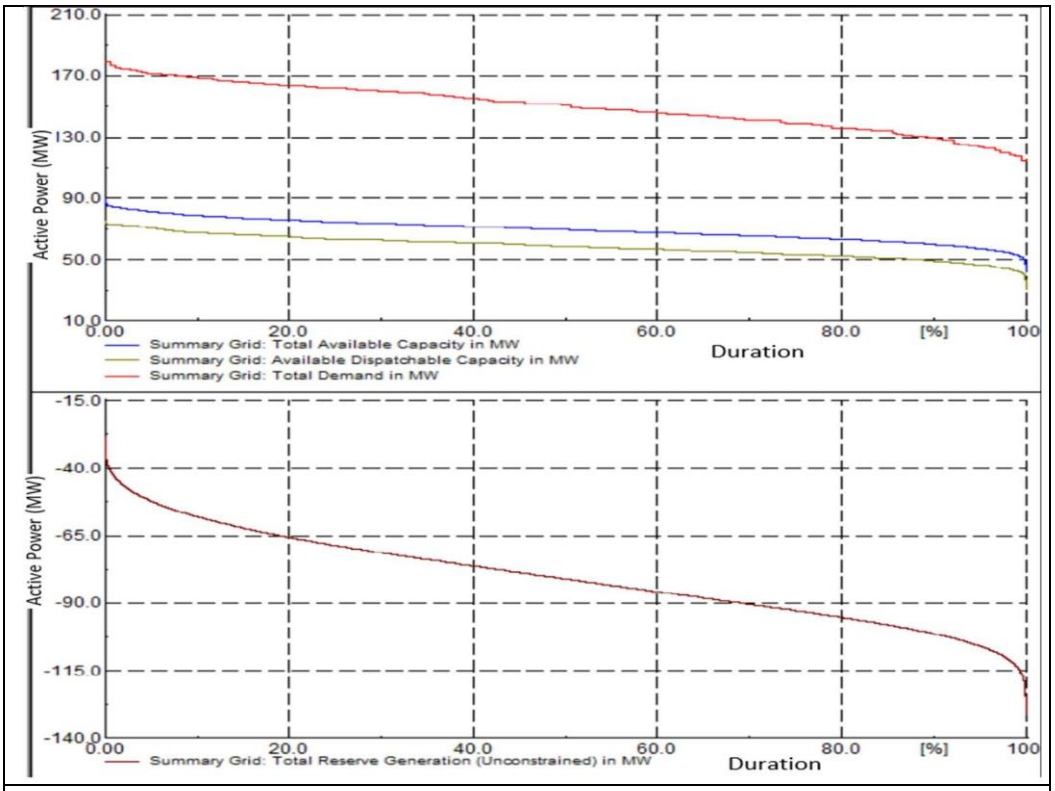

Figure 30: Distribution plots for 'Muela and 50 MW Ha-Ramarothole solar PV in June

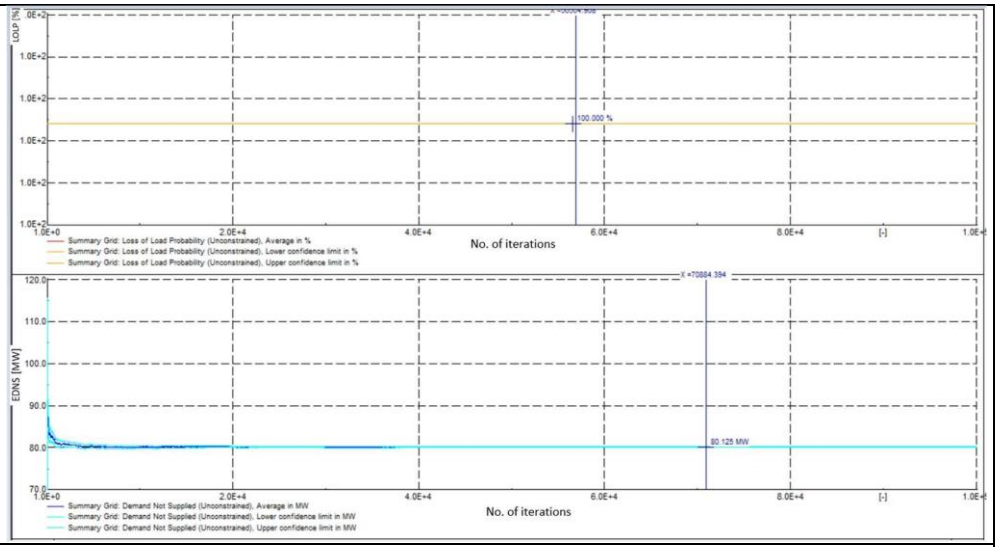

Figure 31:Convergence plots for 'Muela and 50 MW Ha-Ramarothole in June showing EDNS and LOLP

Considering the scenario of 'Muela when operating with the wind farms (Figure 32), about 50% of the time the total available capacity ranges from 80 to 128 MW, which shows a great improvement in the network's ability to supply the load. Because there are times when the load drops to a range of 90 to 110 MW in winter, usually at night, then it already indicates that there will be periods when the available capacity exceeds the load. This can be understood by examining the total reserve generation now ranging from -120 MW to 10 MW, being slightly above zero margin less than 1% of the time and subsequently indicating that the LOLP has slightly decreased from 100% to about 99.4%, and the EDNS has dropped to 65.138 MW in winter (see Figure 33). In this regard, the duration of time that the total reserve capacity is above zero margin indicates when power can be exported or simply when there is excess energy from local generators.

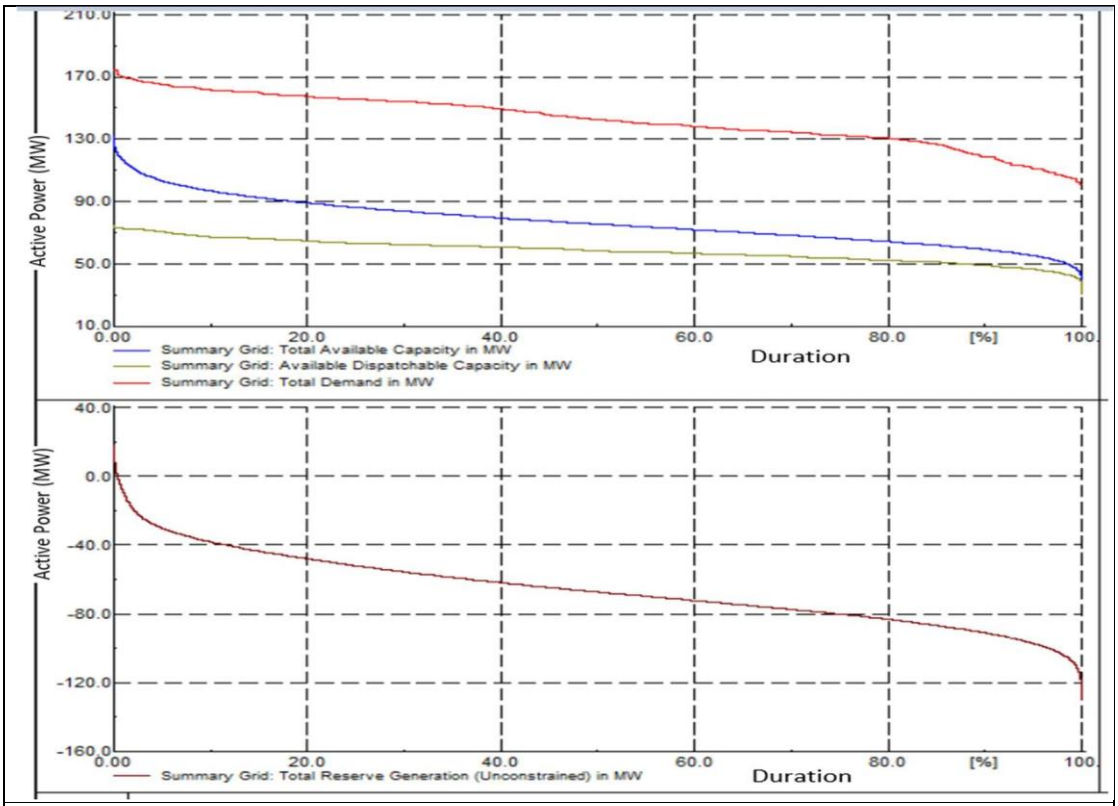

Figure 32: Distribution plots for 'Muela, 24 MW Masitise and 34 MW Lets'eng wind farms in June

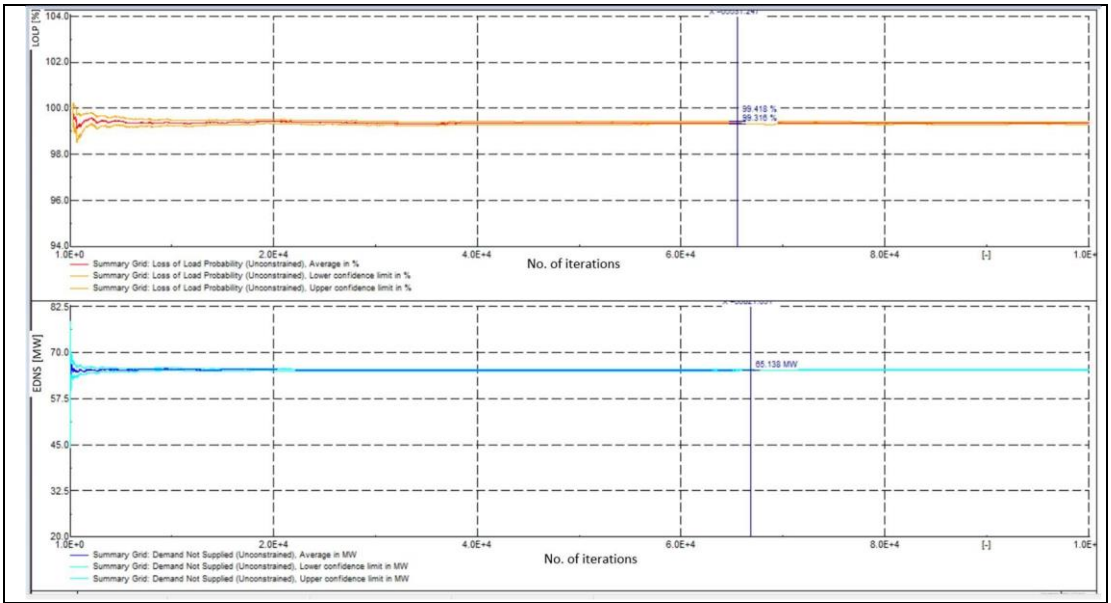

Figure 33:Convergence plots for 'Muela, 24 MW Masitise and 34 MW Lets'eng wind farms in showing EDNS and LOLP in June

Moreover, under the scenario of all the local generators combined with their respective capacities (Figure 34), there is an appreciable increase in the total available capacities and about 50% of the time there is about 85 MW to 145 MW available in the network. It is also worth noting that, only about 10% of the time, the available capacity is greater than 100 MW. This indicates that only 10% of the time in winter (June), all these generators combined are operating almost at their full capacities. In this case, the total reserve generation ranges from 0 to 20 MW only 1.4% of the time and about 98.6% of the time, the network will have insufficient power to supply the load and therefore power will be drawn from imports (Eskom and EdM). The EDNS and LOLP in this case drops to 55.54 MW and 98.56% as shown by Figure 35, respectively. In all cases, the Monte Carlo algorithm seems to converge even before 70 000 iterations and it takes about 5 minutes.

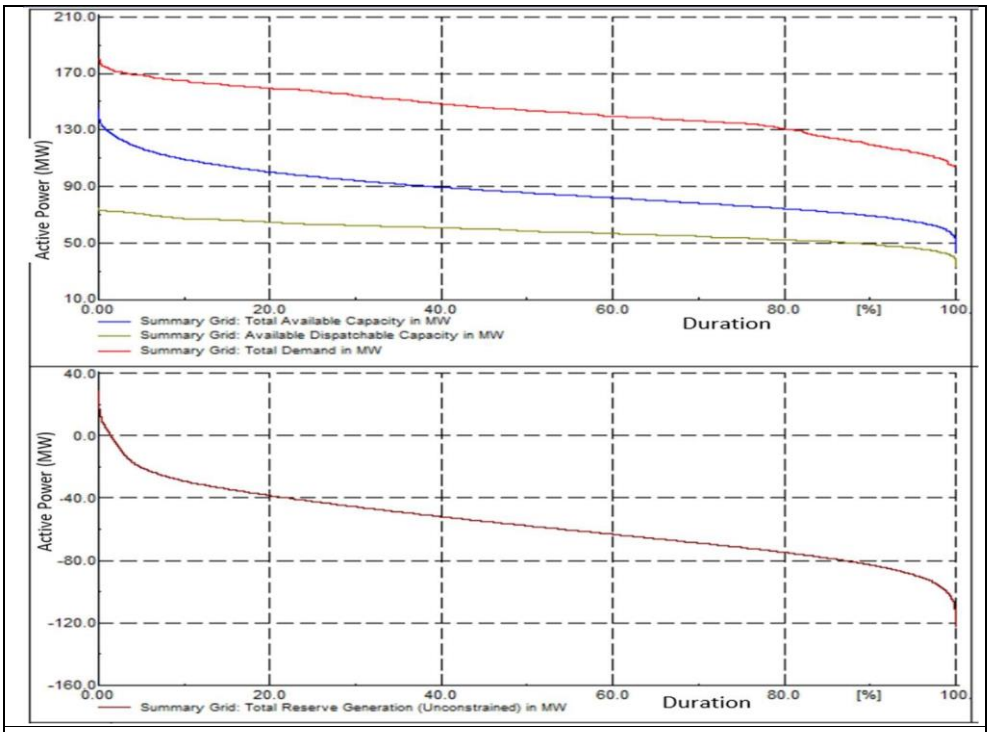

Figure 34: Distribution Plots of 'Muela,50 MW Ha-Ramarothole solar PV, 24 MW Masitise and 34 MW Lets'eng wind farms

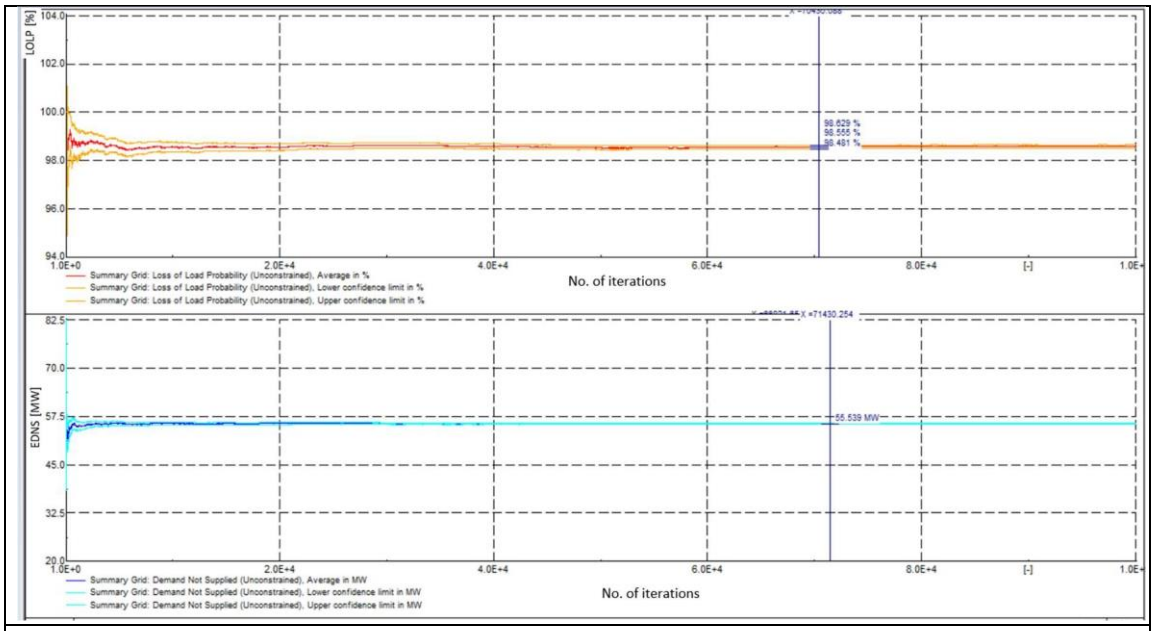

Figure 35: Convergence Plots of 'Muela,50 MW Ha-Ramarothole solar PV, 24 MW Masitise and 34 MW Lets'eng wind farms showing EDNS and LOLP

4.5 Summarized Generation Adequacy analysis results for yearly period under different capacities of solar PV and wind farms

In summary, the indices of EDNS and LOLP for yearly period under different capacities which were obtained from the Monte Carlo simulations are compared in Figure 36 and Figure 37 for generation adequacy analysis. Figure 36 depicts EDNS and LOLP considering 'Muela with HaRamarothole solar PV at 50 and 90 MW plotted also with the scenario of 'Muela combined with 24 MW Masitise and 34 MW Lets'eng wind farms. In all the presented cases, the worst case for the highest EDNS and LOLP is June and July with January and February having lowest EDNS and LOLP. When Ha-Ramarothole solar PV is at 50 MW, the highest EDNS is around 80 MW which occurs in June and the least is 46 MW in January. However, the LOLP for all the months never drops below 98% and from April to October, it is 100%. Considering the expansion stage of HaRamarothole at 90 MW, there is a great improvement with the decrease in both EDNS and LOLP. The highest EDNS is 49 MW occurring in both June and July with LOLP declining to about 98% whereas the least month with EDNS is January with about 24 MW and the LOLP drastically declines to 86%. Lastly, under the scenario of 'Muela and wind farms, the EDNS ranges from 28 to 65 MW while the LOLP is maintained between 94 and 99.2%.

Further, the generation adequacy analysis for all the local generators combined under different capacities of Ha-Ramarothole solar PV is shown in Figure 37 When Ha-Ramarothole is at 50 MW and backed up by wind farms, the EDNS ranges from 17 to 55.6 MW, with the least month being January and the highest being June. The LOLP ranges from 84 to 98.6%. Also, under the scenario of expanded 90 MW Ha-Ramarothole solar PV and wind farms, the EDNS ranges from 8 to 31 MW while the LOLP is maintained between 52 to 77%. The heavy drop in LOLP and EDNS emanates from the compensation profiles of solar PV and wind farms as already discussed considering their predicted performance or generation in the network. As such, combining solar PV and wind farms in the network, shows a significant increase in the reliability of the network to supply the load only with local generators and minimum support from imports. However, at night when solar is unavailable, the indices can be approximated using the scenario of wind farms alone.

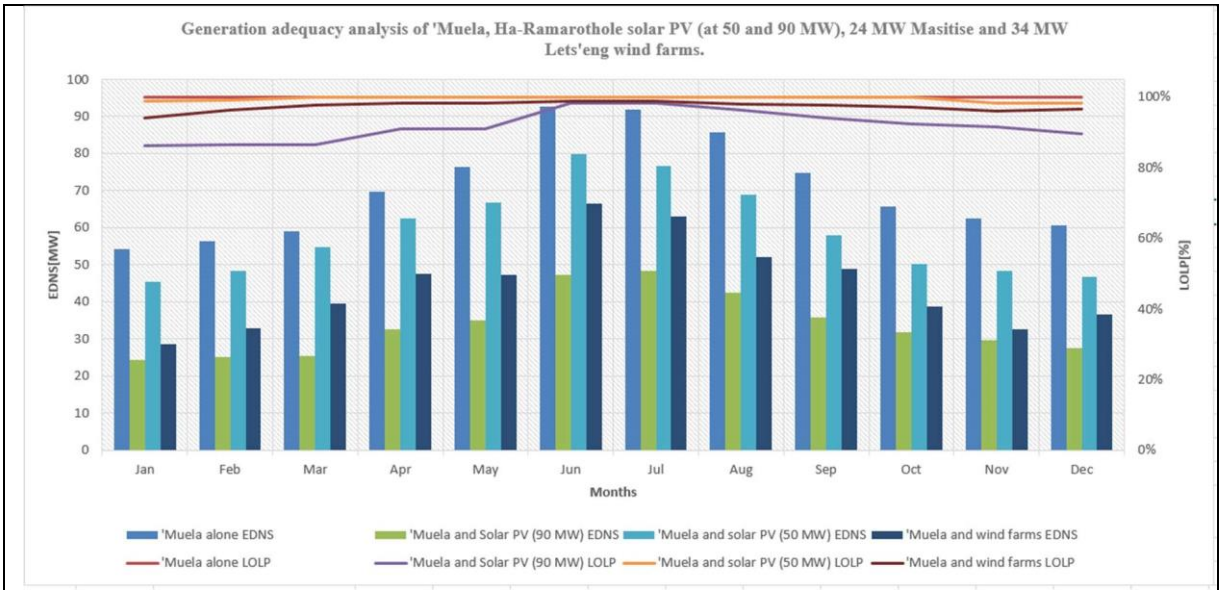

Figure 36: Yearly generation adequacy analysis for: 'Muela+solar PV, and 'Muela+ wind farms

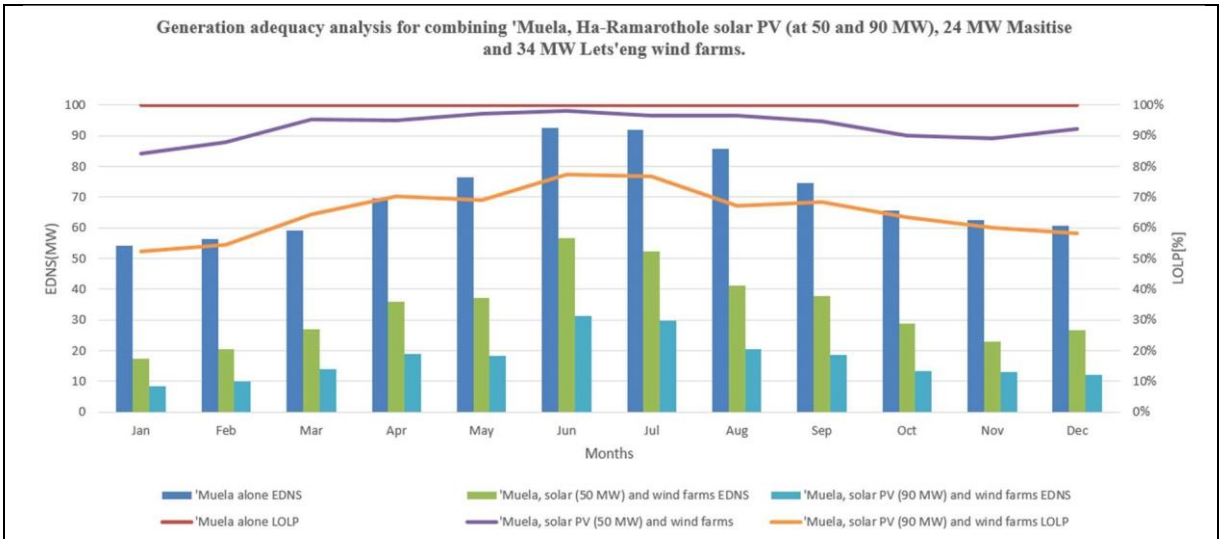

Figure 37: Yearly generation adequacy analysis for: 'Muela+solar PV+ wind farms

4.6 Energy and Costs Estimation through Fixed Bilateral (2018_ 2019)

Table 4 illustrates the monthly modelled energy exchange patterns from DIgSILENT simulations as observed from ‘Muela and imports on every intake point. The highest consumption of imports is 35394.14 MWh which came through in October as ‘Muela was undergoing maintenances. The

percentage contributions from every entry point are demonstrated in Figure 38 which better interprets Table 4. It is seen that, ‘Muela contributes 40-66% to serve the load, while Maseru bulk intake point ranges from 25-46%. Khukhune intake point and Letloepe contributes about 9% and 2% respectively. This means the overall main grid imports (Maseru bulk+Khukhune) contributes between 34-55%, with least imports coming between April and May, when ‘Muela starts to operate at almost its full capacity. This says 'Muela, local generation, supports majority of the load as it is dispatched and imports taking the deficit which is fairly less than ‘Muela. Table 4: Monthly Energy Exchange at different entries

	Energy Consumed (in MWh)					
	Letloepe (Qacha's Nek)	Khukhune (Clarens)	Maseru Bulk (Eskom+EDM)	Muela	Total Imports	Overall Total Energy
Jan	1142.93	5829.45	32858.33	31660.73	39830.71	71491.44
Feb	1016.10	4462.32	24481.82	35175.35	29960.24	65135.60
Mar	1163.52	4837.54	25422.01	40498.54	31423.07	71921.61
Apr	1244.13	4316.26	20247.16	50901.36	25807.55	76708.91
May	1362.27	4975.15	22133.62	52279.80	28471.03	80750.83
Jun	1425.88	5805.94	29943.62	50449.24	37175.44	87624.68
Jul	1483.17	6355.95	31480.38	51603.27	39319.51	90922.78
Aug	1397.18	6506.05	32102.20	46442.47	40005.43	86447.90
Sep	1305.34	5993.22	30397.46	40730.54	37696.02	78426.56
Oct	1304.29	6590.01	35394.14	34621.13	43288.44	77909.56
Nov	1246.93	5654.89	33450.57	32298.18	40352.38	72650.56
Dec	1423.66	6400.44	34582.03	31329.24	42406.12	73735.36
Total	15515.39	67727.23	352493.33	497989.85	435735.95	933725.80

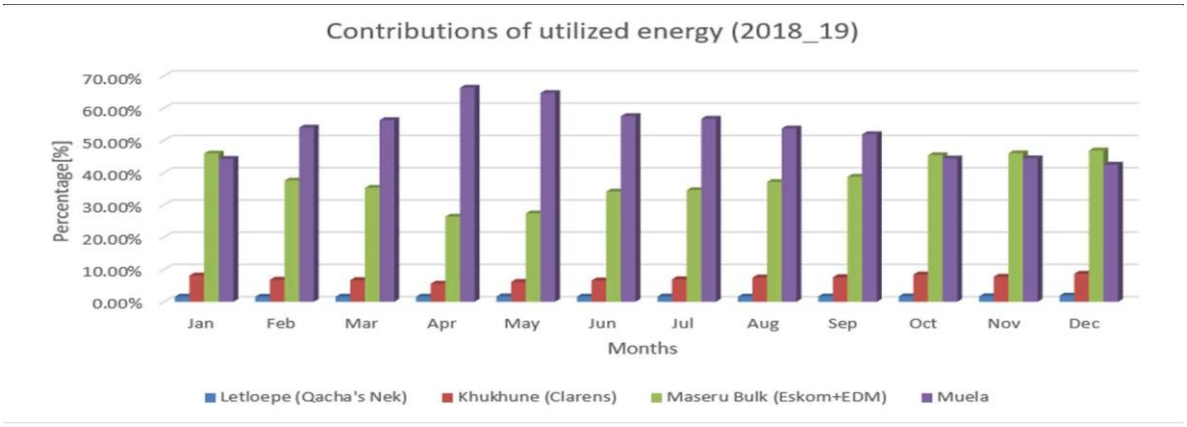

Figure 38: Percentage Contributions from 'Muela and Imports

To model the yearly costs on hourly basis, equation (21) was used to capture every cost of energy at every entry point. Although majority of power supply throughout the year emanates from ‘Muela, because of its low prices, its costs is very cheap as compared to the highly priced imports.

This can be verified by Figure 39 which was extracted from monitoring the yearly costs with respect to power exchange patterns in serving the load. Pointing out the date 20.08.2018 at 10:00 AM, it can be seen that even though 'Muela was supporting about 55% of the load, the cost of its energy is LSL 6700.00 which is even less than Khukhune intake point (LSL 9787.00) which was supporting less than 10% of the load. The most expensive energy costs emanate from Maseru bulk supply (with LSL 70 404.28), which was supporting about 38% of the load.

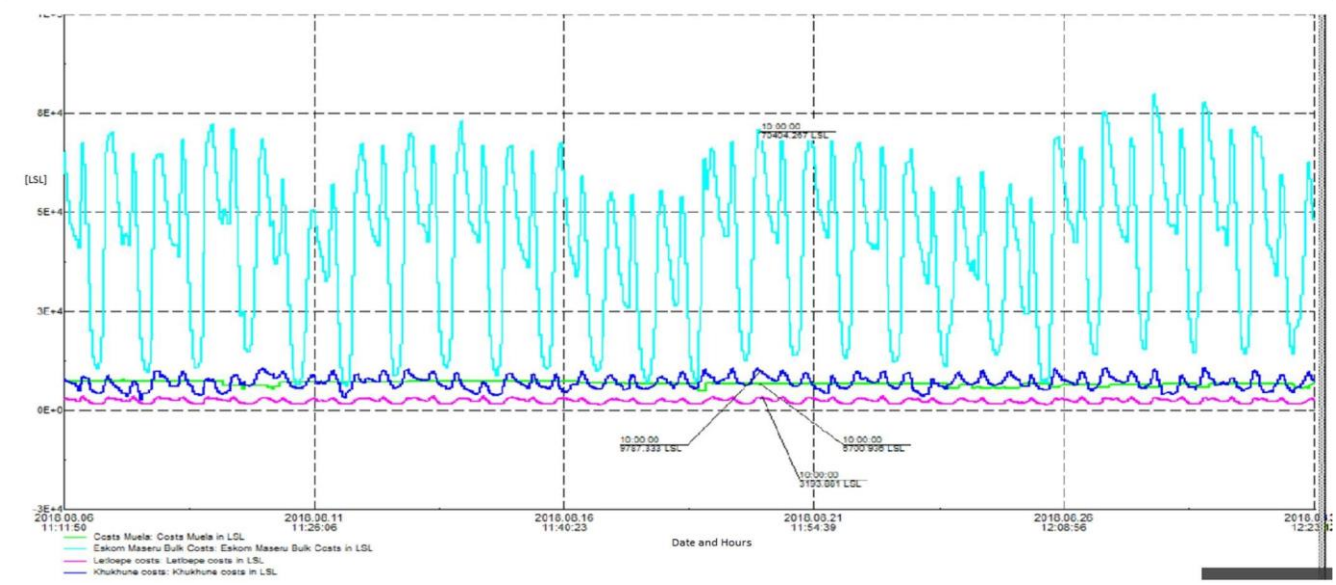

Figure 39: Costs of energy based on hourly exchange patterns

Adding on, the overall yearly costs of energy can be viewed in Table 5 which can be better interpreted using Figure 40 considering percentage contributions. The cost of energy for 'Muela in power procurement are relatively low (8-18%) while from 'Maseru bulk intake point are relatively high ranging from 63-77% with October to December being the highest months in which most money was spent for imports (between LSL 32 447 048.98 and LSL 34 332 312.01). This shows that even though 'Muela supports majority of the load at most times, imports are very expensive even though they support minority of the load. The simulated overall costs from 'Muela in the year is LSL 54 778 883.15, while for imports is LSL 419 324 742.20, which is slightly higher than the actual value of LSL 418.36 million as reported by LEC for 2018_19 financial year. This difference emanates from the difficulty in disaggregating the 'Mabote intake point which consists of power from EDM combined with Eskom, so in this study it was estimated with the Maseru bulk supply charge. The overall costs of energy incurred both locally and from imports sum up to LSL 474 103 625.32, with imports amounting to 88.4% of the total costs. Table 5: Yearly costs based on monthly

	Costs of Energy (in LSL)					
	Letloepe (Qacha's Nek)	Khukhune (Clarens)	Maseru Bulk (Mabote)	Muela	Total Imports	Overall Total Costs
Jan	1451519.59	4955031.89	31872579.57	3482680.62	38279131.05	41761811.67
Feb	1290443.98	3792975.27	23747367.50	3869288.71	28830786.75	32700075.46
Mar	1477673.47	4111911.91	24659348.75	4454838.96	30248934.13	34703773.09
Apr	1580039.90	3668823.89	19771968.33	5599149.47	25020832.13	30619981.59
May	1730082.50	4228875.32	21469607.14	5750777.53	27428564.95	33179342.48
Jun	1810866.31	4935050.09	29046607.66	5549416.88	35792524.06	41341940.93
Jul	1883629.61	5402560.81	30535967.10	5676360.03	37822157.52	43498517.55
Aug	1774415.59	5530144.17	31139137.22	5108671.26	38443696.99	43552368.24
Sep	1657786.95	5094235.95	29485531.79	4480359.61	36237554.68	40717914.29
Oct	1656447.36	5601511.34	34332312.01	3808323.88	41590270.71	45398594.59
Nov	1583596.88	4806657.80	32447048.98	3552799.75	38837303.65	42390103.40
Dec	1808046.30	5440370.10	33544569.16	3446216.46	40792985.56	44239202.02
Total Costs	19704548.44	57568148.53	342052045.20	54778883.15	419324742.17	474103625.32

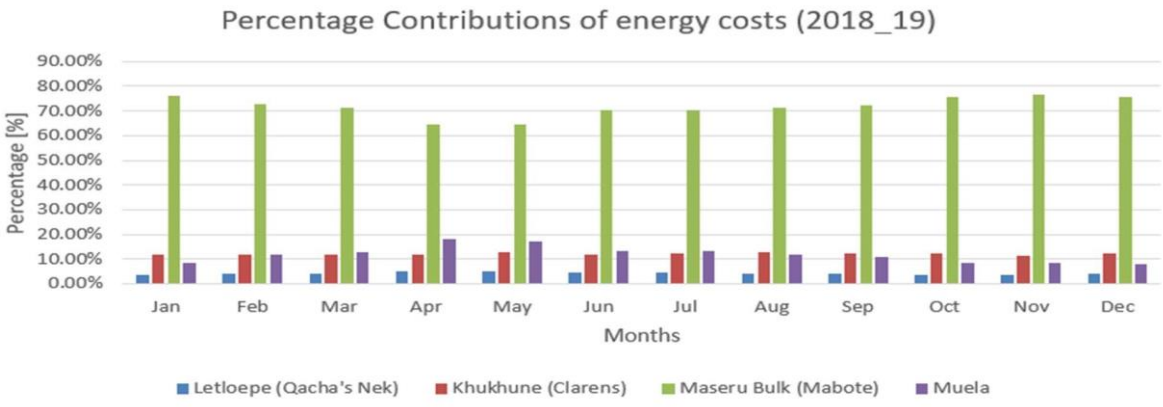

Figure 40: Percentage Contributions of yearly costs of energy from different sources

4.7 Energy contributions and cost of energy considering renewable energy sources and SAPP markets

4.7.1 Yearly energy contributions of 'Muela, VREGs and imports

With introduction of solar PV and wind farms to the network, the yearly consumption of energy from imports declines as shown from Figure 41 and Figure 43. With introduction of solar PV and wind farms to the network, the yearly consumption of energy from imports is expected to decline. Under Scenario 2 of 'Muela and 50 MW solar PV (see Figure 41), the solar farm brings monthly contribution ranging between 4.9 to 10.5 GWh of energy. Also, from June to August, all the energy from solar PV will be consumed, while other months of the year there is small unused or exported energy (ranging from 0.002 to 0.12 GWh) emanating from solar. The main grid imports are reduced to a monthly range of 17.4 to 31.20 GWh and most imports will still be needed in winter when

generation from solar PV declines. The overall used energy from the 50 MW Ha-Ramarothole solar PV is about 93.77 GWh, which is 99.6% of its yearly expected generation. In total, the exported or unused energy is about 0.36 GWh. Hence, in total the overall main grid imports are reduced by 22.3% to about 326.45 GWh.

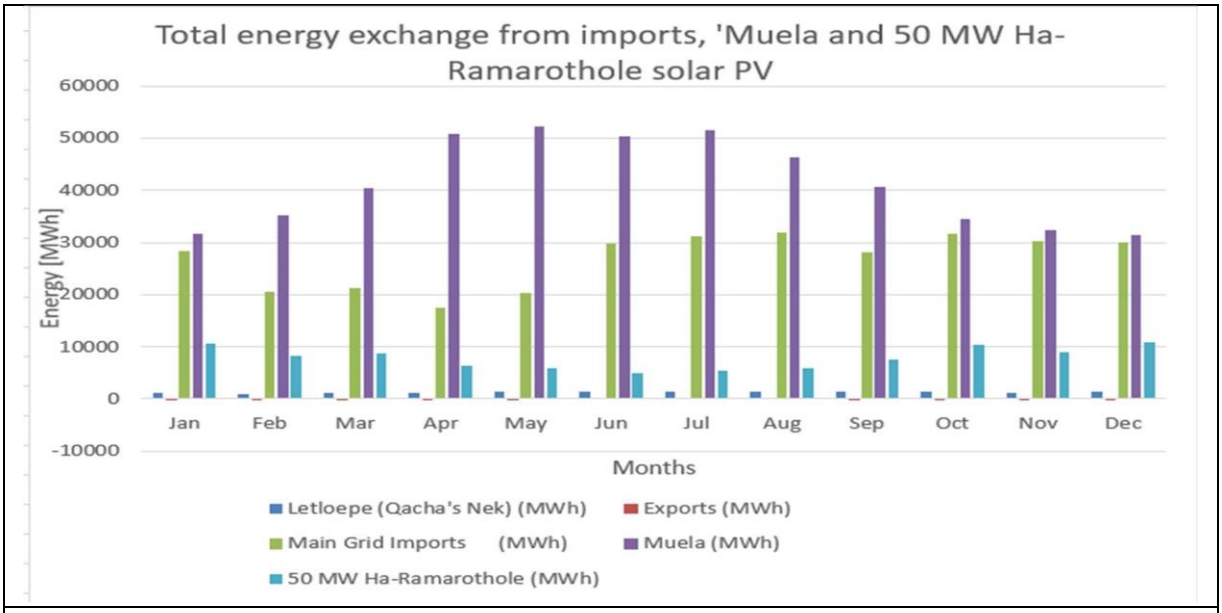

Figure 41: Energy consumption from 'Muela, 50 MW Ha-Ramarothole solar PV and Imports

Considering the Scenario 3 of the 58 MW wind farms operating with 'Muela (as shown in Figure 42), the main grid imports are reduced to a monthly range of about 13.00 to 27.40 GWh which translates to yearly reduction of about 40.2% to 251.48 GWh in total. Masitise wind farm (which is dispatched first) injects a monthly energy of 3.00 to 5.00 GWh while for Lets'eng wind farm, about 7.50 to 14.00 GWh is absorbed in the grid. Out of all the energy these wind farms inject to the network, about 98% of the available energy from Masitise is used to serve the load, while 93% of the available energy from Lets'eng wind farm will be utilized. Most export or unused energy from wind farms is seen to be occurring from January to May and December (with a monthly range of 1.00 to 2.00 GWh), giving annual total of about 13.46 GWh which is about 7.4% of the yearly generation (182.20 GWh) from the wind farms combined.

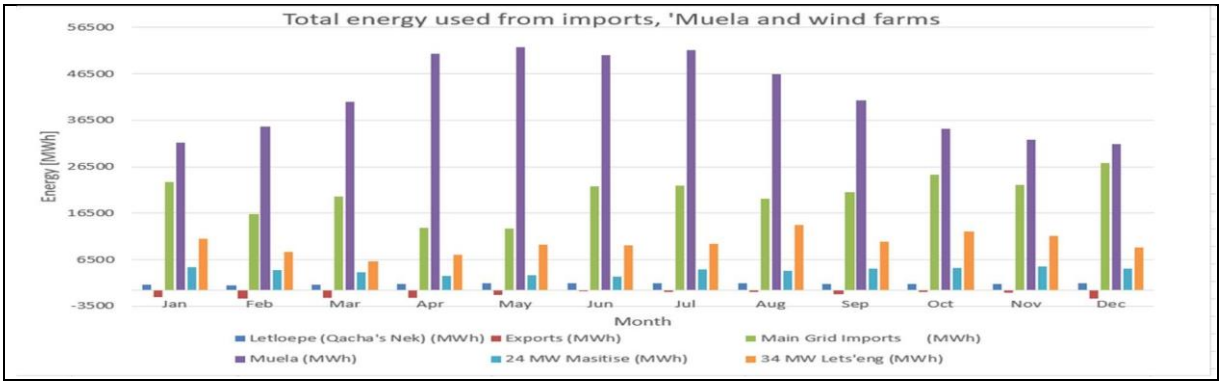

Figure 42: Energy consumption from 'Muela, 24 MW Masitise and 34 MW Lets'eng wind farms and Imports

Combining ‘Muela, solar and wind farms under the fourth scenario (illustrated by Figure 43), the main grid imports are reduced to a monthly range of 8.00 to 18.00 GWh, which brings a significant reduction of about 59.7% yearly consumption of imports to what about 169.23 GWh. The monthly energy contributions of the wind farms drop to ranges of 3.00 to 4.40 GWh and 5.00 to 12.50 GWh for Masitise and Let’seng, respectively. When combined with solar PV, the wind energy injected into the main grid declines to 91% and 81% for Masitise and Lets’eng wind farms, respectively. In all these scenarios, about 99.6% of Ha-Ramarothole solar PV energy will be absorbed to serve the load and exported energy emanates mainly from wind farms since solar is dispatched first ahead of wind. Under the last scenario, exports (or unused energy) are seen to occur even in winter season. This is because wind generation is available even at night (during off-peak periods). On top of that, in most cases both the wind farms are almost at their rated capacities, with ‘Muela included as it operates at around 99.3% of its rated capacity most of the time regardless of whether it is day or night. The exported or unused energy increases to about 25.34 GWh under this scenario. In all scenarios, since Qacha’s Nek grid is isolated, the imports are maintained at about 15.52 GWh.

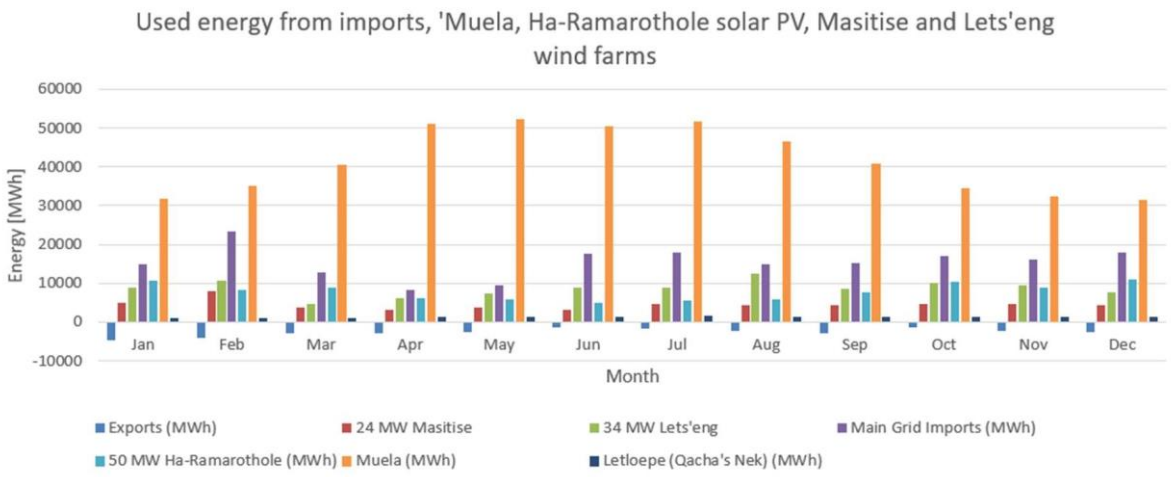

Figure 43: Energy consumption from 'Muela, 50 MW Ha-Ramarothole solar PV 24 MW Masitise and 34 MW Lets'eng wind farms and Imports

4.7.2 Yearly cost of local energy ('Muela+50 MW Ha-Ramarothole solar PV) and imports under SAPP markets

As already discussed from the previous section of generation adequacy analysis, introduction of solar PV and wind farms brings certain level of energy security to the network as seen by decrease in LOLP and EDNS. Therefore, with the introduction of renewable energy sources to the network, the aim is to shift the power procurement strategy from fixed bilateral contracts and procure under SAPP markets being DAM, FPM weekly and FPM monthly. Under all the scenarios of DAM, FPM weekly and monthly, the cost of local power will remain as stated above (because of a fixed charge per kilowatt hour) and the varying costs will be only for imports due to fluctuating hourly prices from these markets.

From Figure 44 to Figure 46 is an illustration of the costs of energy considering DAM, FPM weekly and monthly that would be incurred if 50 MW Ha-Ramarothole solar PV and 'Muela were combined. Under DAM, the monthly cost main grid imports range from LSL 8.56 million to LSL 29.7 million illustrated in Figure 44. However, with the same amount of energy consumed, the costs of main grid imports increases to a range of LSL 14.9 million to LSL 52.1 million and LSL 6.54 million to LSL 78.8 million for FPM weekly and monthly as shown by Figure 45 and Figure 46 respectively. In all cases, the least costs of imports is incurred in April and most expenses incurred

in July, the high demand month. Hence, in April LEC could opt for FPM monthly and continue with DAM throughout the year as it would incur roughly LSL 2 million less than the overall costs of main grid imports.

Furthermore, the overall costs of importing from Qacha's Nek intake point reduces by 47.7% to about LSL 10.4 million from the status quo under DAM. On the other hand, the figure slightly declines by LSL 2.29 million to LSL 17.4 million under FPM weekly and slightly decreases by LSL 1.83 million to LSL 17.9 million under FPM monthly. It is seen that under all markets, the costs of imports for Qacha's Nek (Letloepe) are lower than the yearly costs of imports from the base case with the same utilized energy. This implies that, if LEC procured under SAPP markets in 2018_19 financial year, it would have endured less costs when compared with the usual practice of fixed bilateral contracts. Because of the fact that Letloepe is an isolated grid, this cost of energy under SAPP markets will not be affected with the penetrations of renewable generators.

Moreover, the total yearly cost of imports (main grid imports and Qacha's Nek imports) under DAM with introduction of solar PV adds up to about LSL 240.79 million with main grid imports taking a share LSL 230.42 million and the rest is due to Letloepe imports. Nonetheless, with the same energy utilized from imports, the yearly costs of energy for the overall imports is LSL 407.81 million for FPM weekly (Figure 45) and LSL 410. 95 million for FPM monthly (Figure 46) with main grid imports taking a share of 95.7% of the overall costs. The FPM monthly is slightly higher than the FPM weekly (with about LSL 3.14 million) and about 1.71 times the cost of imports under DAM.

Additionally, the overall costs of energy (local+imports) under this scenario translates to LSL 373.39 million considering DAM and further sums up to LSL 540.42 million and LSL 543.56 million for FPM weekly and monthly, respectively. In all cases, solar PV contributes a monthly range of LSL 4.09 million to LSL 9.08 million, which sums up to LSL 77.8 million to the costs of energy utilized. However, if the same energy used from solar was imported, it would costs about LSL 65.5 million under DAM, LSL 109.16 million with FPM weekly and LSL 119.56 million under FPM monthly. Hence, indicating that, importing from DAM is cost effective when compared with purchasing local energy from solar and more expensive to import using other markets.

Comparing all the markets under this scenario as shown from Figure 44 to Figure 46, DAM is the most cost effective market to procure power, followed by FPM weekly as for majority of the

months, the costs of imports from DAM is always less than other markets for the same energy consumed. FPM weekly are almost 1.5 times the costs of DAM in winter season, while for FPM monthly the costs are almost double the costs of energy incurred in winter from DAM. Comparing local energy with mainly the imports from the main grid, it is seen that even though the main grid imports are reduced, under FPM weekly and monthly their monthly costs are always higher than energy from 'Muela and solar PV. Furthermore, from June to August, the costs of main imports are almost double the costs incurred even in the first scenario of fixed bilateral contracts when 'Muela was alone. This is because of the highly fluctuating and expensive peak prices in the SAPP markets.

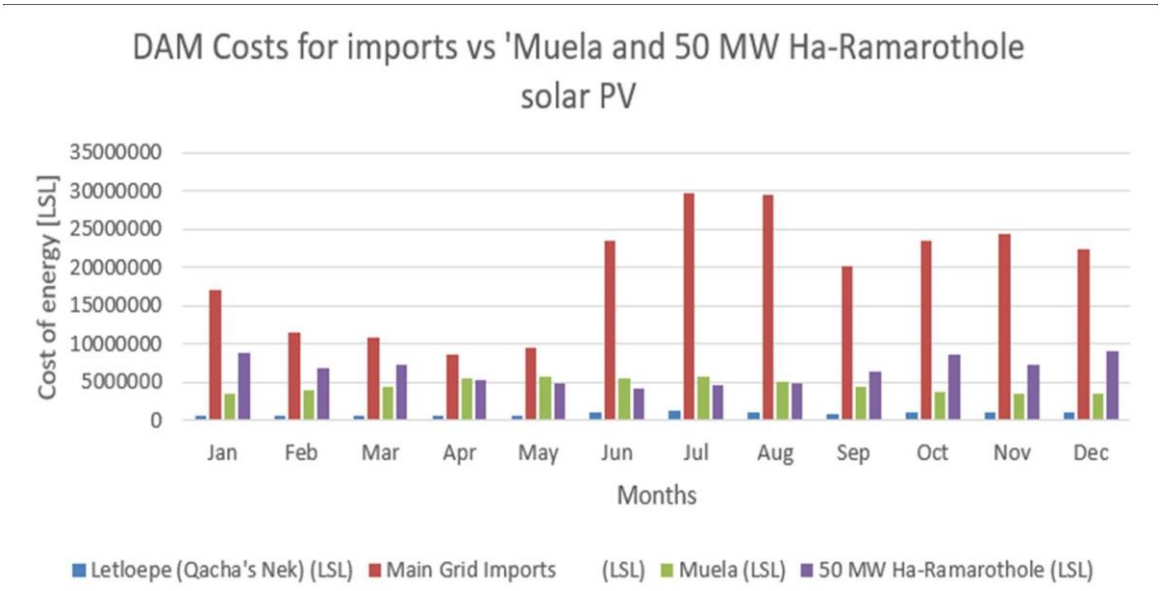

Figure 44:DAM costs for imports combined with cost from 'Muela and 50 MW Ha-Ramarothole

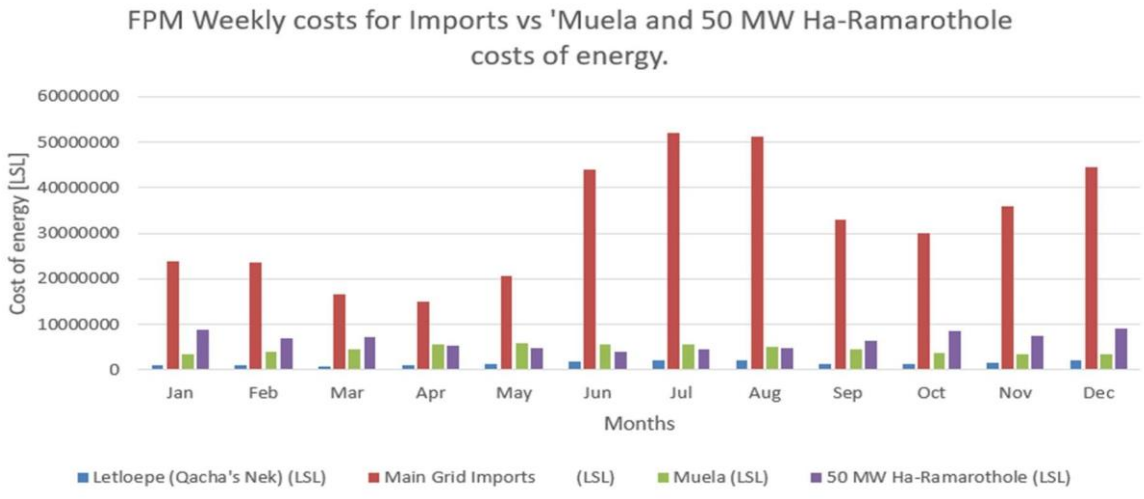

Figure 45:FPM weekly costs for imports combined with cost from 'Muela and 50 MW Ha-Ramarothole

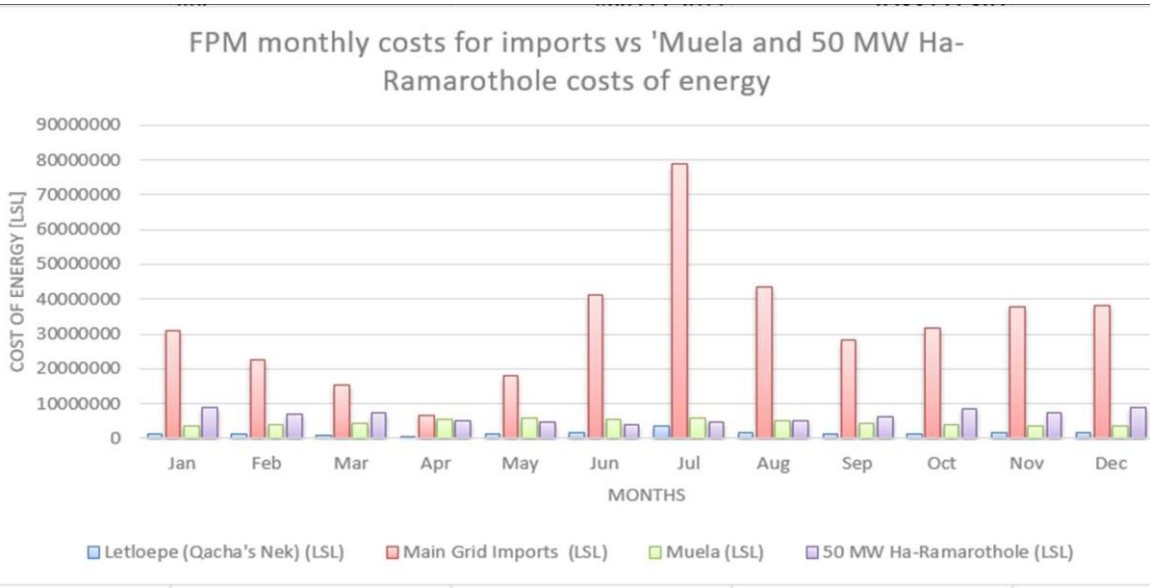

Figure 46:FPM monthly costs for imports combined with cost from 'Muela and 50 MW Ha-Ramarothole

4.7.3 Yearly costs of local energy ('Muela+24 MW Masitise and 34 MW Lets'eng wind farms) and imports under SAPP markets

Figure 47 to Figure 49 illustrates the costs of imports considering SAPP markets vs local energy costs that are calculated to be incurred considering penetrations of wind farms operating with 'Muela. As the main grid imports are greatly minimized under this scenario as compared to solar

and ‘Muela alone, the costs of energy also declines to a monthly range of about LSL 6.29 million to LSL 21.9 million under DAM, as shown in Figure 47. Thus with the same energy utilized from imports, the costs translates to a monthly range of LSL 13.9 million to LSL 42.1 million and LSL 4.97 million to LSL 62.2 million considering FPM weekly and FPM monthly as shown by Figure 48 and Figure 49, respectively. The overall cost of energy for imports under DAM add up to LSL 193.57 million with main grid imports taking a chunk of LSL 183.20 million. On the other hand, the main grid imports costs LSL 320.54 million for FPM weekly and LSL 330.34 million under FPM monthly with main grid imports contributing an average of 95% to the overall costs of imports. This great minimization of imports and their cost is attributed to the mostly available wind energy, during day and night.

Considering the scenario of DAM, the sum of local energy combined with imports sum up to LSL 425.52 million which is about LSL 52.13 million higher when compared to the total cost of energy incurred with the scenario of solar PV and ‘Muela. Taking cases of other markets, the overall sum of the costs considering imports and local energy drastically escalates to LSL 570.78 million and LSL 579.71 million for FMP weekly and monthly, respectively. This great increase in costs can be attributed to high increase in wind energy absorption. Hence, minimizing imports with wind energy, the overall costs of local energy greatly increases due to cost-reflective wind energy. The monthly costs incurred for utilizing wind energy fall to a monthly range of LSL 10 million to LSL 18.2 million, with the least cost occurring in March and the highest in August. The total costs of wind energy is LSL 177.18 million with Masitise contributing about 30% to the overall cost. However, if the same energy of wind was procured under the presented SAPP markets, the costs would translate to LSL 108.11 million under DAM, LSL 182.29 million with FPM weekly and LSL 192.24 million under FPM monthly. Therefore, indicating that procuring from wind could be a better alternative than FPM weekly and monthly markets. Even so, under this scenario of wind farms and ‘Muela, the DAM is still found to be more cost effective when combined with local energy as it is seen to offset the expensive costs from wind energy.

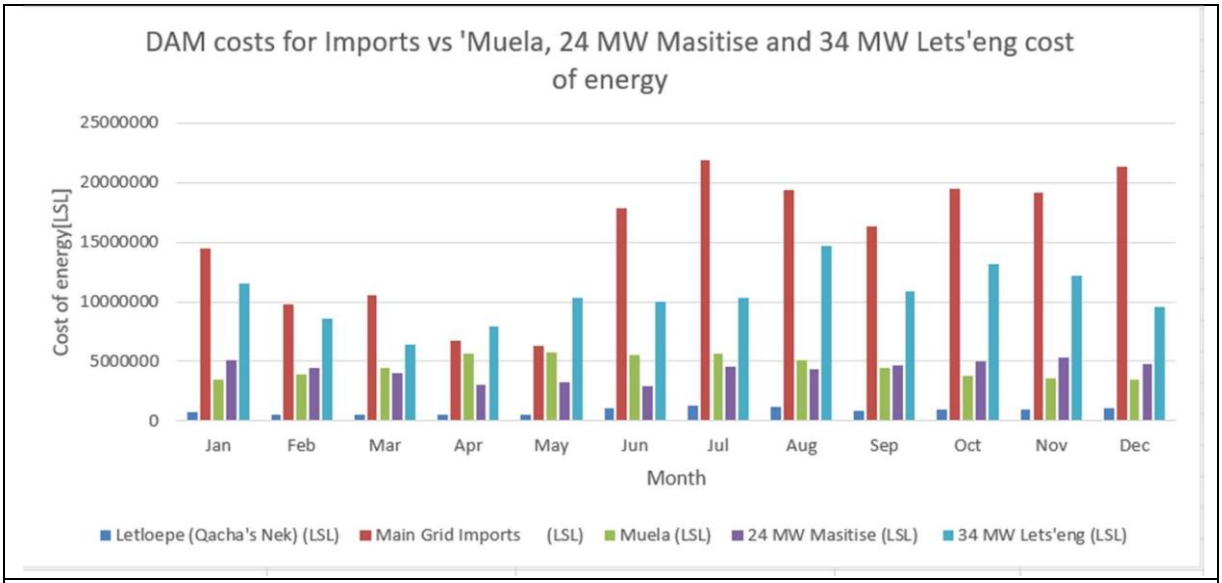

Figure 47:DAM costs for imports combined with cost from 'Muela, 24 MW Masitise and 34 MW wind farms, and Imports

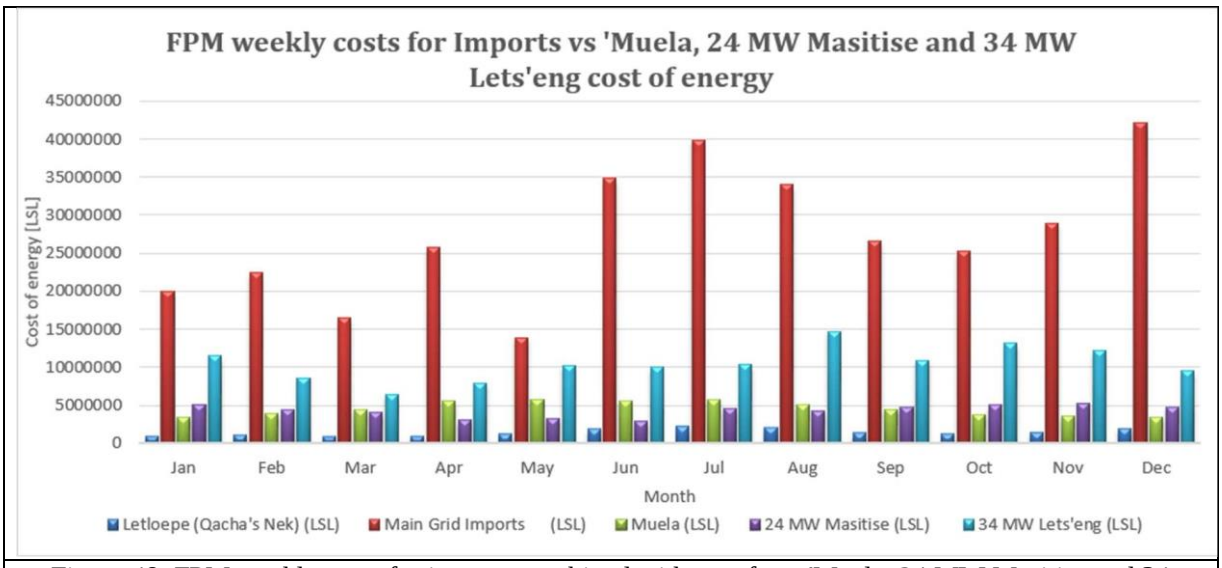

Figure 48: FPM weekly costs for imports combined with cost from 'Muela, 24 MW Masitise and 34 MW wind farms, and Imports

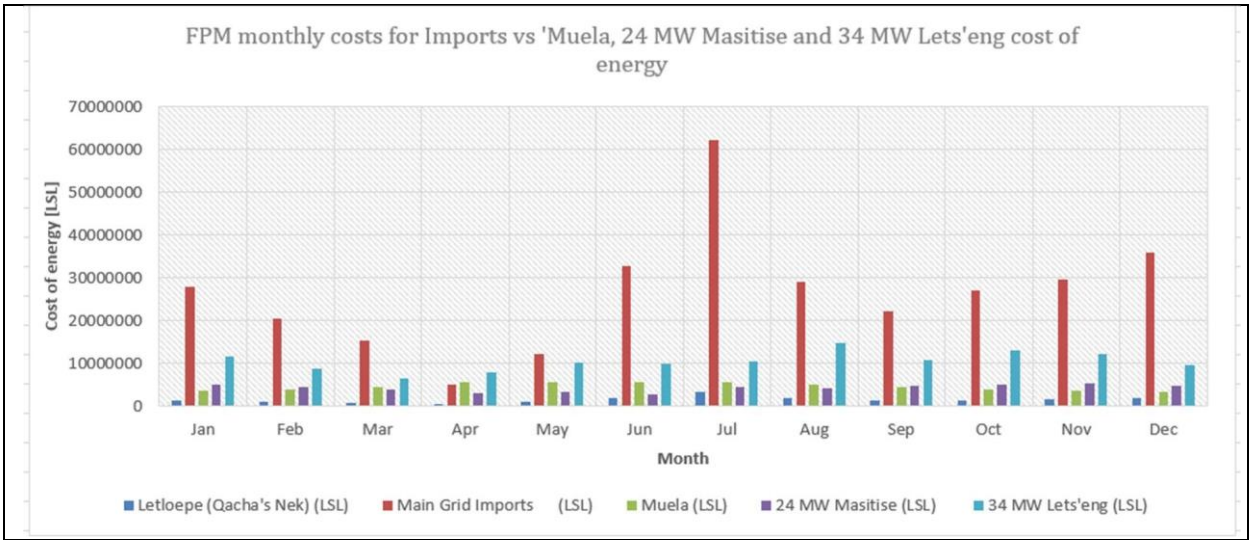

Figure 49:FPM monthly costs for imports combined with cost from 'Muela, 24 MW Masitise and 34 MW wind farms, and Imports

4.7.4 Yearly costs of local energy ('Muela+50 MW Ha-Ramarothole solar PV+24 MW Masitise and 34 MW Lets'eng wind farms) and imports under SAPP markets

As already discussed that backing up 'Muela with both solar PV and wind farms results in heavy decline hourly EDNS and much reduced LOLP when compared to other cases, then under this scenario, the imports are heavily minimized as well as their costs considering all the markets as portrayed from Figure 50 to Figure 52 considering SAPP markets under study. Under DAM, shown in Figure 50, the monthly costs of main grid imports never exceeds LSL 20 million, while FPM weekly a maximum of costs incurred arises in July with about LSL 32.86 million as portrayed by Figure 51. Similarly, with FPM monthly the highest costs incurred for importing is July with LSL 48.98 million as shown in Figure 52. The yearly costs of imports under DAM in this case amount to LSL 157.88 million with main grid imports constituting to 94% of the overall costs. Also, the costs of imports are seen to sum up to LSL 249.51 million and LSL 250.74 million for FPM weekly and monthly, respectively, with main grid imports taking a share of about 93% of average for both markets.

In this case, it is seen that imports costs are greatly minimized due to increased absorption of local energy. As already stated, solar and 'Muela still retain their stated costs throughout, in this scenario, wind energy is minimized due to consumption of solar energy. Therefore, the costs of overall wind

energy declines to LSL 165.08 million, with Lets'eng contributing to about 66% of the overall costs of wind. As such, the overall costs of imports combined with local energy adds up to LSL 455.57 million under DAM and the overall cost of energy amount to LSL 547.21 million and LSL 548.43 million for FPM weekly and monthly, respectively. Like all other scenarios of different renewable energy penetration, DAM is still more favorable and cost effective than all the markets.

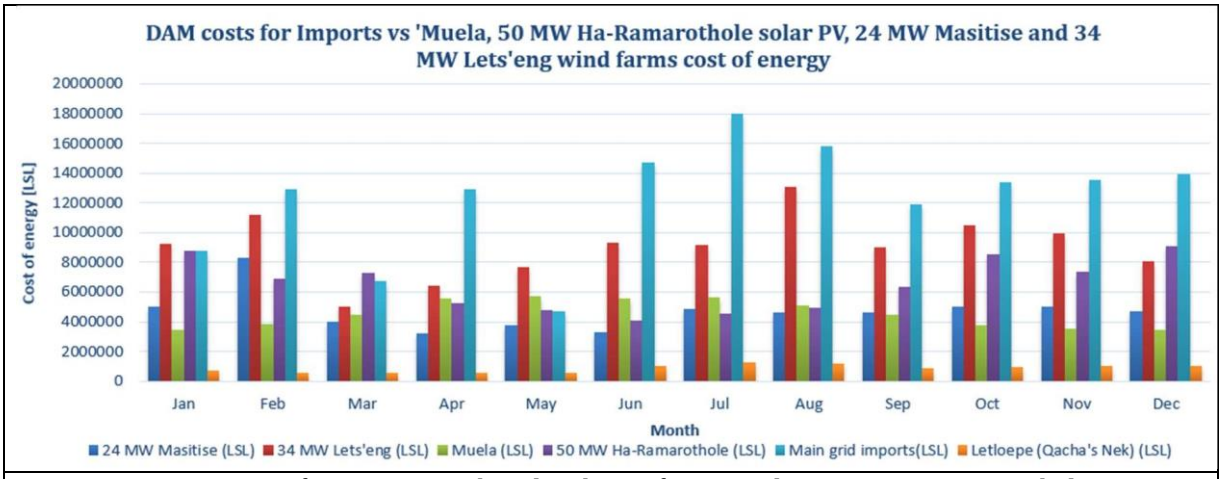

Figure 50: DAM costs for imports combined with cost from 'Muela, 50 MW Ha-Ramarothole 24 MW Masitise and 34 MW wind farms, and Imports

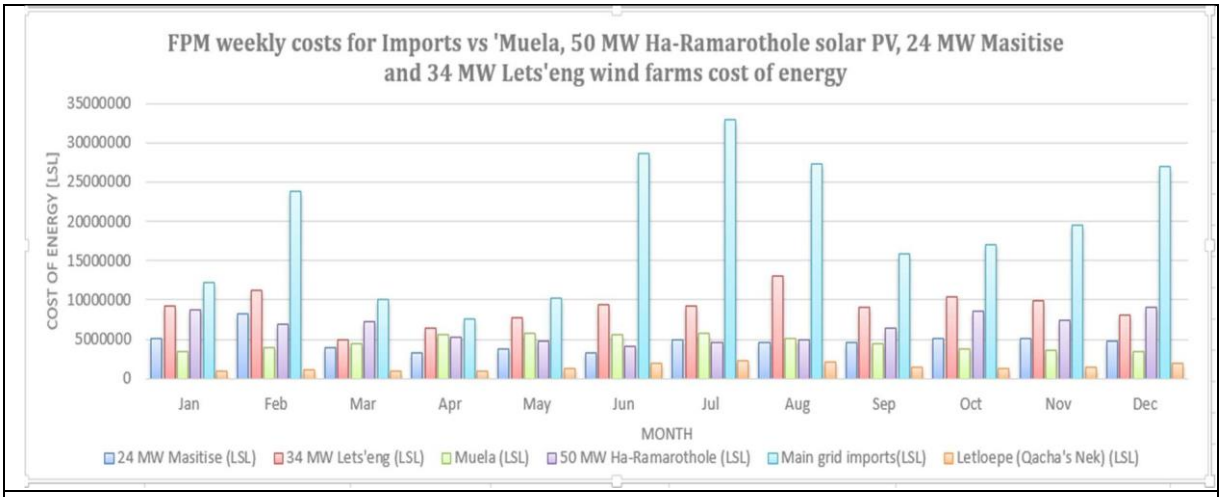

Figure 51: FPM weekly costs for imports combined with cost from 'Muela, 50 MW Ha-Ramarothole 24 MW Masitise and 34 MW wind farms, and Imports

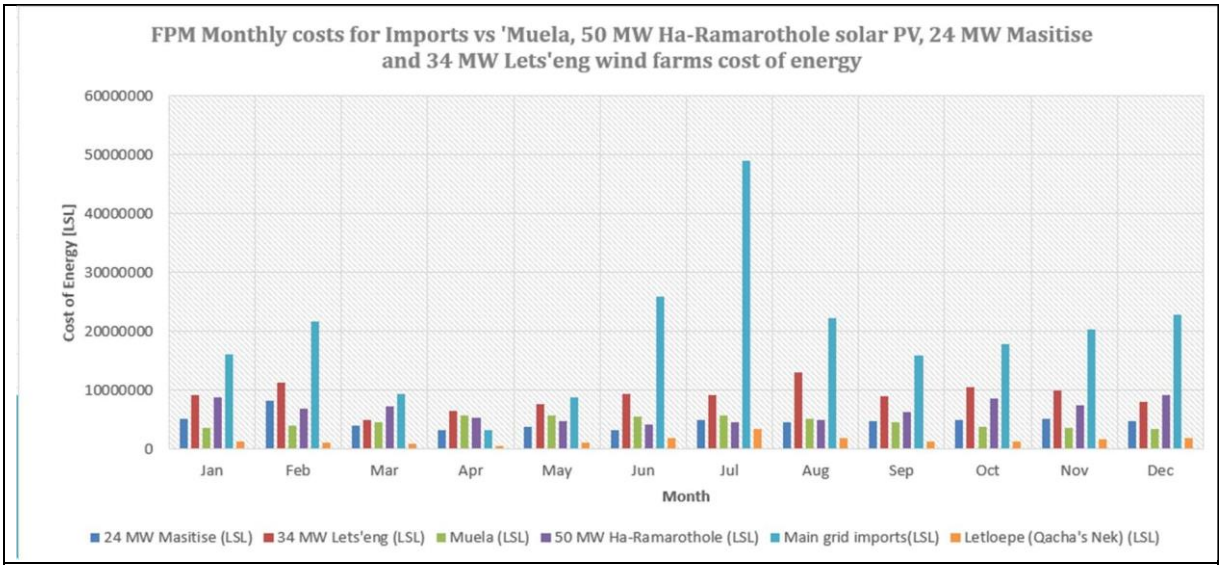

Figure 52: FPM monthly costs for imports combined with cost from 'Muela, 50 MW Ha-Ramarothole 24 MW Masitise and 34 MW wind, and Imports

In this work, the generation adequacy of locally committed generators was analyzed using the Monte Carlo method, as well as the performance of local generators when they were dispatched, using the DiGSILENT software. The study effort provided a power dispatching strategy where local renewable generators are dispatched first ahead of imports, using a similar approach to the ELD problem incorporating renewable generators, whereby renewable generators are dispatched first, and prior to coal or thermal generators. The findings indicate that the 50 MW HaRamarothole solar PV farm has the ability to minimize imports by 22.3% with almost all its annual production exhausted and fed to the grid. Additionally, only 0.5% of its annual production is surplus, demonstrating excellent use of solar output when available. In all scenarios involving wind farms and local generators, more than 80% of the overall estimated generation from the two wind farms can always be incorporated into the network. Furthermore, in all of the offered scenarios, the addition of wind farms to the network resulted in a significant reduction of the absorption of imports by over 40%. As a result, minimization of imports is accomplished in every situation, and excellent local generation use is demonstrated.

The network's generation adequacy analysis showed a significant improvement with the addition of renewable generators, as seen by a decrease in LOLP and EDNS in all scenarios compared to 'Muela alone. The network's security of power supply has not really improved when solar at 50

MW and 'Muela are coupled, as the least LOLP is shown to be 98% and from April to October the LOLP is still stagnant at 100%, which is similar to that of 'Muela alone. Therefore, more imports will still be anticipated for a consistent supply of the load during this time when LOLP is at its highest. The highest LOLP achieved when solar generation is increased to 90 MW is 98%, and the lowest is roughly 86%. Consequently, it becomes clear that substantially higher solar capacities and the potential for future storage are needed in order to attain much more stable supply with solar and 'Muela alone. The networks' ability to deliver the load has greatly improved in the case of wind at 58 MW, nevertheless, as the greatest LOLP is almost 99% and the lowest is 94%. The LOLP results of solar at 90 MW are practically equivalent to those of wind farms at 58 MW, demonstrating that smaller wind capacities as compared to solar can be more adequate for meeting the load. In every scenario, the EDNS is observed to decline from the base case ('Muela alone) by more than 10 MW over the course of the full year. Higher margins of around 40 MW are seen with every combination of adding local generators and expanding the network's capacity. Therefore, diversifying LEC power sources with local renewable energy generators can improve local energy security and further enable the network to be more adequate in supplying the load with the minimum support from imports.

The study evaluated the cost implications of acquiring power locally and through SAPP markets as the network becomes more reliable to provide the load with various combinations of local generators, as evidenced by a drop in LOLP and EDNS. When 'Muela is the only local source of power for LEC, the base case of power procurement from imports with fixed bilateral contracts can be compared to in order to arrive at the conclusion that procuring from solar at 50 MW and 'Muela combined with DAM is less expensive by roughly LSL 45 million. However, it is expected that other markets (FPM weekly and monthly) will cost about LSL 120 million more than the base scenario. The results indicate that the overall cost of energy in the scenarios of the wind farms, 'Muela and DAM is approximately LSL 6.2 million higher than the expenses of energy incurred in the base case. When other markets are taken into account, the cost of energy increases significantly by to a range of LSL 150 million to LSL 160 million from the base scenario. The overall cost translate to LSL 36 million more than the base case when all local generators are combined and paired with DAM, and they increase further by around LSL 129 million under different markets. In conclusion, diversifying the power sources of LECs with solar and using DAM appear to be more cost-effective alternative than other markets and the customary method of using fixed bilateral contracts. However, even with the DAM, when compared to the base case, the overall costs that

LEC bears are significantly higher with the addition of wind in all scenarios. But in every scenario, purchasing through DAM is viewed as being less expensive as compared to other markets. This leads to the conclusion that by using DAM in conjunction with local generators, LEC may purchase power at a lower cost than other markets.

5.0 Conclusions and Recommendations

The study presented a power dispatching approach whereby all power from local generators must be dispatched and procured first by LEC ahead of imports. 'Muela alone being the only source of power for LEC can only meet about 40-66% of the load demand and at all times it is insufficient to meet the load alone. Therefore, introduction of 50 MW Ha-Ramarothole solar PV increases the local energy security and the main grid imports are reduced by 22.3% with overall used energy from solar PV being 99.6% of its yearly expected generation. If wind farms under the stated capacities could operate alone with 'Muela, the main grid imports could be reduced by 40.2% and significantly minimized by 59.7% through combination of solar PV at 50 MW, wind farms and 'Muela scenario. However, introduction of wind and solar PV to the main network does not affect the contribution of imports to Qacha's Nek region, as it is isolated. Out of all the energy these wind farms inject to the network, about 98% of the available energy from Masitise is used to serve the load, while 93% from the available energy from Lets'eng wind farm will be utilized, under the scenario of 'Muela and wind farms. However, when combined with solar PV at 50 MW, their utilized energy declines to 91% and 81% for Masitise and Lets'eng wind farms, respectively. Despite of combination of wind, 99.62% of 50 MW Ha-Ramarothole solar PV energy will be absorbed to serve the load because solar is consumed first ahead of wind, as the power dispatching strategy.

Apart from that, the study demonstrated that with penetrations of solar PV and wind generators, specifically under the capacities of 50 MW Ha-Ramarothole solar PV, 24 MW Masitise and 34 MW Lets'eng wind farms, there are times when the available energy exceeds the local demand, and energy could be exported to Eskom. Furthermore, the generation adequacy analysis for all local generators was performed for the entire year and through all the scenarios of different penetrations of solar PV and wind farms, the EDNS and LOLP were both seen to decline from when 'Muela was operating alone. Although it was revealed that the EDNS never drops to 0 MW and the LOLP is seen to never drop even below 50% for all scenarios considered, there is a great or positive improvement in the network's ability to supply the load with introduction of solar PV for both different capacities and wind farms. Also, solar PV is more adequate at higher capacities and backing up solar PV with wind farms illustrate great decline in EDNS and LOLP and show less dependency on imported power from imports as there are times when imports are not needed into the main grid. Therefore, the study performed an analysis by evaluating different SAPP markets on how power could be procured under these markets to minimize the costs of purchasing power from imports.

Comparing all the markets, DAM is the cheapest or cost-effective market to procure power, with the FPM monthly being the most expensive. However, FPM weekly is comparable to FPM monthly except for winter season. FMP monthly is only seen to be cheaper than all markets only in April and therefore it can be a viable option instead of DAM during this month.

As the network is seen to be more adequate to supply the load with local generators and imports being heavily minimized through the introduction of solar PV and wind farms into the network, the cost of power procurement locally increases as well considering the given charges of energy per kilowatt hour from both solar PV and wind. Importing from DAM the same amount of energy that solar contributes, LEC could save LSL 12.3 million. Nevertheless, when compared with other markets, the same amount of energy costs about LSL 30 to 41 million more when compared with solar. In the case of wind, purchasing the same energy from DAM is seen to be more cost effective as opposed to buying it locally from wind. This is because of the cost reflective wind energy. However, LEC can save between LSL 5 and 15 million when compared to other markets, making wind energy a more affordable choice. To mitigate the high costs of renewable energy, introduction of auction programs for IPPs, procuring power locally could be affordable and ease the burden from LEC as well as end users. As such, these programs could help promote renewable energy absorption in Lesotho.

Although the cost of local power procurement was done on 50 MW Ha-Ramarothole solar PV, 24 MW Masitise and 34 MW Lets'eng wind farms, it can still be performed in the similar manner with any other capacities. Also, even though this study did not use any forecasting methodologies in procuring power under these markets, LEC will require at least two trained and licensed cross border traders to provide efficient price signals, forecast load demand, and outputs of renewable generators, for the procurement and transmission of electricity from imports. Furthermore, a more in-depth assessment with a focus on the generating adequacy analysis can be carried out given the plans to expand the LEC electrical network over the next years and the addition of new local generators to the network to boost local energy security.

These power dispatch and costing model assumptions neglect the economic risks of power not being bought in the SAPP markets as well as having to dump the excess local energy. Nevertheless, the importance of allowing excess energy, is to show the significance of having enough or more than enough local power that LEC can buy, resell it to end-users as well as grant an opportunity to

participate in SAPP markets for generating revenues or economical gain. Also, if there is any excess, this will introduce the need to store this energy for later use. This can be done in future studies through an analysis of whether it would be more beneficial to export the power or store it for night time as a reserve.

References

[1] S. Mokeke and L. Z. Thamae, “The impact of intermittent renewable energy generators on Lesotho national electricity grid,” Electr. Power Syst. Res., vol. 196, p. 107196, Jul. 2021, doi:

10.1016/j.epsr.2021.107196.
[2] “Renewables 2021: Global Status Report.” Paris: REN21 Secretariat, 2021. Accessed: Sep. 30, 2021. [Online]. Available: https://erc.nul.ls/publications/reports
[3] Y. Sasaki, T. Tsurumi, N. Yorino, Y. Zoka, and A. Beni Rehiara, “Real-time dynamic economic load dispatch integrated with renewable energy curtailment,” J. Int. Counc. Electr. Eng., vol. 9, no. 1, pp. 85–92, Jan. 2019, doi: 10.1080/22348972.2019.1686861.
[4] M. Nemati, M. Braun, and S. Tenbohlen, “Optimization of unit commitment and economic dispatch in microgrids based on genetic algorithm and mixed integer linear programming,” Appl. Energy, vol. 210, pp. 944–963, Jan. 2018, doi: 10.1016/j.apenergy.2017.07.007.
[5] V. K. Jadoun, V. C. Pandey, N. Gupta, K. R. Niazi, and A. Swarnkar, “Integration of renewable energy sources in dynamic economic load dispatch problem using an improved fireworks algorithm,” IET Renew. Power Gener., vol. 12, no. 9, pp. 1004–1011, Jul. 2018, doi: 10.1049/iet-rpg.2017.0744.
[6] J. Kim and K.-K. K. Kim, “Dynamic programming for scalable just-in-time economic dispatch with non-convex constraints and anytime participation,” Int. J. Electr. Power Energy Syst., vol. 123, p. 106217, Dec. 2020, doi: 10.1016/j.ijepes.2020.106217.
[7] H. Wu, X. Liu, and M. Ding, “Dynamic economic dispatch of a microgrid: Mathematical models and solution algorithm,” Int. J. Electr. Power Energy Syst., vol. 63, pp. 336–346, Dec. 2014, doi: 10.1016/j.ijepes.2014.06.002.
[8] J. K. Pattanaik, M. Basu, and D. P. Dash, “Dynamic economic dispatch: a comparative study for differential evolution, particle swarm optimization, evolutionary programming, genetic algorithm, and simulated annealing,” J. Electr. Syst. Inf. Technol., vol. 6, no. 1, Dec. 2019, doi: 10.1186/s43067-019-0001-4.
[9] C. Kumar and T. Alwarsamy, “Dynamic Economic Dispatch – A Review of Solution Methodologies,” European Journal of Scientific Research, vol. 64, no. 4, p. 22, 2011.
[10] T. G. Hlalele, R. M. Naidoo, J. Zhang, and R. C. Bansal, “Dynamic Economic Dispatch With Maximal Renewable Penetration Under Renewable Obligation,” IEEE Access, vol. 8, pp. 38794–38808, 2020, doi: 10.1109/ACCESS.2020.2975674.
[11] N. Tyagi, H. M. Dubey, and M. Pandit, “Economic load dispatch of wind-solar-thermal system using backtracking search algorithm,” Int. J. Eng. Sci. Technol., vol. 8, no. 4, pp. 16–27, Jan. 1970, doi: 10.4314/ijest.v8i4.3.
[12] J. Stanojevic, A. Djordjevic, and M. Mitrovic, “Influence of battery energy storage system on generation adequacy and system stability in hybrid micro grids,” in 2016 4th International Symposium on Environmental Friendly Energies and Applications (EFEA), Belgrade, Serbia, Sep. 2016, pp. 1–6. doi: 10.1109/EFEA.2016.7748813.
[13] F. K. Ariyo, “Investigation of Nigerian 330 Kv Electrical Network with Distributed Generation Penetration − Part III: Determinis c and Probabilistic Analyses.,” Am. J. Electr. Power Energy Syst., vol. 2, no. 1, p. 7, 2013, doi: 10.11648/j.epes.20130201.12.
[14] R. Billinton and W. Li, Reliability Assessment of Electric Power Systems Using Monte Carlo Methods. Boston, MA: Springer US, 1994. doi: 10.1007/978-1-4899-1346-3.
[15] W. Wangdee and R. Billinton, “Considering Load-Carrying Capability and Wind Speed Correlation of WECS in Generation Adequacy Assessment,” IEEE Trans. Energy Convers., vol. 21, no. 3, pp. 734–741, Sep. 2006, doi: 10.1109/TEC.2006.875475.
[16] B. M. Taele, L. Mokhutšoane, I. Hapazari, S. B. Tlali, and M. Senatla, “Grid electrification challenges, photovoltaic electrification progress and energy sustainability in Lesotho,” Renew. Sustain. Energy Rev., vol. 16, no. 1, pp. 973–980, Jan. 2012, doi: 10.1016/j.rser.2011.09.019.
[17] Bureau of Statistics, “Energy Report 2019.” 2020. Accessed: Mar. 05, 2021. [Online]. Available: http://www.bos.gov.ls/Publications.htm

[18] M. Senatla, M. Nchake, B. M. Taele, and I. Hapazari, “Electricity capacity expansion plan for Lesotho – implications on energy policy,” Energy Policy, vol. 120, pp. 622–634, Sep. 2018, doi: 10.1016/j.enpol.2018.06.003.
[19] M. Mpholo et al., “Determination of the lifeline electricity tariff for Lesotho,” Energy Policy, vol. 140, p. 111381, May 2020, doi: 10.1016/j.enpol.2020.111381.
[20] “Tracking The SDG7: Progress Report 2021.” Accessed: Sep. 28, 2021. [Online]. Available: https://trackingsdg7.esmap.org/downloads
[21] D. P. Thyrsos Hadjicostas, “Formulation of The Lesotho Electrification Master Plan: Grid Development Plan Report (Draft).” Department of Energy, Jul. 22, 2018.
[22] Department of Energy (DoE), “Lesotho Sustainable Energy for All: Country Action Agenda.” 2018. Accessed: Sep. 28, 2021. [Online]. Available: https://erc.nul.ls/publications/reports
[23] Lesotho Electricity Company (LEC), “Lesotho Services for Renewable Energy Grid Integration Study.” 2019. Accessed: Sep. 28, 2021. [Online]. Available: https://www.afdb.org/fileadmin/uploads/afdb/Documents/Procurement/Project-related-Procurement/EOI_-_Lesotho_-_Services_for_Renewable_Energy_Grid_Integration_Study.pdf
[24] European Commission. Joint Research Centre., Power grid recovery after natural hazard impact. LU: Publications Office, 2017. Accessed: Oct. 10, 2021. [Online]. Available: https://data.europa.eu/doi/10.2760/87402
[25] J. Lin and F. Magnago, Electricity markets: theories and applications. Hoboken, NJ: Wiley / IEEE Press, 2017.
[26] T. Hove, “A method for predicting long-term average performance of photovoltaic systems,” Renew. Energy, vol. 21, no. 2, pp. 207–229, Oct. 2000, doi: 10.1016/S0960-1481(99)00131-7.
[27] M. Zare Oskouei and B. Mohammadi-Ivatloo, Integration of Renewable Energy Sources Into the Power Grid Through PowerFactory. Cham: Springer International Publishing, 2020. doi: 10.1007/978-3-030-44376-4.
[28] M. Rastegar and M. Fotuhi-Firuzabad, “Load management in a residential energy hub with renewable distributed energy resources,” Energy Build., vol. 107, pp. 234–242, Nov. 2015, doi: 10.1016/j.enbuild.2015.07.028.
[29] C. Tao, D. Shanxu, and C. Changsong, “Forecasting power output for grid-connected photovoltaic power system without using solar radiation measurement,” in The 2nd International Symposium on Power Electronics for Distributed Generation Systems, Hefei, China, Jun. 2010, pp. 773–777. doi: 10.1109/PEDG.2010.5545754.
[30] S. Diaf, G. Notton, M. Belhamel, M. Haddadi, and A. Louche, “Design and techno-economical optimization for hybrid PV/wind system under various meteorological conditions,” Appl. Energy, vol. 85, no. 10, pp. 968–987, Oct. 2008, doi: 10.1016/j.apenergy.2008.02.012.
[31] M. C. Argyrou, P. Christodoulides, C. C. Marouchos, and S. A. Kalogirou, “A grid-connected photovoltaic system: Mathematical modeling using MATLAB/Simulink,” in 2017 52nd International Universities Power Engineering Conference (UPEC), Heraklion, Aug. 2017, pp. 1–6. doi: 10.1109/UPEC.2017.8232009.
[32] I. Hamdan, A. Maghraby, and O. Noureldeen, “Stability improvement and control of gridconnected photovoltaic system during faults using supercapacitor,” SN Appl. Sci., vol. 1, no. 12, p. 1687, Dec. 2019, doi: 10.1007/s42452-019-1743-2.
[33] M. Gustavo and P. Enrique, “Modelling and Control Design of Pitch-Controlled Variable Speed Wind Turbines,” in Wind Turbines, I. H. Al-Bahadly, Ed. InTech, 2011. doi: 10.5772/15880.
[34] W. Tong, “Fundamentals of wind energy,” in WIT Transactions on State of the Art in Science and Engineering, 1st ed., vol. 1, WIT Press, 2010, pp. 3–48. doi: 10.2495/978-1-84564-205-1/01.

[35] V. Sohoni, S. C. Gupta, and R. K. Nema, “A Critical Review on Wind Turbine Power Curve Modelling Techniques and Their Applications in Wind Based Energy Systems,” J. Energy, vol. 2016, pp. 1–18, 2016, doi: 10.1155/2016/8519785.
[36] R. Veena, S. M. Manuel, S. Mathew, and I. Petra, “Parametric Models for Predicting the Performance of Wind Turbines,” Mater. Today Proc., vol. 24, pp. 1795–1803, 2020, doi: 10.1016/j.matpr.2020.03.604.
[37] J. Hetzer, D. C. Yu, and K. Bhattarai, “An Economic Dispatch Model Incorporating Wind Power,” IEEE Trans. Energy Convers., vol. 23, no. 2, pp. 603–611, Jun. 2008, doi: 10.1109/TEC.2007.914171.
[38] P. Giorsetto and K. F. Utsurogi, “Development of a new procedure for reliability modeling of wind turbine generators,” IEEE Trans. Power Appar. Syst., vol. 102, no. 1, pp. 131–143, 1983.
[39] M. K. Deshmukh and S. S. Deshmukh, “Modeling of hybrid renewable energy systems,” Renew. Sustain. Energy Rev., vol. 12, no. 1, pp. 235–249, Jan. 2008, doi: 10.1016/j.rser.2006.07.011.
[40] W. R. Powell, “An analytical expression for the average output power of a wind machine,” Sol. Energy, vol. 26, no. 1, pp. 77–80, 1981, doi: 10.1016/0038-092X(81)90114-6.
[41] Pallabazzer, R, “Evaluation of wind-generator potentiality,” Sol. Energy U. S., vol. 55, no. 1, 1995, doi: https://doi.org/10.1016/0038-092X(95)00040-X.
[42] Sathyajith Mathew, “wind_energy_-_fundamentals_resource_analysis_and_economics.pdf.”
[43] G. Gualtieri and S. Secci, “Methods to extrapolate wind resource to the turbine hub height based on power law: A 1-h wind speed vs. Weibull distribution extrapolation comparison,” Renew. Energy, vol. 43, pp. 183–200, Jul. 2012, doi: 10.1016/j.renene.2011.12.022.
[44] R. Byrne, N. J. Hewitt, P. Griffiths, and P. MacArtain, “Observed site obstacle impacts on the energy performance of a large scale urban wind turbine using an electrical energy rose,” Energy Sustain. Dev., vol. 43, pp. 23–37, Apr. 2018, doi: 10.1016/j.esd.2017.12.002.
[45] M. Mpholo, T. Mathaba, and M. Letuma, “Wind profile assessment at Masitise and Sani in Lesotho for potential off-grid electricity generation,” Energy Convers. Manag., vol. 53, no. 1, pp. 118–127, Jan. 2012, doi: 10.1016/j.enconman.2011.07.015.
[46] “Wind energy: fundamentals, resource analysis and economics,” Choice Rev. Online, vol. 44, no. 01, pp. 44-0337-44–0337, Sep. 2006, doi: 10.5860/CHOICE.44-0337.
[47] “Renewable energy market analysis: Africa and its regions,” p. 318.
[48] “World Energy Transitions Outlook: 1.5°C Pathway,” p. 312.
[49] N. T. Mbungu, R. M. Naidoo, R. C. Bansal, M. W. Siti, and D. H. Tungadio, “An overview of renewable energy resources and grid integration for commercial building applications,” J. Energy Storage, vol. 29, p. 101385, Jun. 2020, doi: 10.1016/j.est.2020.101385.
[50] T. García-Sánchez, E. Gómez-Lázaro, and A. Molina-García, “A Review and Discussion of the GridCode Requirements for Renewable Energy Sources in Spain,” Renew. Energy Power Qual. J., pp. 565–570, Apr. 2014, doi: 10.24084/repqj12.410.
[51] C. Sourkounis and P. Tourou, “Grid Code Requirements for Wind Power Integration in Europe,” Conf. Pap. Energy, vol. 2013, pp. 1–9, Jun. 2013, doi: 10.1155/2013/437674.
[52] A. Eberhard and K. N. Gratwick, “IPPs in Sub-Saharan Africa: Determinants of success,” Energy Policy, vol. 39, no. 9, pp. 5541–5549, Sep. 2011, doi: 10.1016/j.enpol.2011.05.004.
[53] T. Ackermann et al., “Integrating Variable Renewables in Europe : Current Status and Recent Extreme Events,” IEEE Power Energy Mag., vol. 13, no. 6, pp. 67–77, Nov. 2015, doi: 10.1109/MPE.2015.2461333.
[54] O. Langniß, J. Diekmann, and U. Lehr, “Advanced mechanisms for the promotion of renewable energy—Models for the future evolution of the German Renewable Energy Act,” Energy Policy, vol. 37, no. 4, pp. 1289–1297, Apr. 2009, doi: 10.1016/j.enpol.2008.11.007.
[55] D. Jacobs et al., “Analysis of renewable energy incentives in the Latin America and Caribbean region: The feed-in tariff case,” Energy Policy, vol. 60, pp. 601–610, Sep. 2013, doi:

10.1016/j.enpol.2012.09.024.
[56] G. Sreenivasan and S. Sivanagaraju, “Power System Operation and Control,” p. 925.
[57] K. Y. Lee, “Applications of Modern Heuristic Optimization Methods in Power and Energy Systems,” p. 888.
[58] S. P. Boyd and L. Vandenberghe, Convex optimization. Cambridge, UK ; New York: Cambridge University Press, 2004.
[59] K. Y. Lee and M. A. El-Sharkawi, Eds., Modern heuristic optimization techniques: theory and applications to power systems. Piscataway, N.J. : Hoboken, N.J: IEEE Press ; Wiley-Interscience, 2008.
[60] A. J. Wood, B. F. Wollenberg, eacute Shebl&amp, and Gerald B, “Power Generation, Operation and Control,” p. 658.
[61] X. Xia and A. M. Elaiw, “Optimal dynamic economic dispatch of generation: A review,” Electr. Power Syst. Res., vol. 80, no. 8, pp. 975–986, Aug. 2010, doi: 10.1016/j.epsr.2009.12.012.
[62] V. R. Pandi, B. K. Panigrahi, R. C. Bansal, S. Das, and A. Mohapatra, “Economic Load Dispatch Using Hybrid Swarm Intelligence Based Harmony Search Algorithm,” Electr. Power Compon. Syst., vol. 39, no. 8, pp. 751–767, Apr. 2011, doi: 10.1080/15325008.2010.541411.
[63] A. Mahor, V. Prasad, and S. Rangnekar, “Economic dispatch using particle swarm optimization: A review,” Renew. Sustain. Energy Rev., vol. 13, no. 8, pp. 2134–2141, Oct. 2009, doi: 10.1016/j.rser.2009.03.007.
[64] F. N. Lee and A. M. Breipohl, “Reserve constrained economic dispatch with prohibited operating zones,” IEEE Trans. Power Syst., vol. 8, no. 1, pp. 246–254, Feb. 1993, doi: 10.1109/59.221233.
[65] S. Prabakaran, V. Senthilkuma, and G. Baskar, “Economic Dispatch Using Hybrid Particle Swarm Optimization with Prohibited Operating Zones and Ramp Rate Limit Constraints,” J. Electr. Eng. Technol., vol. 10, no. 4, pp. 1441–1452, Jul. 2015, doi: 10.5370/JEET.2015.10.4.1441.
[66] W. T. El-Sayed, E. F. El-Saadany, H. H. Zeineldin, and A. S. Al-Sumaiti, “Fast initialization methods for the nonconvex economic dispatch problem,” Energy, vol. 201, p. 117635, Jun. 2020, doi: 10.1016/j.energy.2020.117635.
[67] E. Arriagada, E. López, M. López, R. Blasco-Gimenez, C. Roa, and M. Poloujadoff, “A probabilistic economic dispatch model and methodology considering renewable energy, demand and generator uncertainties,” Electr. Power Syst. Res., vol. 121, pp. 325–332, Apr. 2015, doi: 10.1016/j.epsr.2014.11.018.
[68] T. Nguyen, N. Vu Quynh, M. Duong, and L. Van Dai, “Modified Differential Evolution Algorithm: A Novel Approach to Optimize the Operation of Hydrothermal Power Systems while Considering the Different Constraints and Valve Point Loading Effects,” Energies, vol. 11, no. 3, p. 540, Mar. 2018, doi: 10.3390/en11030540.
[69] K. Kazda and X. Li, “A Critical Review of the Modeling and Optimization of Combined Heat and Power Dispatch,” Processes, vol. 8, no. 4, p. 441, Apr. 2020, doi: 10.3390/pr8040441.
[70] M.-H. Lin, J.-F. Tsai, and C.-S. Yu, “A Review of Deterministic Optimization Methods in Engineering and Management,” Math. Probl. Eng., vol. 2012, pp. 1–15, 2012, doi: 10.1155/2012/756023.
[71] Parmvir Singh Bhullar, Jaspreet Kaur Dhami, and B.B.S.B.E College Fatehgarh Sahib, “Particle Swarm Optimization Based Economic Load Dispatch with Valve Point Loading,” Int. J. Eng. Res., vol. V4, no. 05, May 2015, doi: 10.17577/IJERTV4IS050998.
[72] C. A. Floudas, Deterministic Global Optimization, vol. 37. Boston, MA: Springer US, 2000. doi: 10.1007/978-1-4757-4949-6.
[73] Z. N. Jan, “Economic Load Dispatch using Lambda Iteration, Particle Swarm Optimization & Genetic Algorithm,” Int. J. Res. Appl. Sci. Eng. Technol., vol. 9, no. 8, pp. 972–977, Aug. 2021, doi: 10.22214/ijraset.2021.37527.

[74] H. Xing, Z. Lin, and M. Fu, “Distributed augmented lambda-iteration method for economic dispatch in smart grid,” in 2017 Chinese Automation Congress (CAC), Jinan, Oct. 2017, pp. 3302–3307. doi: 10.1109/CAC.2017.8243347.
[75] J. P. Zhan, Q. H. Wu, C. X. Guo, and X. X. Zhou, “Fast λ-Iteration Method for Economic Dispatch With Prohibited Operating Zones,” IEEE Trans. Power Syst., vol. 29, no. 2, pp. 990–991, Mar. 2014, doi: 10.1109/TPWRS.2013.2287995.
[76] D. R. Morrison, S. H. Jacobson, J. J. Sauppe, and E. C. Sewell, “Branch-and-bound algorithms: A survey of recent advances in searching, branching, and pruning,” Discrete Optim., vol. 19, pp. 79–102, Feb. 2016, doi: 10.1016/j.disopt.2016.01.005.
[77] K. O. Alawode, A. M. Jubril, L. O. Kehinde, and P. O. Ogunbona, “Semidefinite programming solution of economic dispatch problem with non-smooth, non-convex cost functions,” Electr. Power Syst. Res., vol. 164, pp. 178–187, Nov. 2018, doi: 10.1016/j.epsr.2018.07.026.
[78] T. Ding, R. Bo, F. Li, and H. Sun, “A Bi-Level Branch and Bound Method for Economic Dispatch With Disjoint Prohibited Zones Considering Network Losses,” IEEE Trans. Power Syst., vol. 30, no. 6, pp. 2841–2855, Nov. 2015, doi: 10.1109/TPWRS.2014.2375322.
[79] A. Bhadoria, V. K. Kamboj, M. Sharma, and S. K. Bath, “A Solution to Non-convex/Convex and Dynamic Economic Load Dispatch Problem Using Moth Flame Optimizer,” INAE Lett., vol. 3, no. 2, pp. 65–86, Jun. 2018, doi: 10.1007/s41403-018-0034-3.
[80] J. Kim, C. S. Kim, and Z. W. Geem, “A Memetic Approach for Improving Minimum Cost of Economic Load Dispatch Problems,” Math. Probl. Eng., vol. 2014, pp. 1–11, 2014, doi: 10.1155/2014/906028.
[81] Shewit Tsegaye and Fekadu Shewarega, “Recent Trends on Security Constrained Economic Dispatch: A Bibliographic Review,” Jun. 2019, doi: 10.5281/ZENODO.3300384.
[82] G. Chicco and A. Mazza, “Metaheuristic Optimization of Power and Energy Systems: Underlying Principles and Main Issues of the ‘Rush to Heuristics,’” Energies, vol. 13, no. 19, p. 5097, Sep. 2020, doi: 10.3390/en13195097.
[83] C. K. Panigrahi, P. K. Chattopadhyay, R. N. Chakrabarti, and M. Basu, “Simulated Annealing Technique for Dynamic Economic Dispatch,” Electr. Power Compon. Syst., vol. 34, no. 5, pp. 577–586, May 2006, doi: 10.1080/15325000500360843.
[84] S. Venkatraj and B. Mugunthan, “An Intelligent Soft Computing Technique based Solution to Economic Load Dispatch Problem in Power System,” p. 10, 2021.
[85] H. Shahinzadeh, S. M. Nasr-Azadani, and N. Jannesari, “Applications of Particle Swarm Optimization Algorithm to Solving the Economic Load Dispatch of Units in Power Systems with Valve-Point Effects,” Int. J. Electr. Comput. Eng. IJECE, vol. 4, no. 6, Dec. 2014, doi: 10.11591/ijece.v4i6.6720.
[86] S. Hemavathi and N. Devarajan, “Efficient Dynamic Economic Load Dispatch Using Parallel Process of Enhanced Optimization Approach,” Circuits Syst., vol. 07, no. 10, pp. 3260–3270, 2016, doi: 10.4236/cs.2016.710278.
[87] S. P. Singh, R. Tyagi, and A. Goel, “Genetic Algorithm for Solving the Economic Load Dispatch,” p. 7.
[88] S. Mirjalili, “Genetic Algorithm,” in Evolutionary Algorithms and Neural Networks, vol. 780, Cham: Springer International Publishing, 2019, pp. 43–55. doi: 10.1007/978-3-319-93025-1_4.
[89] F. K. Khosa, M. F. Zia, and A. A. Bhatti, “Genetic algorithm based optimization of economic load dispatch constrained by stochastic wind power,” in 2015 International Conference on Open Source Systems & Technologies (ICOSST), Lahore, Pakistan, Dec. 2015, pp. 36–40. doi: 10.1109/ICOSST.2015.7396399.

[90] M. Akmal, S. Ali, Y. A. Khalil, N. B. Iqbal and S. Alzaabi, “Integration of solar energy and optimized economic dispatch using genetic algorithm: A case-study of Abu Dhabi,.” IEEE Power & Energy Society Innovative Smart Grid Technologies Conference (ISGT, 2017. [Online]. Available: doi: 10.1109/ISGT.2017.8085990.
[91] L. B. Shi, R. Wang, L. Z. Yao, and Y. J. Liu, “Study on the Dynamic Economic Dispatch for a Windhydro Hybrid Power System,” in International Conference on Renewable Power Generation (RPG 2015), Beijing, China, 2015, p. 6 .-6 . doi: 10.1049/cp.2015.0334.
[92] S. Banerjee, K. Dasgupta, and C. K. Chanda, “Short term hydro–wind–thermal scheduling based on particle swarm optimization technique,” Int. J. Electr. Power Energy Syst., vol. 81, pp. 275–288, Oct. 2016, doi: 10.1016/j.ijepes.2016.01.031.
[93] S. Titus and A. Ebenezer Jeyakumar, “Hydrothermal Scheduling Using an Imporoved Particle Swarm Optimization Technique Considering Prohibited Operating Zones.” International Journal of Soft Computing,2: 313-319., 2007. Accessed: Nov. 15, 2021. [Online]. Available: https://medwelljournals.com/abstract/?doi=ijscomp.2007.313.319
[94] K. Gholami and E. Dehnavi, “A modified particle swarm optimization algorithm for scheduling renewable generation in a micro-grid under load uncertainty,” Appl. Soft Comput., vol. 78, pp. 496–514, May 2019, doi: 10.1016/j.asoc.2019.02.042.
[95] R. Bouddou, “The Dynamic Economic Dispatch in An Integrated Wind-Thermal Electricity Market Using Simulated Annealing Algorithm,” PRZEGLĄD ELEKTROTECHNICZNY, vol. 1, no. 11, pp. 57–62, Nov. 2020, doi: 10.15199/48.2020.11.12.
[96] M. Basu, “Dynamic economic dispatch with demand-side management incorporating renewable energy sources and pumped hydroelectric energy storage,” Electr. Eng., vol. 101, no. 3, pp. 877– 893, Sep. 2019, doi: 10.1007/s00202-019-00793-x.
[97] K. Vaisakh, P. Praveena, S. Rama Mohana Rao, and K. Meah, “Solving dynamic economic dispatch problem with security constraints using bacterial foraging PSO-DE algorithm,” Int. J. Electr. Power Energy Syst., vol. 39, no. 1, pp. 56–67, Jul. 2012, doi: 10.1016/j.ijepes.2012.01.005.
[98] M. F. Zaman, S. M. Elsayed, T. Ray, and R. A. Sarker, “Evolutionary Algorithms for Dynamic Economic Dispatch Problems,” IEEE Trans. Power Syst., vol. 31, no. 2, pp. 1486–1495, Mar. 2016, doi: 10.1109/TPWRS.2015.2428714.
[99] S. Titus and A. E. Jeyakumar, “A Hybrid EP-PSO-SQP Algorithm for Dynamic Dispatch Considering Prohibited Operating Zones,” Electr. Power Compon. Syst., vol. 36, no. 5, pp. 449–467, Apr. 2008, doi: 10.1080/15325000701735256.
[100] T. A. A. Victoire and A. E. Jeyakumar, “Deterministically guided PSO for dynamic dispatch considering valve-point effect,” Electr. Power Syst. Res., vol. 73, no. 3, pp. 313–322, Mar. 2005, doi: 10.1016/j.epsr.2004.07.005.
[101] G. C. Oliveira, S. H. F. Cunha, and M. V. F. Pereira, “A direct method for multi-area reliability evaluation,” Power Syst. IEEE Trans., vol. 2, no. 4, pp. 934–940, 1987.
[102] E. Tomasson and L. Soder, “Generation Adequacy Analysis of Multi-Area Power Systems With a High Share of Wind Power,” IEEE Trans. Power Syst., vol. 33, no. 4, pp. 3854–3862, Jul. 2018, doi: 10.1109/TPWRS.2017.2769840.
[103] M. P. Blanco, A. Spisto, and G. Fulli, “GENERATION ADEQUACY METHODOLOGIES REVIEW,” p. 108.
[104] V. Pillai N, “Loss of Load Probability of a Power System,” J. Fundam. Renew. Energy Appl., vol. 05, no. 01, 2014, doi: 10.4172/2090-4541.1000149.
[105] S. Jaehnert and G. Doorman, “Analysing the generation adequacy in power markets with renewable energy sources,” in 11th International Conference on the European Energy Market (EEM14), Krakow, Poland, May 2014, pp. 1–6. doi: 10.1109/EEM.2014.6861225.

[106] F. Vallee, J. Lobry, and O. Deblecker, “System Reliability Assessment Method for Wind Power Integration,” IEEE Trans. Power Syst., vol. 23, no. 3, pp. 1288–1297, Aug. 2008, doi: 10.1109/TPWRS.2008.926090.
[107] A. Ahadi, S. E. Reza, and X. Liang, “Probabilistic reliability evaluation for power systems with high penetration of renewable power generation,” in 2017 IEEE International Conference on Industrial Technology (ICIT), Toronto, ON, Mar. 2017, pp. 464–468. doi: 10.1109/ICIT.2017.7913275.
[108] B. Do, T. Tran, and N. Nguyen, “Renewable Energy Integration in Vietnam’s Power System: Generation Adequacy Assessment and Strategic Implications,” Energies, vol. 14, no. 12, p. 3541, Jun. 2021, doi: 10.3390/en14123541.
[109] F. M. Gonzalez-Longatt and J. Luis Rueda, Eds., PowerFactory Applications for Power System Analysis. Cham: Springer International Publishing, 2014. doi: 10.1007/978-3-319-12958-7.
[110] A. Ilinca, E. McCarthy, J.-L. Chaumel, and J.-L. Rétiveau, “Wind potential assessment of Quebec Province,” Renew. Energy, vol. 28, no. 12, pp. 1881–1897, Oct. 2003, doi: 10.1016/S09601481(03)00072-7.
[111] “JRC Photovoltaic Geographical Information System (PVGIS) - European Commission.” https://re.jrc.ec.europa.eu/pvg_tools/en/ (accessed Mar. 24, 2022).